BIOFABRICATION OF THREE-DIMENSIONAL LIVER CELL-EMBEDDED TISSUE CONSTRUCTS FOR IN VITRO DRUG METABOLISM MODELS

A Thesis

Submitted to the Faculty

of

Drexel University

by

Robert Chao Chang

in partial fulfillment of the

requirements for the degree

of

PhD in Mechanical Engineering

June 2009

DEDICATIONS

This work is dedicated to my dear parents for their loving support, advice, and unyielding faith in me and my brother for his constant encouragement throughout my doctoral studies.

ACKNOWLEDGMENTS

First and foremost, I would like to sincerely express my deepest gratitude to my advisor and mentor, Dr. Wei Sun, for his guidance throughout my doctoral studies and helping me with my professional development and maturation as a researcher. I would also like to thank my thesis committee members Dr. Honglu Wu, Dr. Moses Noh, Dr. Min Jun Kim, Dr. Alan Lau, and Dr. Fred Allen for their participation, time, and helpful suggestions to improve my dissertation. I would like extend my thanks to all the faculty, staff, and students I've been fortunate to encounter in the Department of Mechanical Engineering and Mechanics for their constant support during my graduate studies at Drexel. I would like to thank NASA-JSC for supporting our collaborative project, especially working with Kamal Emami, Dr. Chris Culbertson, Dr. Antony Jeevarajan, Dr. Heidi Holtorf, and Julie Leslie. I also would like to acknowledge both the past and current lab members who have made my years at Drexel a truly memorable one: Andrew Darling, Lauren Shor, Connie Gomez, Milind Gandhi, Xun Zhou, Jie Li, Qudus Hamid, and Jessica Snyder. A special thanks to Saif Khalil and Binil Starly who helped guide me along the way and Eda Yildirim for her constant friendship and a multitude of helpful suggestions. I greatly value my experience at Drexel which has inspired me to pursue a career in research.

TABLE OF CONTENTS

LIST OF TABLES

LIST OF FIGURES

ABSTRACT

Biofabrication of three-dimensional liver cell-embedded tissue constructs for in vitro drug metabolism models

Robert Chao Chang

Wei Sun, Ph.D

In their normal *in vivo* matrix milieu, tissues assume complex well-organized three-dimensional architectures. Therefore, a primary aim in the tissue engineering design process is to fabricate an optimal analog of the *in vivo* scenario. This challenge can be addressed by applying emerging layered biofabrication approaches in which the precise configuration and composition of cells and bioactive matrix components can recapitulate the well-defined three-dimensional biomimetic microenvironments that promote cell-cell and cell-matrix interactions. Furthermore, the advent of and refinements in microfabricated systems can present physical and chemical cues to cells in a controllable and reproducible fashion unrealizable with conventional tissue culture, resulting in high-fidelity, high-throughput *in vitro* models. As such, the convergence of layered solid freeform fabrication (SFF) technologies along with microfabrication techniques, a three-dimensional micro-organ device can serve as an *in vitro* platform for cell culture, drug screening, or to elicit further biological insights, particularly for NASA's interest of a flight-suitable high-fidelity microscale platform to study drug metabolism in space and planetary environments. A proposed model in this thesis involves the combinatorial setup of an automated syringe-based, layered direct cell writing bioprinting process with micro-patterning techniques to fabricate a microscale *in vitro* device housing a chamber of

bioprinted three-dimensional cell-encapsulated hydrogel-based tissue constructs in defined design patterns that biomimics the cell's natural microenvironment for enhanced performance and functionality. In order to assess the structural formability and biological feasibility of such a micro-organ, reproducibly fabricated tissue constructs are biologically characterized for both viability and cell-specific function. Another key facet of the *in vivo* microenvironment that is recapitulated with the *in vitro* system is the necessary dynamic perfusion of the three-dimensional microscale liver analog with cells probed for their collective drug metabolic function and suitability as a drug metabolism model. This thesis details the principles, methods, and engineering science basis that undergird the direct cell writing fabrication process development and adaptation of microfluidic devices for the creation of a drug screening model, thereby establishing a novel drug metabolism study platform for NASA's interest to adopt a microfluidic microanalytical device with an embedded three-dimensional microscale liver tissue analog to assess drug pharmacokinetic profiles in planetary environments.

CHAPTER 1. INTRODUCTION AND BACKGROUND

1.1 Biomanufacturing for Tissue Engineering

Tissue engineering has classically been defined as the application of the principles and methods of engineering and life sciences for the development of biological substitutes to restore, maintain, or improve tissue function (Langer et al., 1993). In the process of establishing a shift or directional change for the field of tissue science and engineering, the 2007 Federal Multi-Agency Strategic Plan, initiated by the NIH, NSF, DoD and other Federal agencies, has redefined tissue engineering as "the use of physical, chemical, biological, and engineering processes to control and direct the aggregate behaviors of cells" as opposed to developing functional tissues for implantation. In accordance with this paradigm shift, living cells can be used as basic building blocks to manufacture cell-integrated biological structures. Just as central processing units (CPUs) form the cores of computers, living cells may form the cores of the next generation of biological systems, constructs, and devices. Incidentally, the convergence of engineering and the life sciences as the foundation for robust biology-based engineering design and analysis has enabled the emergence of a novel interdisciplinary field of biomanufacturing or biofabrication (terms that will be used interchangeably in this thesis) which employs cells or bioactive factors as nature's fundamental structural and functional elements from which biological models, systems, devices, and products are assembled. Specific examples of new broader biomanfacturing applications include the incorporation of cells into engineered tissue scaffolds, microfluidic devices, biochips and biosensors, drug delivery and toxicity screening platforms, and tissue or organ-on-a-chip devices.

From a purely mechanistic standpoint, biomanufacturing represents a broad array of methods that employ mechanical means to manufacture products that incorporate living cells into their systems as well as enable precision multi-scale control of material, architecture, and cells (Sun et al., 2007). Successful biofabrication for new broad applications, however, must include both an appropriate environment for cell viability and function at the microscale level, as well as macroscale-level properties that allow sufficient transport of nutrients, provide adequate mechanical properties, and facilitate coordination of multicellular processes (Tsang et al., 2004). This *in vivo*-like milieu, or local cellular microenvironment, aims to present biochemical, cellular, and physical stimuli that orchestrate cellular fate processes such as proliferation, differentiation, migration, and apoptosis. Pivotal in the phenomenological replication of these microenvironmental stimuli are the relative composition of cells and biomaterials in a tissue engineered scaffold or construct which can be tuned to recapitulate the biophysical and biochemical milieus that direct cellular behavior and function (Lutolf et al., 2005). Discussed below is an overview of the two general biomanufacturing approaches to engineer three-dimensional tissue, i.e. acellular polymer tissue scaffold methods and cell-integrated tissue construct systems. The sections below will specifically address tissue scaffold and cell-integrated tissue construct biofabrication processes involving both cells and biomaterials as integral components in the tissue engineered system.

1.1.1 Acellular Tissue Scaffold Biofabrication Processes

The first set of biofabrication processes are classified as ones that exclude cells during the initial biomaterial processing phase of scaffold fabrication, but are typically seeded on the surface with cells subsequent to the scaffold fabrication and any additional post-processing steps for improved scaffold bioactivity. Within the category of acellular tissue scaffold biofabrication, the biomaterial processing phase can be classified as being heat-based, light mediated, governed by adhesives, or indirectly fabricated with molds. In heat-based scaffold biofabrication techniques, the heat energy is applied to a biopolymer, thereby elevating the material above its glass transition temperature to facilitate sequential fusion of laminated sheets through the application of pressure (Yang et al., 2002). Currently, these biofabricated laminated sheets exhibit a low void volume that is prohibitive of high cell density integration. Another example of heat-based scaffold biofabrication is the selective laser sintering (SLS) technique which uses a CO_2 laser beam to sinter thin layers of powdered polymeric materials. The interaction of the laser beam with the powder raises the powder temperature and sintering occurs at just beyond the glass transition temperature, thereby causing the particles to fuse together to form a solid three-dimensional structure. Application of SLS with formulated suspensions of calcium polyphosphate (CPP) and a photocurable monomer as well as other polymer blends can lead to the formation of bioresorbable skeletal implants (Porter et al., 2001, Tan et al., 2003). The pattern resolution, however, of SLS is limited by the diameter of the laser beam to about 400 μm (Yang et al., 2002), and maximum pore size is about 50 μm due to the powder particle size (Leong et al., 2003). Fused deposition modeling

(FDM) is another acellular biofabrication process that combines heat and extrusion techniques to create three-dimensional scaffolds layer-by-layer. A nozzle deposits a strand of molten plastic or ceramic onto a previously deposited layer of material. Zein et al. have implemented this method to produce biodegradable poly(ε-caprolactone) (PCL) scaffolds exhibiting various honeycomb geometries with strut widths of 250–700 μm (Zein et al., 2002). A variation of the FDM process, the precision extruding deposition (PED) system, has been developed and characterized in which the hallmark difference between PED and conventional FDM is that the scaffolding material can be directly deposited without filament preparation (Shor et al., 2007). Pellet-formed polycaprolactone (PCL) is fused by a liquefier temperature provided by two heating bands and respective thermal couples and is then extruded by pressure created by a turning precision screw.

1.1.2 Cell-Integrated Tissue Construct Biofabrication Processes

Acellular tissue scaffolds possess excellent mechanical integrity on the whole, but may be difficult to efficiently populate with cells during the cell-seeding phase. In contrast, tissue constructs provide high tissue density but may be mechanically unstable without a biomaterial support environment. Furthermore, for various tissue engineering applications, when cells are seeded onto preformed scaffolds, the result is a non-directed, homogenous coating of cells on the scaffold's surface (Williams et al., 2005, Cortesini, 2005). Although several cell types can be simultaneously seeded onto scaffolding, there

currently exists no way to place different cell types in different parts of the scaffolding, much less on a length scale comparable to the heterogeneity found in natural tissue.

Cell-integrated tissue constructs, particularly those composed of hydrogel biopolymers, have therefore become increasingly popular because of their ability to provide both structural biomaterial support and a sufficiently high tissue density with tissue heterogeneity while maintaining an *in vivo*-like microenvironment for cells. The incorporation of cells in the biomanufacturing process has led to the development of various cell printing methods which can be subdivided into structural and conformal cell printing (Ringeisen et al., 2006). Both approaches are similar in that the finished printed cell construct would be fabricated from the bottom up (i.e., layer-by-layer or cell-by-cell) and has heterogeneous cell and biomolecular structure in three dimensions. The distinction lies in the fact that structural cell printing requires that the same tool print the scaffolding, cells, and biomolecules simultaneously or sequentially, while conformal cell printing is a hybrid approach that would print cells and biomolecules on top of thin layers of prefabricated scaffolding. Jet-based cell printing methods is an example that has shown promise for structural cell printing for simultaneous printing of cells and materials, but has been for the most part applied as a conformal printing approach.

Jet-based printing approaches can be appropriately classified into several distinct categories including laser guidance direct writing (LGDW), modified laser-induced forward transfer techniques (modified-LIFT), and modified ink jet printers. The distinctions between these methods are often related to resolution, print speed, cell

throughput, and load volume, which will all have varying levels of relevancy depending upon the application (organ, tissue, injury site, etc.) being addressed. The first jet-based printing approach is laser guidance direct writing, which utilizes radiation pressure to direct particle deposition with micrometer resolution. Odde et al. have demonstrated the use of laser-based optical forces to precisely deliver a stream of embryonic chick spinal cord cells and 'write' them into arbitrary positions on a substrate (Odde et al., 2000, Odde et al., 1999). However, if the parameters are not optimized it could lead to further problems like fiber clogging because of higher cell density and potential for cell damage by using more intense light. The modified laser induced forward transfer technique (modified-LIFT) has demonstrated the ability to print patterns of living E. coli (Ringeisen et al., 2001) with acceptable cell viability and retained functionality of the printed bacteria. This technique has also been successfully implemented to print pluripotent embryonal carcinoma cells with near 100% viability and phenotype retention after the printing process (Ringeisen et al., 2004). Modified-LIFT possesses the added advantage of being an orifice/capillary-free technique to forestall clogging events as well as enable orders of magnitude more concentrated cell solutions to be used for printing compared to other jet-based technologies. One weakness of the modified-LIST for cell printing is that the reproducibility and resolution in prior experiments are low, resulting in a relatively small array of pluripotent cells being printed with low resolution and high numbers of cells/spot. The final example of jet-based printing techniques is thermal inkjet printing. Applying this technique, Mironov et al. have positioned cell aggregates and fused together embryonic heart mesenchymal fragments within biocompatible gels of varying

chemical and mechanical properties (Mironov et al., 2003). Boland et al. have modified thermal ink jet printers to assemble functional three-dimensional cardiac "pseudo-tissue" constructs with mechanical properties similar to native tissue (Boland et al., 2007, Boland et al., 2006). Maintaining cells in the ink cartridge for long periods of time, however, is often difficult and make rapid deposition or replacement/replenishment of the cells, biomaterials, or bioactive factors necessary to achieve successful cell printing.

The cell printing method that is of particular interest in this thesis relates to structural cell printing in which cells and polymers can be printed simultaneously to result in a cell-embedded tissue construct. While structural cell printing has great potential for novel tissue engineered constructs, it is important to note that there are a few recent examples in the literature demonstrating that technologies capable of the direct assembly of cells and extracellular matrix materials for the construction of functional cell-laden three-dimensional tissue constructs with stable structures. The few that are documented in literature have managed to adopt technologies that have previously been used to print scaffolding materials alone (i.e. without cells). Most of these techniques utilize a micro-pen, syringe, or plotter head to print polymer solutions into three-dimensional assemblies with microscopic structure (Landers et al., 2002, Vozzi et al., 2003). Moreover, most of these techniques utilize extrusion mechanisms (i.e., pushing material through an orifice rather than "jetting" that implies a higher velocity fluid stream), and therefore not considered jet-based technologies. Khalil et al. have explored the use of a solid freeform based fabrication process where heterogeneous three-dimensional structures could be developed with cells using a multinozzle dispensing

device (Khalil et al., 2005) where the cell viability through the system has been studied and reported as well (Chang et al., 2008a). This process, namely the direct cell writing (DCW) system is the biofabrication method of choice in this thesis and is discussed further in Section 1.4.

Many processes have been developed in the area of biomanufacturing for the development of tissue engineered systems. In this thesis, the scope of the biomanufacturing technique implemented is solid freeform fabrication (SFF), which collectively refers to a group of technologies capable of manufacturing objects in a layer-by-layer fashion from a three-dimensional computer design of the object. This layer-by-layer approach allows the manufacturing of objects not feasible with traditional manufacturing methods in which precise control over the macroscopic geometry, internal architecture, and interconnectivity is problematic. Computer-aided rapid-prototyping technologies have been adapted towards the fabrication of three-dimensional scaffolds with precise spatial and temporal control at the macro- and micro-scale levels (Chen et al., 2006). This technology aids design and manufacturing customized tissue substitutes based on clinical imaging data and computer aided design-based freeform fabrication techniques. For example, layered technology that incorporates cells in resorptive materials has been implemented for the development of whole organ and/or complex functional living systems. Specifically, cell printing methods can be used to deposit cells in precise spatial patterns to enhance cell–cell communication, reduce the reliance on cell migration to populate the tissue construct, and create artificial tissue structures that more closely resemble the *in vivo* state. Another recent promising approach of

biomanufacturing techniques is to furnish biologists with sophisticated *in vitro* physiological models for studying fundamental biological problems.

1.2 Tissue Engineering In Vitro Physiological Models

In order to engineer biological tissues *in vitro*, cultured cells are typically coaxed to grow on bioactive porous degradable tissue scaffolds, i.e. temporary synthetic extracellular matrices that provide the biological, chemical, and mechanical cues to guide the cell's eventual differentiation and assembly into three-dimensional tissues. While regeneration of different tissues and organs for therapeutic applications continues to undergo active investigation and development, new applications of tissue engineering for designing *in vitro* physiological models also show great promise. Researchers are increasingly identifying a need to engineer tissues amenable for probing the fundamental mechanisms of human physiology as well as the evolution of disease processes. In fact, Griffith et al. speculates that the greatest impact of tissue engineering in the coming decade will be for designing *in vitro* physiological models for studying disease pathogenesis and developing molecular therapeutics (Griffith et al., 2002).

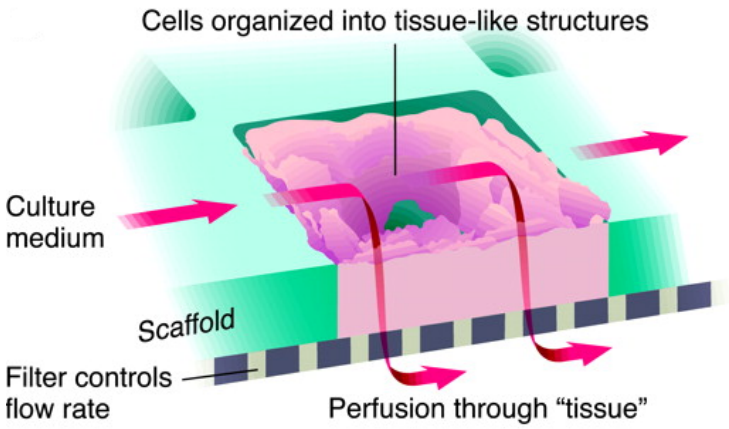

Figure 1-1: A microfabricated bioreactor for perfusing three-dimensional liver tissue engineered *in vitro* (Griffith et al., 2002)

This statement nicely encapsulates a new conceptual framework that could potentially find more near-future applicability, i.e. the design and fabrication of *in vitro* physiological models for the purposes of diagnostics, therapeutics, and pathology. These physiological surrogates can potentially contribute meaningful advances in prevention, diagnosis, and molecular treatment of diseases that are currently considered potential targets for tissue engineering.

The recent development of three specific technologies has greatly facilitated the engineering of tissues for *in vitro* applications: 1) the microfabrication tools that serve to both define the cellular microenvironment and enable parallelization of cell-based assays, 2) tunable hydrogels to create three-dimensional microenvironments; and 3) bioreactors to control nutrient transport and fluid shear stress (Khetani et al., 2006). This chapter explores previous work along with related technologies for the creation of *in vitro*

microfluidic devices to simulate physiological or pathogenetic human responses to the microenvironment. These microtechnology-based processes have several practical applications for cells, materials, and tissues cultured on a microscale platform. These include, but are not limited to drug screening, biosensors, and the study of cell-cell or cell-matrix interactions in both normal cell biology and disease pathogenesis.

1.2.1 Drug and Toxicology Screening Models

One possible near-future application of *in vitro* physiological models established from biology-based engineering analysis is in the area of pharmaceutical drug and toxicology screening for drug discovery and development. In these *in vitro* drug screening models, the liver organ is the focus of study due to its primary role in drug metabolism. Currently, liver cell-based drug screening is used in pharmaceutical development, followed by several rounds of animal testing. A high-fidelity *in vitro* drug metabolism platform, however, can serve as an effective bridge between cell-based assays and animal studies by enabling tissue-based drug screening, resulting in more accurate assessments of drug action as well as mitigating the use of animals in pre-clinical drug testing. Additionally, preclinical animal studies are limited for evaluating toxicity due to species-specific variation between human and animal liver-specific functions, necessitating supplementation of animal data with assays to assess human responses (Pritchard et al., 2003). Existing *in vitro* cell culture models with human liver cells have already shown great potential in predicting drug toxicity and metabolism in the pharmaceutical industry (Powers et al., 2002). For example, a microfabricated array

bioreactor has been designed for perfused three-dimensional liver culture at reported near-physiological ranges of perfusate flow rates and fluid shear stresses. Primary rat liver cells cultured within these microchannels for a two-week duration undergoes rearrangement to form tissue-like structures. Others have reported the modeling of a microscale *in vitro* system to serve as a human surrogate for drug analysis which adheres stringently to a physiologically-based pharmacokinetic (PBPK) model in which disparate organs are serially connected by channels to comprise a fluid circuit of modular systems. This methodology is then applied to mechanistically simulate and predict drug biotransformation, distribution, and efficacy *in vivo*. Therefore, one can imagine the design and fabrication of a stamp-sized animal-on-a-chip microfluidic device which, with great fidelity, accurately simulates the process of an experimental drug being broken down by the metabolizing liver, absorbed by the intestines, and held onto by fat (Ghanem et al., 2000, Shuler et al., 1996, Viravaidya et al., 2004). These models mark the far-reaching potential for *in vitro* drug screening technology as well as highlight the current availability of crude analogs for the organ functions they're intended to biomimic. The inadequacies of current testing methods include, but are not limited to the lack of a high-fidelity three-dimensional microenvironment and the ability to reproducibly fabricate three-dimensional tissue constructs. The current state-of-the-art for *in vitro* drug toxicology platforms is described in greater detail in Section 1.3.2.

1.2.2 Biosensors

Currently, chemical and biological sensors are delicate, complex devices with very limited range and scope that do not accurately predict the human response to environmental toxins. Furthermore, molecular sensors are capable of detecting only single pathogens or chemicals. The limitations of biological sensors are primarily associated with two-dimensional culture on tissue culture plastic which has been a mainstay in conventional cell culture by dispersing complex tissues into single cells and ignoring higher-order processes. Tissue-based sensors fabricated enlisting the precision approaches and processes of microfabrication and layered biofabrication technologies can result in cell signaling pathway components as a highly discriminating and sensitive detection mechanism for identifying a wide range of pathogens and chemicals. More robust sensors based on three-dimensional tissue and/or organ fragments may then be used to rapidly detect biological or chemical threats under a variety of conditions and scenarios. Tools of biofabrication technology may enable development of increasingly sophisticated tissue analogs capable of processing complex environmental information and potentially serve as smart sensors in public health surveillance (Bratten et al., 1998, Chen et al., 2003, Meyvantssson et al., 2008).

1.2.3 In Vitro Models of Disease Pathogenesis

High-throughput technologies based on automation, miniaturization, and multiplexing are now feasible for the systematic study of cells. On the one hand, cell-based models have been the prevailing models in studying cancer and disease

pathogenesis verified by testing in animal models of diseases (Borenstein et al., 2007, Holmes et al., 2000, Semino et al., 2003). On the other hand, biofabrication technology introduces three-dimensional human tissue models for probing basic biological insights into cells and tissues as well as understanding human disease processes to curtail the use of animals in research. Among the applications are three-dimensional *in vitro* tissue analogs with tissue-embedded chambers that mimic different cancer tissues to elicit mechanistic information and further elucidate cell-substrate dynamics in cancer biology. For example, the biofabrication of cancer cells patterned with fibrobasts and various angiogenic factors can simulate some of the hallmark features of invasion and metastasis in cancer, which is often accompanied by fibroblast cell proliferation in the neighboring tissues. Another application is in the area of studying the behavior of complex, highly specialized cells such as neurons that possess the fundamental constraint of requiring other specialized cells for its continued growth and maturation. Substantial progress has already been made in two-dimensional patterning of biological substrates for controlled cell-material interactions at micrometer scales. A micromechanical device housing three-dimensional biofabrication tissue constructs, however, can be developed to enable manipulation of these cells in a three-dimensional microenvironment to help explain the fundamental biological processes cell-cell and cell-matrix signaling and coordination.

Furthermore, rooted within biofabricated platforms will be measurable surrogates or indicators called biomarkers charged with assessing the physiological state of condition of the three-dimensional biofabricated tissue constructs. One such application is with stem cells, which have naturally been investigated as a candidate cell source for

tissue engineering applications. Coordinated alterations in gene expression, and stem cell differentiation specifically, however are influenced not only by cell-autonomous programs but also by microenvironmental stimuli, which include neighboring cells, extracellular matrix, soluble factors, and physical factors. In embryonic development, for example, many cell types come into close approximation with one another and communicate towards establishing their final identities. Biofabrication methods can serve to deploy spatially and temporally specified biomarkers for stem cells on a microscale *in vitro* platform at interim stages of development to identify stem cells and determine their state of differentiation.

1.3 In Vitro Drug Metabolism Models

1.3.1 NASA's Interest in an *In Vitro* Platform for Studying Drug Metabolism in Planetary Environments

NASA's exploration of space, the solar system, and beyond will invariably expose biological systems to hostile space and planetary systems for prolonged periods. Novel combinations of stressors and selective pressures will affect all life that has originated from this planet. However, cells respond to the environment in specific and reproducible ways that are often predictive of functional consequences, and, as bioreporters in space, can provide an assessment of combinatorial outcomes from numerous simultaneous environmental factors. Moreover, multiple events may be probed at the organism, organ, tissue, cellular, genetic, and molecular level, enabling a comprehensive assessment of potential synergistic stressor effects.

NASA's interest in microfluidic technology originates in the enabling microscale capabilities to significantly influence the design and implementation of modern bioanalytical systems due to the fact that these miniaturized devices can integrate multiple chemical processing and handling steps in a much more efficient way than conventional instruments. This results in several advantages including reduced reagent volumes, fully automated biochemical analyses, parallel processing capabilities for system redundancy, and remote operation. These properties greatly enhance the value of microfluidic systems to NASA for use on small aircrafts with limited resources for long duration manned and unmanned environmental monitoring missions.

The conducted collaborative research herein between NASA-JSC, Kansas State University, and Drexel University, is specifically intended to explore the development and study of a space flight-suitable *in vitro* three-dimensional Microfluidic Microanalytical Micro-organ Device (3MD) for simulation of human response to drug administrations and toxic chemical exposure under microgravity and space environments. A schematic of the multi-chamber drug metabolism device is shown in Figure 1-2 below in which a non-fluorescent pro-drug is fed into the microfluidic circuit towards the first liver chamber where the drug is metabolized (either activated or deactivated) to a metabolite that can subsequently exert an effect on a downstream epithelial target tissue.

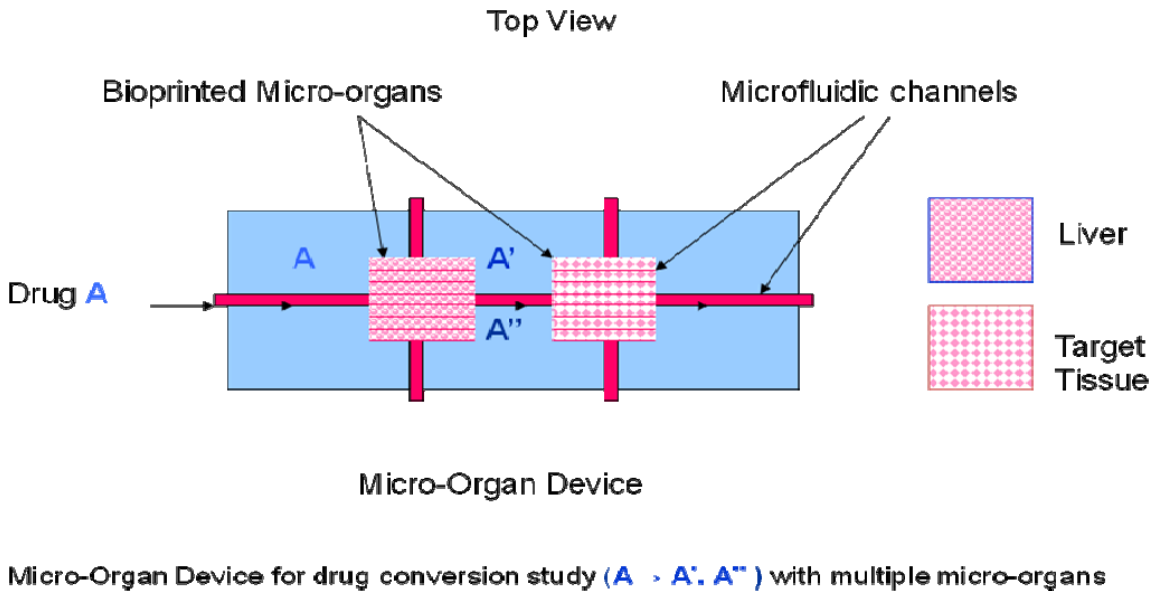

Figure 1-2: Schematic of multi-compartment micro-organ device for drug metabolism studies

1.3.2 The Biopharmaceutical Industry and the Drug Development Process

In recent years, the research and development process in the biopharmaceutical industry sector has become increasingly complex and costly. Clinical trials in particular have become increasingly complicated for a variety of reasons, including difficulty recruiting and retaining volunteers, increasingly complex diseases being studied, and more testing against comparator drugs. As the complexity of the process has increased, so have the associated costs. The trend towards increasing costs is shown in Figure 1-3.

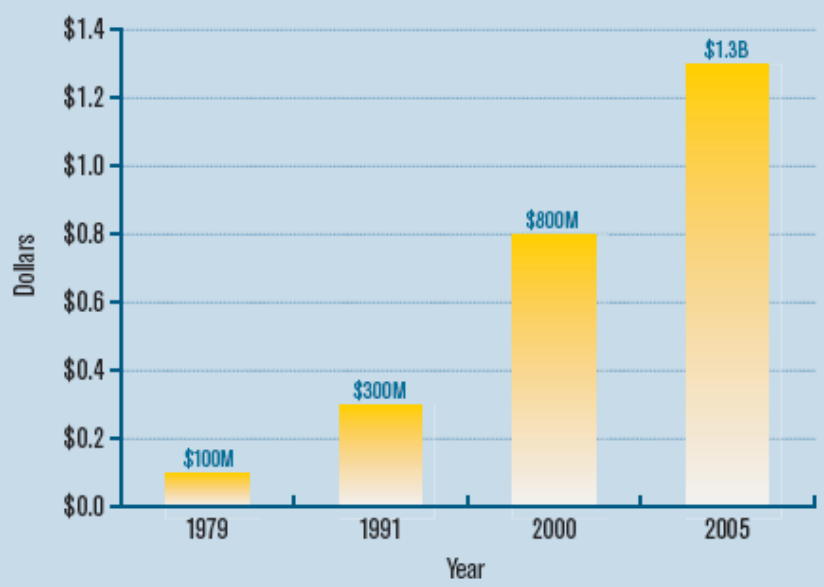

Figure 1-3: Cost to develop an approved drug for the marketplace

On average today, companies spend an estimated $1.3 billion on R&D over a 10-15 year span for each approved drug (Dimasi et al., 2003, Dimasi et al., 2007). Approximately half of this investment takes place during the preclinical testing phases, while the balance is invested during clinical studies. A diagram of the R&D process from drug discovery to FDA approval is depicted in Figure 1-4.

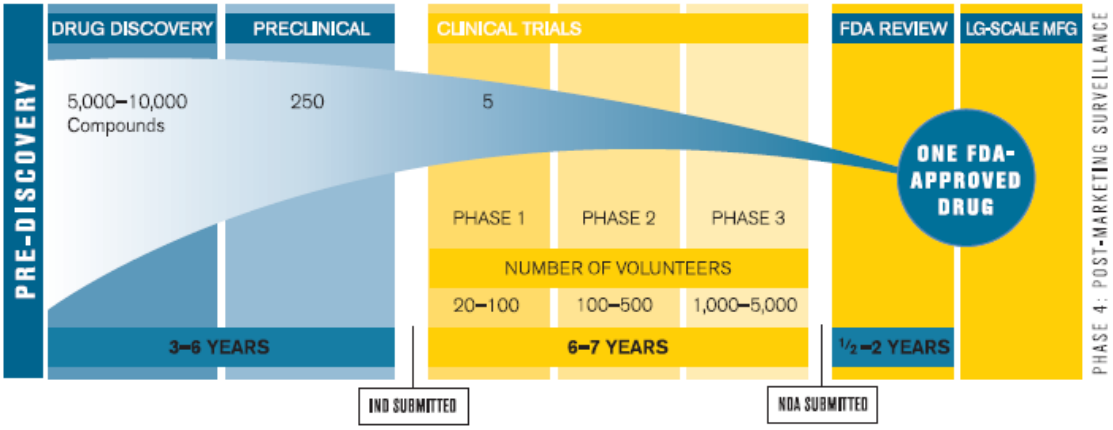

Figure 1-4: The R&D process from drug discovery to approval

Once a compound has demonstrated some activity against the drug target, it undergoes extensive testing in the lab, both in test tubes and animal models. Years of preclinical testing must establish that the candidate medicine is likely to be safe and effective in humans before clinical testing can begin.

Now, since the liver organ is primarily responsible for drug metabolism and detoxification in the human body, the pre-clinical stage of the drug testing and development process typically includes a panel of *in vitro* liver toxicology screens followed by extensive studies in live animals for predicting the pharmacodynamic and pharmacokinetic properties of a new chemical entity or drug. Current methods for evaluating the acute and chronic toxicity of a substance are performed primarily on live animals in which chronic liver toxicity studies are performed over long periods from several months to several years by controlled daily injection of toxic substances that may induce suffering in the animal. The justification for conducting comprehensive liver toxicity studies is the liver's continuous exposure to an array of exogenous substances or

insults. Therefore, a prominent function of the liver is to control the biotransformation and the elimination of toxic waste substances from the body. The liver receives dual blood supply from 1) the gastrointestinal tract via the portal vein and 2) the systemic circulation via the hepatic artery, thereby leaving the liver uniquely susceptible to both acute and chronic injuries. In fact, idiosyncratic drug-induced liver toxicity is the leading cause of post-market drug warnings and withdrawals, despite extensive animal testing (Kaplowitz et al., 2005). This can be explained by the inherent complexity of the body along with a significant number of uncontrolled parameters related to the animal model, resulting in challenges in interpreting *in vivo* analysis that takes into account various undefined or unknown effects, including but not limited to individual variations in the human drug pharmacokinetic response related to genetics, pathophysiology, and environmental factors. The need for an appropriate and predictive *in vitro* preclinical drug evaluation is highlighted by the fact that around 50% of the drugs found to be responsible for liver injury during clinical trials do not render any liver damage in animal experiments (Venkatesh et al., 2000). Consequently, there is a need for an *in vitro* modality to predict both acute toxicity and chronic toxicity owing to repeated exposures to low doses as well as mixtures of compounds in the liver. To address this unmet need for a predictive drug screen, several pertinent *in vitro* physio-toxicological models have been proposed (Baudoin et al., 2006). However chronic toxicity studies using *in vitro* conventional culture on a two-dimensional monolayer are limited in the fact that studies can only be evaluated over a few days as these cellular models cannot preserve liver-specific function for prolonged periods, but rather undergo cell de-differentiation.

However, nearly 90% of the lead candidates identified by existing *in vitro* screens fail to become drugs resulting in an unmet need for systems that are more predictive of the *in vivo* metabolism and toxicity profile of the drug for longer duration studies (Sivaraman et al., 2005). Thus, the challenge of and pre-requisite for a good predictive screen is the preservation of liver functions in culture over long time periods in order to build adequate models for drug screening and development.

In configuring predictive *in vitro* liver systems, hepatocytes (i.e. the primary parenchymal cellular component in the liver) are the primary cell type or common choice for constructing drug screening assays. Cytochrome P450 (CYP) represents the family or complex of enzymes primarily responsible for drug detoxification in the liver. Among the CYP families, CYP1, CYP2, and CYP3 family are the ones involved in drug metabolism. The CYP catalyzed oxidation-reduction drug reactions results in the addition of OH, NH_2 or COOH groups to the molecules (i.e. Phase I of biotransformation). These transformations increase the solubility of the molecules for its future elimination. However, in some cases, CYPs also activates prodrugs or procarcinogens which become toxic through this reaction. Since drug biotransformation that involves a set of Phase I (cytochrome P450 mediated) and Phase II enzyme reactions can affect the overall therapeutic and toxic profile of a drug, several pertinent *in vitro* models have been proposed to understand and mimic *in vivo* drug biotransformation as detailed in the following section on the state-of-the-art of *in vitro* drug screening assays (Baudoin et al., 2006).

1.3.3 Current Status of Drug Screening Assays

In vitro models of the liver have been used as screens for making quantitative and qualitative measurements of pharmacodynamic and pharmacokinetic properties of the candidate drug during the pre-clinical screening stage of the drug development process as well as for bioartificial liver support systems (Davila et al. 1998, Brandon et al., 2003). However, the development of *in vitro* liver cell models in extended culture that stably express functional properties of the *in vivo* liver from which the cells are derived represents a monumental challenge for predicting toxicity of drugs or chemicals. A number of *in vitro* liver culture formats have been developed to replicate the *in vivo* liver biotransformation functions. Among these culture systems are isolated perfused livers, liver tissue slices, primary hepatocyte cultures, immortalized cell lines, and intracellular or subcellular fractions such as microsomes. The advantages of the isolated perfused liver model is that it closest resembles the native *in vivo* liver cell polarity with a three-dimensional histology and three-dimensional architectural organization with a close approximation of *in vivo* drug metabolizing enzyme expression with a full complement of the drug metabolic equipment. The limitations of the isolated perfused liver model is that it is difficulty in sourcing human liver organs, lack of high-throughput capability, and liver function is only transiently preserved (Lee et al., 2008, Brouwer et al. 1996). Next, the advantages of an *in vitro* model implementing liver tissue slices include the *in vivo* like liver architecture and expression that typify the isolated perfused liver model along with improved high-throughput capability and availability over that of whole liver organs. The limitations associated with liver tissue slices include short-term liver-specific

function and viability in addition to the frequent occurrence of necrotic cells at the edges of the liver slice, i.e. diffusional barriers (Catania et al. 2007, LeCluyse et al., 2001, Lerche-Langrand et al., 2000). Now, many *in vitro* drug metabolism model systems to date have implemented liver cells or hepatocytes since hepatocytes represent 70-80% of the total liver cell population and express most xenobiotic metabolizing enzyme activities. For primary hepatocyte cultures, the advantages include ease of use and differentiated function can be maintained in many short-term and some long-term cultures. The deficiencies of primary hepatocyte culture formats include the loss of drug metabolizing enzyme activity in long-term culture and often require specially tailored media supplementation in culture due to the propensity for changes in the fidelity of drug metabolic activity after removal of hepatocytes from the liver organ (LeCluyse et al., 2005, Cross et al., 2000). In the case of immortalized cell lines, the key strengths include unlimited availability with prolonged subculture and drug metabolic functions have been maintained by researchers. The limitations of cell lines include the lack of diversity in the in vivo phenotype and a narrow spectrum of gene expression (Yu et al. 2001). Finally, an example of a subcellular source for *in vitro* liver systems are the liver microsomes which offer the advantage of high-throughput capability and whose Phase I enzyme expression can be maintained. The limitations include the lack of diversity in liver-specific functions due to the absence of dynamic gene expression and the intact cellular machinery required for toxicity testing. Of the culture format alternatives, primary human hepatocytes represent the most pertinent high-throughput model for *in vitro* drug metabolism since they express most of CYP isoforms, but demonstrate limited growth activity and early

phenotypic alterations symptomatic of mammalian primary cultures. Immortalized liver cell lines, however, primarily originate in liver tumors and therefore endowed with an indefinite capacity for proliferation. While liver cell line do lack a variable and substantial set of liver-specific functions including the major CYP related-enzyme activities, human hepatoma (e.g. HepG2) cell lines do contain some of the CYP isoforms essential for *in vitro* drug metabolism studies and affect the overall therapeutic and toxic profile of a drug. While a variety of modifications to conventional cell culture methods have been proposed to foster retention of hepatocyte function at desired *in vivo* levels, including the use of co-culture formats to simulate heterotypic interactions, this thesis will strictly use the HepG2 liver cell line as the most suitable cell source or culture format due to ease of handling and propagation.

A major challenge with cell-based *in vitro* culture formats for drug metabolism studies is that liver cells rapidly lose liver-specific functions when maintained under standard *in vitro* static two-dimensional cell culture conditions (Lecluyse et al., 1996, Baker et al., 2001). Therefore, many approaches have been proposed to preserve the liver functions for extended times in order to construct adequate long-term *in vitro* drug metabolism study platforms. One approach for the enhancement of liver-specific function such as drug metabolization is the judicious selection of an appropriate biomaterial with key extracellular matrix components amenable for optimal culture on single-layer basement membrane gels (Lecluyse et al., 1996, Shuetz et al., 1988, Ben-Ze'ev et al., 1988). Specifically, Shuetz et al. observed that compared to rat hepatocyte culture on type I collagen, incubation of hepatocytes on the reconstituted basement membrane Matrigel

results in the maintenance of hepatocyte morphology and adherence and liver-specific gene expression for more than 1 week *in vitro*. Moreover, Ben-Ze'ev et al. showed that rat hepatocytes cultured on Matrigel resulted in the formation of spherical cellular aggregates that exhibit low DNA, cytoskeletal mRNA, and protein synthesis while simultaneously exhibiting elevated liver-specific mRNAs and albumin production, thereby conforming closely to the *in vivo* liver gene expression program. Additionally, modulating the hepatocyte microenvironment by overlaying collagen gels on top of monolayer cultures, i.e. collagen gel sandwiches, has managed to upregulate liver-specific function sustained over a month period (Dunn et al., 1989, Chen et al., 1998). Specifically, Dunn et al. cultured rat hepatocytes in a collagen sandwich system and maintained normal morphology and physiological rates of liver-specific function for at least 42 days. The same hepatocytes cultured on a single layer of collage gel ceased to express liver-specific function within 1 week, only to recover function with an overlay of a second collagen gel layer. Chen et al. conducted a long-term primary human hepatocyte culture by first maintaining cells on a Matrigel matrix and then transferring to a collagen sandwich gel. These cells maintained the liver-specific ability to secrete albumin, alpha-fetoprotein, and transferring up to a maximum of 5 months. In an additional functional enhancement, Kono et al. demonstrated upregulation of cytochrome P450 activity with the presence of structures resembling in vivo bile caniliculi that exist on the apical side of liver plates (Kono et al., 1997). In order to study the effects of intercellular contacts between hepatocytes on liver-specific function, Abu-Absi et al. cultured hepatocytes to form solid multicellular spheroids possessing tight junctions and micro-villi lined

channels containing bile (Wu et al, 1999, Abu-Absi et al. 2002, Koide et al., 1990, Peshwa et al. 1996). This configuration resulted in the maintenance of liver-specific functions overall several weeks compared to the non-aggregated counterpart, including higher albumin secretion, urea excretion, and cytochrome p450 activity. Another approach utilized to enhance liver-specific function *in vitro* is to recapitulate the heterotypic interactions with co-culture configurations with either non-liver-derived stromal-like cell types on static or perfused two-dimensional substrates (Bhatia et al., 1997, Donato et al., 1990, Gugen-Guillouzo et al., 1983, Khetani et al., 2004, Gebhardt et al., 1996). Bhatia et al., for example, has co-cultivated hepatocytes with fibroblasts using a versatile technique for micropatterning based on existing strategies for surface modification with aminosilanes linked to biomolecules and facile manipulation of the serum content of cell culture media, and shown this culture format to support enhanced liver functions *in vitro* whereby the fibroblasts modulate and stabilize liver function through direct intercellular contacts. Therefore, while the functional relevance of extracellular matrix, cell morphology, and the orchestration of homotypic and heterotypic intercellular contacts is well-accepted, microfabrication tools are only recently emerging to manipulate these tools *in vitro*. Another approach adopted by Mitaka et al. is the development of culture conditions to promote liver characteristics, specifically the addition of exogenous compounds using nutrient-rich medium with 2% DMSO induces proliferating hepatoytes to recover the hepatic differentiated functions with maintenance of function for an extended period (Mitaka et al., 1994). In another modification, culture of cells in a variety of bioreactors employs hydrodynamic flows and fluid handling that

take into account the dynamic effects and transport of media rich in oxygen and nutrients (Bader et al., 1994, De Bartolo et al., 2001, Surapaneni et al., 1997). Nussler et al. designed a hollow fiber bioreactor culture model in order to confer improved metabolic capacity of hepatocytes *in vitro* over a two-week study period (Nussler et al., 2001).

Modifications of traditional culture formats allows *in vitro* liver systems to capture some aspects of in vivo liver physiology, including the appropriate cell interactions, aspects of liver architecture and microenvironment, and fluid flow stresses required to achieve the full spectrum of drug metabolic function. Nevertheless, the primary attributable metabolic or biotransformational function of the liver can as yet be mimic desired *in vivo* levels, prompting continued development of novel culture methods and high-fidelity drug testing platforms. In order to recreate the *in vivo* microenvironment in an *in vitro* liver tissue culture system, it is vitally important to firstly understand the structure and physiology of the liver which confer upon it the distinction as the ideal drug biotransformation organ. Specifically, in the *in vivo* milieu, owing to the close spatial configuration of cells and matrix, the cellular phenotype and viability of the liver cell is influenced by the environment, either by paracrine effects of secreted soluble factors, or by direct cell-matrix and cell-cell interactions, and mechanico-chemical stimuli arising from local perfusion flows.

1.4 Development of a Novel Direct Cell Writing Biomanufacturing System

A proprietary multi-nozzle direct cell writing (DCW) system has been developed at Drexel University for the freeform construction of biopolymer based three-dimensional tissue scaffolds and cell-embedded tissue constructs (Khalil et al., 2005, Khalil et al., 2007, Chang et al., 2008). The schematic of the direct cell writing system configuration is shown in Figure 1-5.

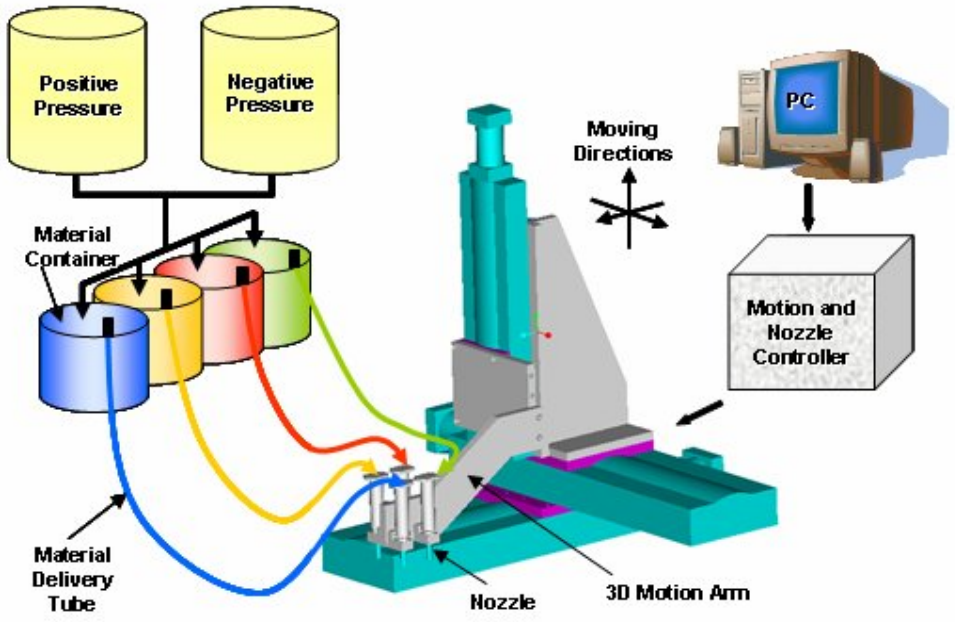

Figure 1-5: Schematic of the direct cell writing system

This direct cell writing process is designed to operate at cell-friendly conditions of room temperature and low pressure conditions to deposit multiple cell types and bioactive factors in controlled amounts with precise spatial positioning to form pre-designed, cell-

embedded tissue constructs with easily adaptable patterned architectures. These unique features of the cell printing system enable the direct printing of cells and biological substances along with the carrying material. Other layered manufacturing methods utilize harsh solvents, high pressures or temperatures, or post-processing methods that are not suitable for working with bioactive materials. Compared to most reported cell dispensing systems that are mostly limited to a single nozzle for cell dispensing or limited to cell printing, this multi-nozzle direct cell writing system as shown in Figure 1-6 enables the simultaneous deposition of cells, growth factors, and scaffold materials to form heterogeneous or functional gradient tissue structures.

Figure 1-6: Direct cell writing system with multinozzle capability

An information pipeline of the direct cell writing system for freeform fabrication of tissue constructs is presented in Figure 1-7.

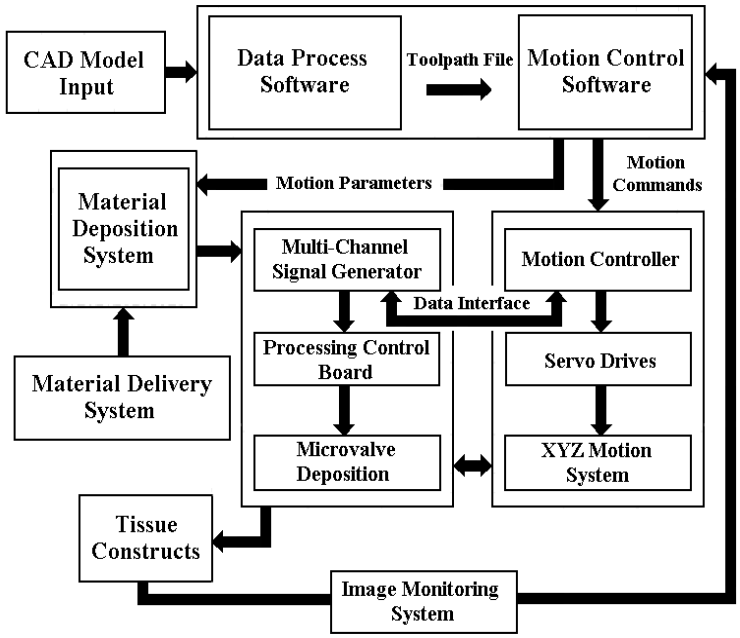

Figure 1-7: Process information pipeline for the direct cell writing biofabrication process

As shown in the figure, the data processing software processes the computer-aided design (CAD) model of the tissue construct and converts it into a layered two-dimensional process tool path. The motion control system is driven by a layered manufacturing technique. The material delivery system supplies various nozzles with the appropriate biopolymer or biological factor. The system consists of an air pressure supply both positive and negative, a material container or reservoir, and a material delivery tube. Each nozzle system has its independent process parameters and material properties adjusted as required such as the air pressure and biopolymer concentration. The system implements multiple nozzles with different types and sizes, thus enabling the deposition of specified

hydrogels with different viscosities for fabricating three-dimensional tissue constructs. Four types of the nozzles can be adapted to the direct cell writing system: solenoid-actuated nozzles, piezoelectric glass capillary nozzles, pneumatic syringe nozzles, and spray nozzles, with deposited diameter size ranges varying from 30 μm to 500 μm. The system can continuously extrude continuous hydrogel strands, or form hydrogels in single droplets with picoliter volumes.

In the development of the direct cell writing system, several micro-nozzle systems have been investigated to evaluate their performances and feasibility to deposit biopolymer solutions for tissue engineered constructs. The specific biopolymer deposition process performed in this study implements a pneumatic microvalve which is a typical mechanical valve that opens and closes the valve via an applied air pressure regulated by a controller detailed in Figure 1-8.

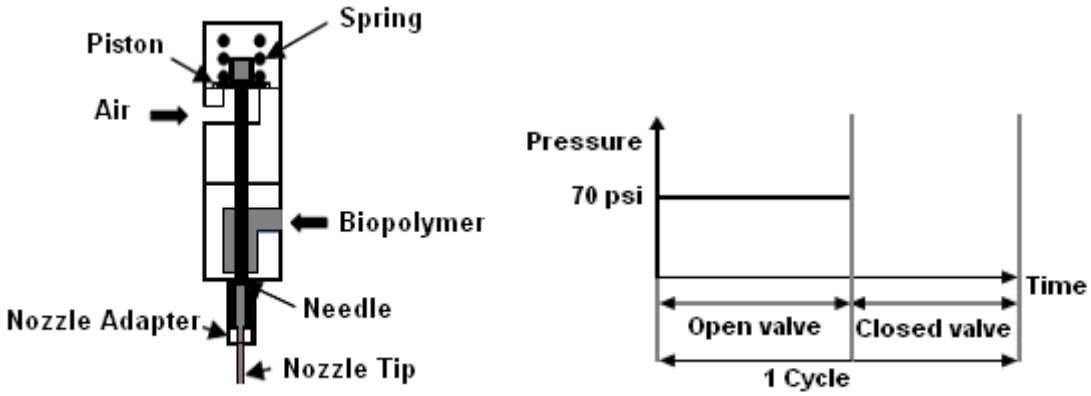

Figure 1-8: Pneumatic microvalve nozzle for direct cell writing. (a) Schematic diagram of the pneumatic microvalve; (b) Schematic diagram of the air control per cycle

The system is capable of operating in extrusion or droplet mode. In extrusion mode, the controller applies pressure to open the valve by lifting the piston against the spring that lifts the needle from the needle seat. The biopolymer material is then extruded from the nozzle tip under an applied pressure that is adjusted through the material delivery system. The extrusion is complete when the controller closes the valve by placing the needle back to the needle seat. The pneumatic microvalve can perform in droplet mode by repeating the continuous mode in a cyclic manner. Multiple pneumatic valves can be simultaneously operated for performing heterogeneous deposition in the development of the three-dimensional tissue constructs.

As a biomanufacturing technology, the direct cell writing system has been developed for the biofabrication of cell-integrated tissue constructs. This novel biomanufacturing technique is amenable for the demonstration of a predetermined engineering design of tissue constructs. The DCW system implements a sub-system to generate the two-dimensional toolpath from a solid scaffold model and to control the motion of the deposition nozzle, namely the two-dimensional toolpath generation and XYZ positioning system displayed in Figure 1-9 along with the motion controller software.

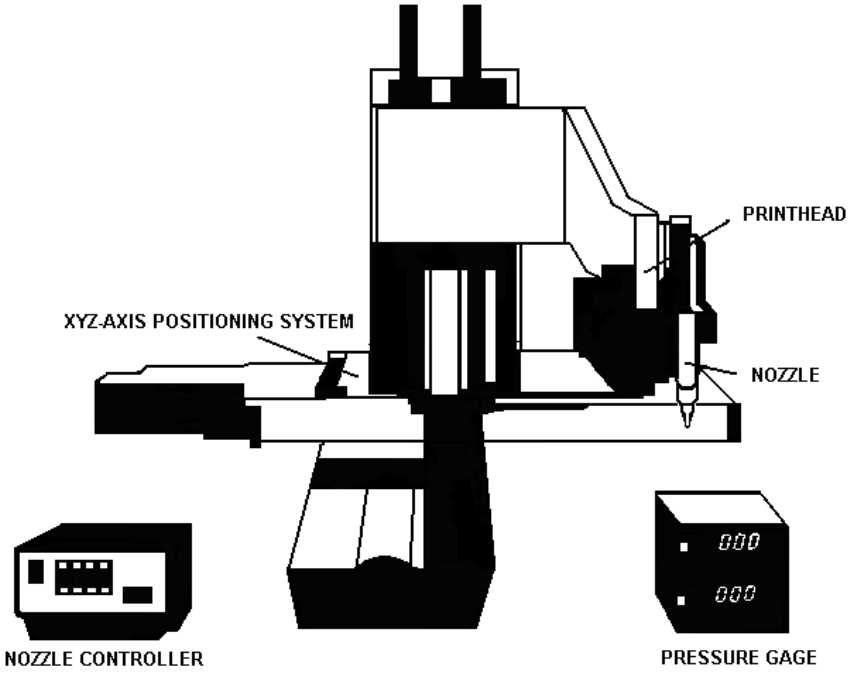

Figure 1-9: Schematic of XYZ-axis positioning system with nozzle pressure controller

The XYZ positioning system is a numerical control (NC) code driven system which drives the deposition nozzles according to the generated toolpath through motion controller software. The motion controlling component is a proprietarily developed software system used to control the speed, location, and movement of XYZ positioning system based on the generated toolpath.

Specifically, the toolpath generation starts with the conversion of a computer aided designed scaffold solid model into stereolithography (STL) format which is a common surface representation format in which the boundary of the object is formed from triangles. Following the format conversion, using commercially available Quickslice software, this STL model is divided into layers, and subsequently each layer is

translated into a toolpath, a single line which doubles back on itself repeatedly to form parallel paths, or multiple tool paths if the layer is discontinuous. Figure 1-10 illustrates the steps for the scaffold design toolpath generation.

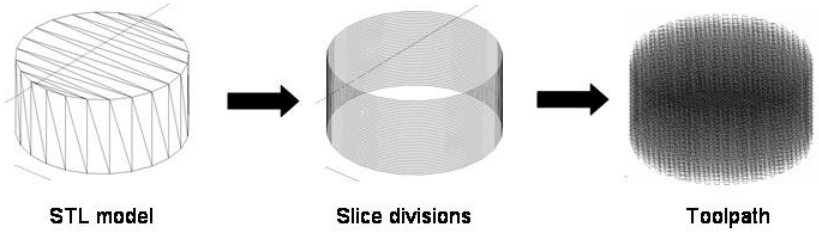

Figure 1-10: Division of STL model into layered toolpath

The variables predetermined by the toolpath are the pore size which is the distance between two parallel lines of the toolpath and the layer height. The pore size is the primary determinant of the porosity, and the layer height represents the diameter of the strut being deposited, which is itself contingent upon nozzle size, material deposition condition, and the lateral speed of the positioning system.

1.5 Research Objectives and Approach

This thesis rests on the hypothesis that the higher order functions of the liver, in particular the drug metabolic capacity, may be optimally simulated in an *in vitro* culture if critical facets of the *in vivo* microenvironment are recapitulated. These include the *in vivo* three-dimensional microenvironment and shear-mediated microfluidic perfusion flows. Therefore, the objective of the conducted research is aimed at the design, modeling, fabrication, and characterization of a three dimensional microfluidic

microanalytical micro-organ (3MD). The scope of the research includes the achievement of high-throughput reproducible fabrication of bioprinted tissue constructs, maintenance of tissue structural integrity, direct integration with the microfluidic platform, and enhancement of cell viability and control of cellular-level differentiation and tissue-level function. The applied rapid prototyping technology presented is a structurally and biologically viable syringe-based direct cell writing (DCW) process for layer-by-layer fabrication of three-dimensional cell-encapsulated hydrogel-based tissue constructs. More specifically, the objective is to develop a viable direct cell bioprinting process for fabrication of reproducible three-dimensional cell-encapsulated alginate-based tissue engineered constructs within three-dimensional tissue chambers as a drug metabolism model. This strategy can be further exploited to fabricate various three-dimensional *in vitro* tissue analogs consisting of an array of channels with tissue-embedded chambers representing different mammalian tissues for a multitude of applications for clinical pharmaceutical screening efficacy and toxicity for the agent of interest.

The conducted collaborative research between NASA-JSC, Kansas State University, and Drexel University, supported through NASA USRA subcontract #09940-008, is intended to explore the development and study of an *in vitro* three-dimensional microfluidic microanalytical micro-organ Device (3MD) for simulation of human response to drug administrations and toxic chemical exposure under microgravity and space environments. By fabricating a three-dimensional *in vitro* tissue analog consisting of an array of channels with tissue-embedded chambers, one can selectively biomimic different mammalian tissues for a multitude of applications, foremost among them liver

tissue for experimental pharmaceutical screening of drug efficacy and toxicity. The objective of research conducted at Drexel University is aimed at the achievement of high-throughput reproducible fabrication of bioprinted three-dimensional tissue constructs into microscale tissue chambers, maintenance of structural integrity, and integration with a microfluidic platform, and enhancement of cell viability and cell phenotype retention. Specifically, specific objectives of this thesis are:

1) to develop the methodology for combining biofabrication with microfabrication to create a microfluidic/microanalytical device for drug metabolism study

2) to develop an optimized biomanufacturing process for reproducible cell-encapsulated three-dimensional structures towards the study of drug metabolism

3) to optimize material/culture conditions for liver cell viability and cell-specific function towards the study of drug metabolism

4) to study the underlying scientific and engineering basis of micro-organ drug metabolic conversion as a function of microfluidic flow pattern design and flow conditions

1.6 Thesis Outline

Chapter 1 introduces the field of biomanufacturing and reviews some of the novel biomanufacturing techniques that encompass a broad range of physical, chemical, biological, and engineering processes, with various applications in tissue science and engineering. Specific emphasis is placed on solid freeform fabrication techniques for

layered biomanufacturing of tissue scaffolds or constructs. Chapter 1 also discusses the application of tissue engineering to *in vitro* physiological models such as biosensors, biological phenomena and diseases processes, with a particular emphasis on *in vitro* drug metabolism models. NASA's interest in such *in vitro* drug metabolism models in space is discussed along with a review on the advantages and limitations of existing platforms for evaluating the behavior of new chemical entities in drug development. This establishes the need for a novel biofabrication system, i.e. the development of the direct cell writing system for reproducibly manufacturing high-fidelity, high-throughput, three-dimensional microscale cell-embedded tissue constructs for the application of drug metabolism studies. Chapter 1 concludes with the research objectives of this dissertation along with the approaches adopted. Chapter 2 explains the design of the three-dimensional micro-organ and microfluidic platform, initiated by a discussion on the key facets of the liver microenvironment that will serve as guiding principles for the design of the micro-organ device for drug metabolism studies. The chapter then proposes specific biopolymer materials as candidates for bioprinting liver micro-organs. Chapter 3 is focused on the biomanufacturing aspects of applying layered fabrication along with microfabrication methods for complete unit assembly of the micro-organ device. Next, Chapter 4 establishes science and engineering basis for the micro-organ device by numeric modeling of fluid dynamics and mass transfer effects of a continuously perfusing drug/media flow through a channel pattern defined by a bioprinted three-dimensional liver micro-organ that biomimicks the *in vivo* liver sinusoidal capillary architecture. Prior to conducting drug perfusion flow experimentation, Chapter 5 and Chapter 6 presents

prefatory data to serve as guideposts for the selection of appropriate parameters, materials, and culture conditions to optimize the drug conversion downstream dynamic flow studies of bioprinted tissue constructs. Chapter 5 specifically examines the effect of the solid freeform fabrication based direct cell writing process, focusing on specific key process parameters, on the viability of liver cells within alginate. Chapter 6, on the other hand summarizes preliminary static culture experiments on bioprinted tissue constructs to 1) validate the need for a three-dimensional microenvironment and 2) elicit the material parameters and nutrient media requirements favorable for optimal drug conversion. Finally, Chapter 7 summarizes the research conducted, concluding remarks, an enumerates the research contributions to the scientific and engineering community, and some suggestions for future work that can either further elaborate and extrapolate my research findings or adopt similar approaches and techniques for novel investigation.

CHAPTER 2. DESIGN OF THE THREE-DIMENSIONAL LIVER MICRO-ORGAN AND MICROFLUIDIC PLATFORM

2.1 Capturing Key Facets of the Liver Microenvironment in an In Vitro System

2.1.1 The In Vivo Liver Hepatic Architecture and Circulation Parameters

Figure 2-1 details the liver with a dual afferent blood supply where (1) the portal vein delivers nutrient rich, relatively deoxygenated blood from the pancreas and intestines to the metabolically-active liver, and (2) the hepatic artery which delivers oxygenated blood after branching off of the celiac axis of aorta that shares cascade arrangement with intestinal vasculature**.**

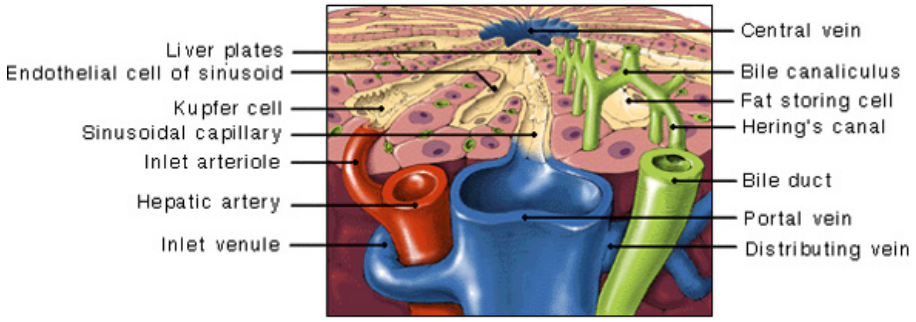

Figure 2-1: The dual afferent blood supply to the liver organ

Small portal venules receive blood from venous outflow of the GI tract by way of portal veins. Portal blood is collected from organs of the GI system and associated glands. The liver can modify the portal blood before it leaves for the systemic circulation. Collected blood flows into hepatic sinusoids (capillary-like) that lie among the hepatocytes and then into the central vein. The hepatocytes surround a central vein, so they are exposed continuously to portal venous blood. The central vein can in turn empty into the hepatic vein and then into the abdominal vena cava. Hepatic arterioles supply lobular tissue

directly with oxygenated blood or may empty into the hepatic sinusoids. The feature dimensions of the liver are shown below in Figure 2-2.

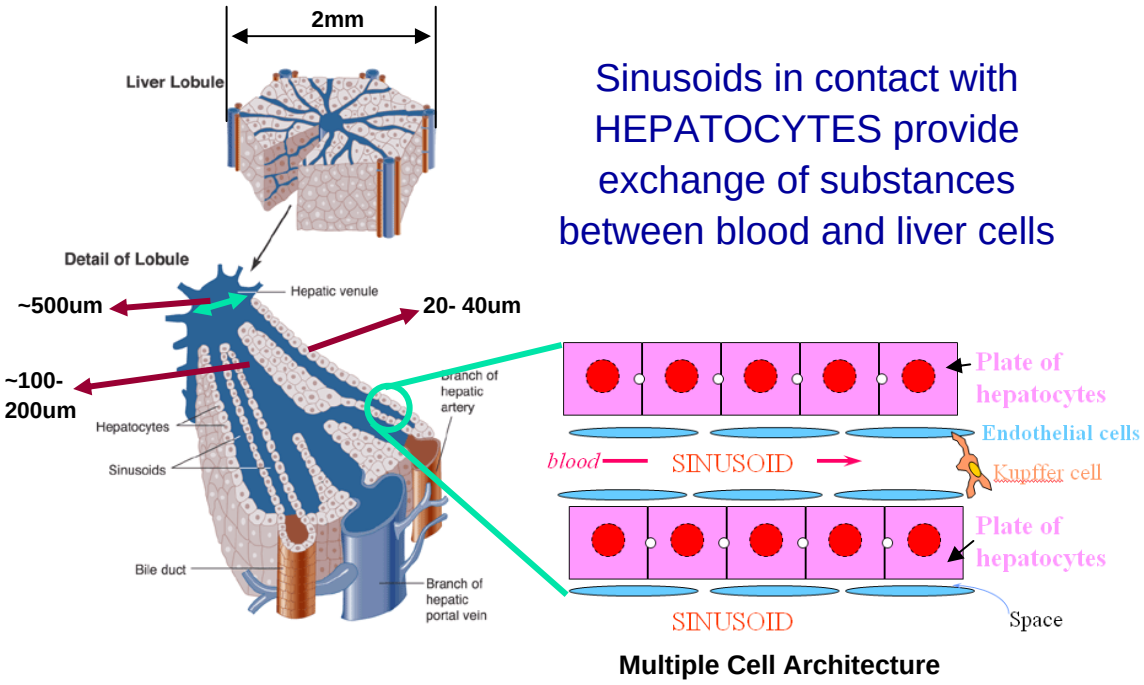

Figure 2-2: Feature dimensions of the liver architecture

This schematic of the liver microenvironment shows the spatial arrangement of cell types allowing both chemical as well as mechanical cues from each other and extracellular matrix facilitated by the flow through of blood. The venous sinusoids are lined by typical endothelial cells and Kupffer cells (macrophages, reticuloendothelial cells). The Kupffer cells can phagocytize bacteria and foreign matter in the blood. The endothelial cells have large pores. Between the rows of hepatocytes and the endothelial cells are narrow spaces, the spaces of Disse. The millions of spaces of Disse are connected with lymphatic vessels in the lobular septa. Excess fluid from the sinusoids passes through the pores of the

endothelial cells lining the sinusoids, into the space of Disse, and is removed through the lymphatics. Even large plasma proteins can diffuse through the endothelial pores into the space of Disse.

About 30% of the resting cardiac output flows through the liver. Blood flows from the portal vein to the hepatic sinusoids at a rate of 1100 ml/min, and about 300 ml/min of blood flows to the sinusoids from the hepatic artery. Therefore, 1400 to 1500 ml/min total blood leaves the liver via the hepatic vein. The resistance to blood flow through the liver sinusoids is usually low. Pressure in the portal vein entering the liver is about 9 mm/ Hg and pressure from the hepatic vein entering the vena cava is about 0 mm /Hg.

2.1.2 The In Vivo Functional Liver Unit Structural Organization

There are two main competing views of the structural organization of the fundamental functional unit of the liver—the lobule and the acinus as shown in Figure 2-3 below.

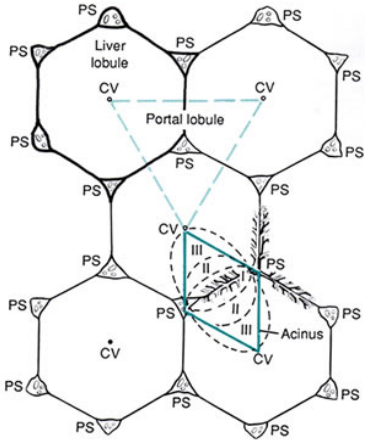

Figure 2-3: Competing views of hepatic structural organization

Both models possess a hexagonal tissue structure with the portal triads at the vertices and the central vein at the centroid. In Kiernan's proposed lobule model, the blood passes into the periphery from the digestive tract via the portal triad, traverses the sinusoid, and then exits via the central vein as depicted in Figure 2-4.

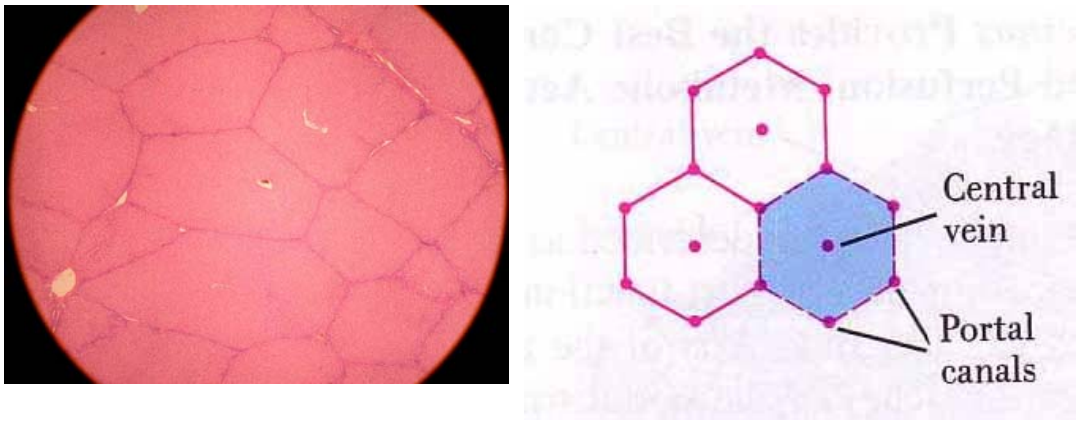

Figure 2-4: Liver lobule model

The portal triad is comprised of three vessels: the hepatic artery bringing oxygenated blood from the heart, the portal vein carrying enriched blood from the intestine, and the bile duct which drains bile from individual bile ducts. These inputs and outputs branch into complex tree structures, which supply and drain the entire liver.

Rappaport proposed the acinar model in 1954 based on the observation that as blood passes through the sinusoids, oxygen content and dissolved solutes are altered at different positions in the sinusoids by the hepatocytes which have contacted it. Consequently, the cell types in the liver represent a heterogeneous population of cells whose function differs relative to the composition of contacted blood. Therefore, the

acinus is subdivided into three zones graded by the depletion of oxygen and other metabolites in adjacent red blood cells as they travel the length of the sinusoid toward the central vein as shown in Figure 2-5.

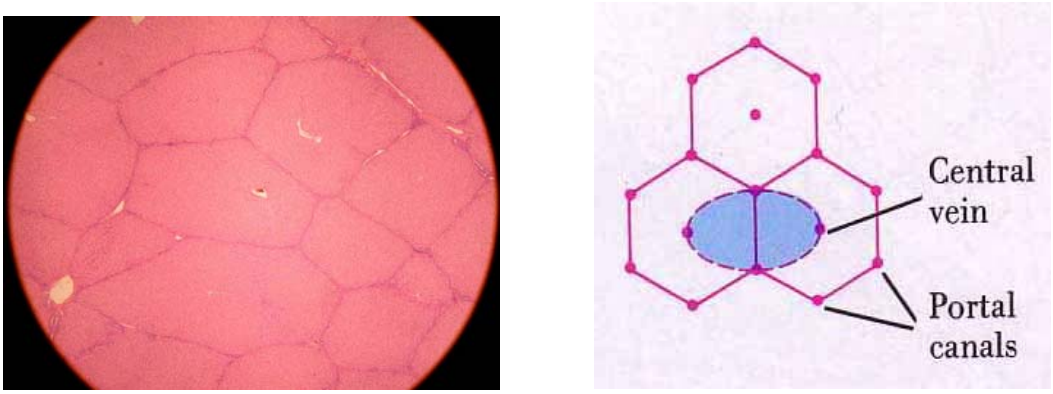

Figure 2-5: Liver acinus model

The hepatic acinus is diamond-shaped with borders defined by lines that connect the central veins of two neighboring classical lobules with two adjacent periportal spaces, functionally defined as the region that is irrigated by the terminal distributing branch of the portal vein that runs around the periphery of the lobule. Based on their proximity to the distributing veins, the cells in the hepatic acinus are subdivided into three zones I-III with the incoming blood passing through zone I first and continuing into zone II and III. The gradient for substances coming in with the blood (nutrients, oxygen, toxic substances) thus define functional differences among the hepatocytes in the different zones. Isolating a single sinusoid shows the fundamental unit of liver structure: a set of thin hepatocyte plates, called the acinus, strung between the portal triad and the hepatic venule.

These two models of the liver, though seemingly disparate, provide the foundation for current physiological models. Further research should result in a more definitive model for the architecture of the basic functional unit of the liver, but for the purposes of this research the liver will be viewed as a heterogeneous hexagonal tissue, which is a simplification and an incorporation of both theories.

Additionally the liver has an equally intricate organization on the cellular level that may be required to be replicated to achieve proper function. The acinus is organized in a perfused, spongelike, capillary bed structure, composed primarily of mature hepatocyte plates of a single cell thickness, known as the parenchyma. These plates have an apical domain which forms bile canalicular networks in the secretion of bile components and metabolites of xenobiotics, and a basal domain which interacts with ECM and participates in cell signaling. These hepatic plates are lined by fenestrated endothelial cells, which create a physical and chemical shield between the sinusoid and the hepatic plate. The region between the endothelium and the hepatic plate, known as the Space of Disse, is traversed by stellate cells, or the resident liver fibroblasts. Interspersed in the sinusoid are kupffer cells, a specialized form of macrophage. Fluid flows through two paths: the bulk travels “down” the acinus from the portal region to the central vein; hepatocytes also form ducts known as bile canaliculi that transport bile retrograde or “up” to the bile duct in the portal triad. These ducts are separated from the rest of the tissue by tight junctions between neighboring hepatocytes in a similar fashion to that of the digestive system.

Most *in vitro* experiments with adherent human cells are performed in conventional monolayer two-dimensional cultures in which cells are plated or seeded onto homogeneous polystyrene plastic substrates treated to simulate cell attachment and spreading. Depending on their type, cells either grow directly on the plastic, secrete ECM components that coat the plastic to facilitate cell adhesion, or require pre-coating of the plastic with ECM. Standard two-dimensional culture conditions are poor mimics of the cellular environment in an animal: soluble growth factors are present at abnormally high concentrations, three-dimensional cues are largely absent, oxygen tension is too high and cell-cell interactions are rarely organized. Therefore, conventional cell culture disperses tissues into single cells while neglecting higher-order processes. Attempts have been made to overcome these problems using organ culture and various laboratory-scale bioreactors, but microscale systems provide much more effective means of controlling cell environment *in vitro*. Particularly promising are various artificial organ systems in which multiple cell types are grown together under conditions that mimic normal three-dimensional environmental and circulatory cues. Microfluidics has the additional advantage of being capable of creating mechanical strain, through shear, in the physiological range. A microscale circulation-type bioreactor system enables the simultaneous evaluation of multiple specimens.

2.2 Material Considerations - Hydrogels

In the design of the three-dimensional liver micro-organ in this work, hydrogel biopolymers are selected as the material to effectively encapsulate hepatocytes within a three-dimensional matrix microenvironment. Hydrogels are either synthetic or naturally-

derived hydrophilic polymer networks that swell in the presence of water. Among numerous applications, hydrogels have been used for cell encapsulation since their mechanical properties resemble that of native soft tissues while intrinsically exhibiting high permeability to oxygen, nutrients, and other water-soluble metabolites. Additionally, hydrogels exhibit mechanical and chemical properties that may be engineered via addition of functional groups or modulation of degradation rates to manifest other desirable characteristics. As a result of this customizability, hydrogels have been widely used in tissue engineering and drug delivery applications.

Hydrogels have many different functions in the field of tissue engineering. They are primarly applied as delivery vehicles for bioactive molecules, and as three-dimensional structures that organize cells and present stimuli to direct the formation of a desired tissue. First of all, bioactive molecules are delivered from hydrogel scaffolds in a variety of applications including promotion of angiogenesis and encapsulation of secretory cells (Drury et al., 2003). Finally, hydrogel scaffolds are being applied to transplant cells and to engineer nearly every tissue in the body, including cartilage, bone, and smooth muscle.

In traditional tissue engineering, cells are seeded upon the surface of porous scaffolds and are induced to migrate and populate the inner regions. In many cases, cells do not evenly seed within the scaffold because of the large distances they must migrate in order to populate the scaffolds. Attempts have been made to homogenize cell seeding distribution through, for example, the application of centrifugal force to surface-seeded

scaffolds or the continuous perfusion of scaffolds with cell suspended solutions. These techniques require cumbersome equipment and have not been demonstrated for microscale scaffold constructs. In contrast, the techniques described here exploit the encapsulation of cells within hydrogel materials. The advantage of cell encapsulation to cell seeding in porous scaffolds for tissue engineering is the homogeneity of cell distribution that may be achieved. In cell encapsulation applications, cells are embedded within hydrogels by suspending the cell in a liquid hydrogel precursor, followed by crosslinking of the polymer network. In this way, uniformly-distributed hydrogel-encapsulated cells are required to migrate shorter distances during the subsequent remodeling of cells into tissue.

2.2.1 Alginate as Tissue Matrix Material

Alginates are naturally derived polysaccharides that are derived primarily from seaweed. They are composed of (1-4) linked β-D- mannuronic acid (M units) and α-L-guluronic acid (G units) monomers along the polymer backbone. The M and G units may vary in ratio depending on the alginate source. The alginate molecule is considered to be a block copolymer with regions of M and G units that both have carboxylic groups. The carboxylic groups are capable of forming salt formations such as sodium alginate, where the sodium monovalent ions are attached ionically to the carboxylic groups as shown in Figure 2-6.

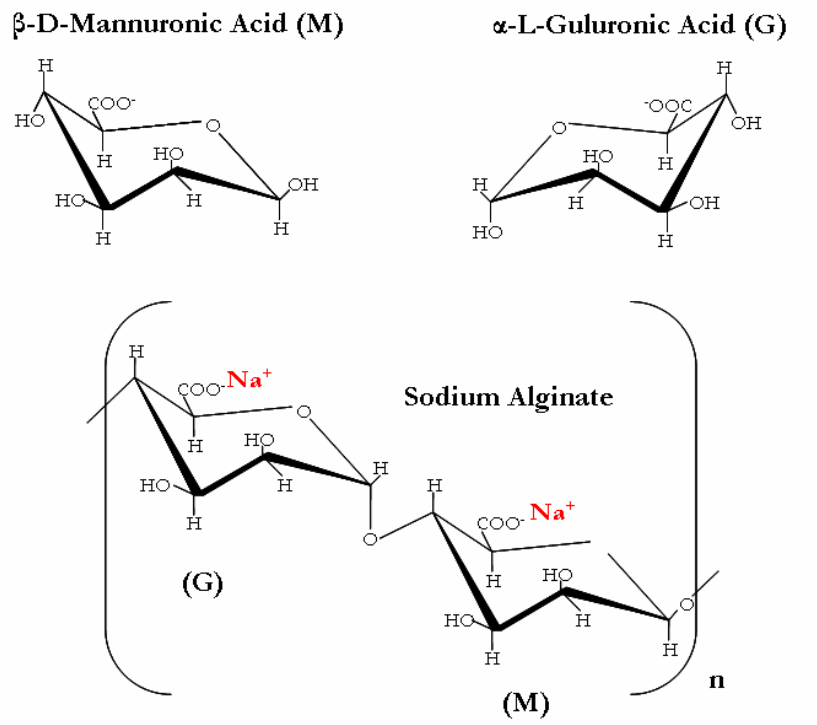

Figure 2-6: Chemical structure of sodium alginate biopolymer

Sodium alginate is soluble in water and when dissolved forms a viscous solution that could vary depending on the concentration and molecular weight of the biopolymer. In the presence of divalent calcium ions, sodium alginate solution is crosslinked ionically between chains to form a hydrogel. The calcium ions exchange with sodium ions on the G blocks and bind together adjacent chains that precipitate the gelation of alginate. It has been reported that ionically crosslinked alginates lose mechanical properties *in vitro* over time. It is presumed that this phenomenon occurs due to an outward flux of crosslinking ions to the surrounding medium (Shoichet et al., 1996). A study by Wang et al. is conducted to investigate the ability of rat bone marrow cells to proliferate and differentiate on alginates of differing composition and purity. It is found that high purity

and high G-type alginate retained 27% of its initial strength after 12 days in culture (Wang et al., 2003). The formation of alginate gels may take place in two known methods; diffusion setting and internal gelation. In the first, alginate solution such as sodium alginate is deposited directly in to a reservoir of divalent ions such as calcium chloride. The gelation process takes place as the calcium ions gel the outer most layer of sodium alginate and then diffuse into the core of the material to gel internally. In the later method, the process is vice versa where the calcium chloride solution is introduced into a reservoir of sodium alginate. The gelation in this method begins at the outer surface of the calcium chloride solution and then proceeds into the sodium alginate outer body. Both gelation methods have been used for various applications.

Tissue engineering biomaterials should fulfill several preconditions such as high level of biocompatibility and biodegradability. These are also required to have low degree of cytotoxicity, high affinity to biological surfaces, mechanical stability to the construct, and serve as a guide for three-dimensional tissue regeneration. Alginate is a nontoxic immunologically inert hydrogel and therefore has been widely used for scaffold material for immobilization of enzymes or cells for bioreactors, and also for tissue engineering. Alginate has been mainly utilized in tissue engineering as a delivery vehicle or supporting matrix cell via encapsulation techniques. Alginate-based microencapsulation is currently a favored approach because animal studies and small scale clinical trials have shown that the requirements for long-term immunoisolation and simultaneous maintenance of transplant function can most likely be fulfilled by this hydrogel (Leinfelder et al., 2003). Many groups have demonstrated various techniques

for producing alginate beads of controlled dimensions for cell encapsulation. The use of alginate in cell encapsulation requires the gel to be of high purity to exploit cytotoxic and apoptosis-inducing impurities. The purification and sterilization processes are time-consuming labor work that is accomplished by filtration techniques. Alginate degradation is not carried out by mammalian cell digestion, instead, divalent calcium ions slowly diffused out of the hydrogel allowing alginate molecules to be excreted in the urine. Alginate has been used extensively in the culturing of chondrocytes, as well as for hepatocytes and Schwann cells for nerve regeneration.

One of the drawbacks of alginate is that there is no specific interaction between mammalian cells alginate gel. That is, alginate does not directly provide active attachment sites for anchorage-dependent cells. In addition, a negative charge balance exists in alginate gels that inhibit protein absorption due to electrostatic repulsion. For this reason, many studies have modified alginate with peptides for cell adhesion. The carboxylic acid on alginate makes it attractive for modification such as in peptide attachments. For example, in a study by Kreeger et al., the roles of peptide density in alginate on murine granulose cell adhesion, morphology, and steroid secretion are conducted (Kreeger et al., 2003). Their results show that murine granusola cells attached and spread on the modified surfaces with morphologies specific to the peptide identity and density.

Several studies have emphasized the importance of maintaining hepatocyte cell lines in culture conditions that impose a three-dimensional architecture on cells, and have

highlighted the advantage of alginate encapsulation (Khalil et al., 2005). Compared with other matrix support systems or monolayer cultures, alginate encapsulated cells maintained significantly higher expression of differentiated function, and for many liver-specific products the synthetic capacity per cell performance was equivalent to that seen in vivo. Specifically, compared with cells in monolayer culture, alginate-encapsulated cells have an approximately 10-fold higher expression of a panel of protein synthetic and secretory functions, and an expression of cytochrome P450-mediated functions.

2.2.2 Matrigel as Tissue Matrix Material

Much effort in tissue engineering has focused on controlling the microscale environment of three-dimensional matrices. Recently, Matrigel has been a biomaterial of interest in certain applications for this purpose. Norman et al. studied the effects of discrete microscale structures (microrods) on cell proliferation in three-deimensional Matrigel gels (Norman, et al., 2008). Experimentally, 100 μm x 15 μm x 15μm (length x height x width) microrods fabricated out of SU-8 are incorporated into Matrigel seeded with fibroblasts. The results demonstrate that the three-dimensional microrod-Matrigel composite gels inhibit the proliferation of fibroblasts compared to cells seeded in Matrigel alone. Furthermore, it is determined that the suspended microrods can regulate cell proliferation in a dose-dependent manner. Advancements in this type of research will enable the development of a biocompatible system in which long term cell growth and proliferation can be modulated in three-dimensional cultures.

Another recent tissue engineering advancement by Wong and colleagues has utilized Matrigel for adjustable three-dimensional cellular microenvironments *in vitro* using microfluidics (Wong et al., 2008). More specifically, they have developed a method that allows controlled spatial distribution (patterning) of multiple types of cells within three-dimensional Matrigel gels along with the controlled application of gradients of soluble factors, such as cytokines, across the Matrigel constructs. Their technique uses laminar flow to divide a microchannel into multiple subchannels separated by microslabs of hydrogel, making it possible to design model systems to study cellular communication mediated by the diffusion of soluble factors within three-dimensional matrices. The authors suggests that their technique would be especially useful for studying cells such as those of the immune system, which are often weakly adherent and difficult to position precisely with standard cell culture systems.

In tissue engineering, Matrigel has also been used as a scaffold biomaterial. However, it is commonly believed that Matrigel "with the maximum thinkable likelihood, will never be granted (FDA) approval," and therefore, "is not a suitable option in human tissue engineering" (Polykandriotis et al., 2008). Despite this, the potential benefits of Matrigel as a scaffold/ECM material have continued to drive its use in the development of many tissue engineering organs *in vitro*. Matrigel has shown promise as a scaffold for vascular graft development (Abilez et al., 2006). Under pulsatile conditions, undifferentiated mouse embryonic stem cells (mESC) have been grown in three-dimensional Matrigel matrices. Recent efforts in the reconstruction of engineered uterine tissues (EUTs) have also utilized Matrigel. Epithelial cells were mixed with stromal cells

in a 1:2 collagen:Matrigel gel to form an endometrial layer on top of a smooth muscle layer (Lu et al., 2008). The epithelial cells showed self assembly in the EUTs, and the reconstructed EUTs demonstrated the ability to support the development of embryos. Three-dimensional pulmonary tissue constructs *in vitro* have also shown positive results using Matrigel. Three-dimensional FPC constructs were created using Matrigel and synthetic polymer scaffolds of poly-lactic-co-glycolic acid (PLGA) and poly-L-lactic-acid (PLLA) fabricated into porous foams and nanofibrous matrices (Modrinos et al., 2006). The experimental results demonstrated that the three-dimensional Matrigel constructs contained alveolar forming units with proper cellular ultrastructure, gene expression, and gene product. Furthermore, the addition of specific growth factors induced the formation of branching and sacculated epithelial structures similar to distal lung architecture *in vivo*. Matrigel matrices have also been explored as a method for tissue engineering cartilage implants using embryonic stem cells (Jukes et al., 2008).

Advancements in tissue engineering nerve cells have also benefited from the use of Matrigel. Laminin, an important component of Matrigel, promotes the attachment and growth of neurites *in vitro*, and seems a logical choice for nerve regeneration. Madison *et al* have shown that laminin-rich Matrigel enhanced sciatic nerve regeneration through biodegradeable nerve guide channels (Madison et al., 1985). Furthermore, Kjavin *et al.* has shown that laminin-containing gels, such as Matrigel, enhanced regeneration of mouse sciatic nerves within silicon tubular prosthesis compared to similar silicon tubes filled with collagen gel (Kjavin et al., 1991). Experimentally, when presented with two-dimensional PDL-adsorbed surfaces, three-dimensional Matrigel, and grooved

topography, neuritis preferred extending into the three-dimensional gel layers of Matrigel rather than along the PDL surfaces of the grooved topographical substrates (Li et al., 2008). The mechanical and dimensional properties of the matrix materials have been shown to be of great importance to the characteristics of the developed neurons. Experimentally, the stiffer three-dimensional matrix of collagen supported longer neurons than two-dimensional collagen matrices. However, softer three-dimensional Matrigel matrices supported shorter neurons than two-dimensional Matrigel matrices.

A recent effort in tissue engineering skeletal muscle tissue networks has used innovative techniques in controllable gel architecture and reproducible fabrication (Bian et al., 2009). This reproducible techniques involves injecting a cell/gel mixture composed of fibrinogen, collagen type 1, Matrigel at 10% (v/v) , C2C12 myoblasts, and primary rat skeletal myoblasts into a microfabricated PDMS mold. The research group claims that this approach produces relatively large skeletal muscle tissue networks made of viable, densely packed, highly aligned, cross-striated, and spontaneously contractile myofibers.

For liver tissue applications, Babensee et al. studied hepatoma cells (HepG2), an anchorage-dependent cell line, and microencapsulated them in a HEMA-MMA polyacrylate membrane to which the cells do not adhere (Babensee et al., 1992). This environment is altered by the coencapsulation of Matrigel, a reconstituted extracellular matrix derived from the Engelbreth-Holm-Swarm (EHS) mouse tumor basement membrane, to provide sites for cell attachment. The effect on the cells of these two capsule microenvironments during a 2-week *in vitro* culture period is assessed by

examining the spatial arrangement, morphology, and viability of the cells using light microscopy and scanning electron microscopy (SEM). In the absence of Matrigel, cells in HEMA-MMA capsules are found to form aggregates in intracapsular pockets with central necrosis occurring at day 7 in large aggregates. The coencapsulation of HepG2 cells with Matrigel, resulted in an initially uniform distribution of essentially individual cells with aggregates appearing later within the Matrigel. Many cells within these capsules had remained viable when examined up to day 14 with only limited cellular necrosis, implying a favorable environment for microencapsulated HepG2 cells.

CHAPTER 3. BIOFABRICATION OF THE THREE-DIMENSIONAL LIVER MICRO-ORGAN AND MICROFLUIDICS

There has been keen interest recently in microscale systems for cell culture because microsystems offer capabilities either unavailable or difficult to implement in conventional macroscale cell culture systems. For example, microscale tools enable more precise control of the microenvironment by allowing precise control of direct cell-cell interactions, cell-matrix interactions, soluble factors, and mechanical forces (Thomas et al., 2002, Chen et al., 1997, McBeath et al. 2004). Microscale cell cultures also support higher-throughput experimentation along with enabling integration onto a microfluidic chip for dynamic profiling assays. Specifically, the unique capability microfluidic technologies to miniaturize assays and increase experimental throughput have generated significant interest in the drug discovery and development domain.

This chapter therefore explores the development for the design and biofabrication of an *in vitro* three-dimensional microfluidic microanalytical micro-organ device (3MD) for simulation of the physiological human response to drug administrations and toxic chemical exposure. The applied solid freeform fabrication technology is a viable bioprinting freeform fabrication process for layer-by-layer extrusion of three-dimensional cell-encapsulated hydrogel-based tissue constructs. By fabricating a three-dimensional *in vitro* tissue analog consisting of an array of channels with tissue-embedded chambers, one can selectively biomimic different mammalian tissues for a multitude of applications for pharmaceutical screening of drug efficacy and toxicity. The research conducted is aimed at the achievement of high-throughput reproducible fabrication of bioprinted tissue

constructs and three-dimensional organ chambers, maintenance of structural integrity and direct integration with the microfluidic platform, and enhancement of cell viability and display of cellular-level differentiation and tissue-level function. More specifically, the objective is to develop a viable direct cell writing process for fabrication of reproducible three-dimensional cell-encapsulated alginate-based tissue engineered constructs within three-dimensional liver tissue chambers as a drug metabolism model. An overview of this biofabricated drug metabolism platform is show in schematic in Figure 3-1.

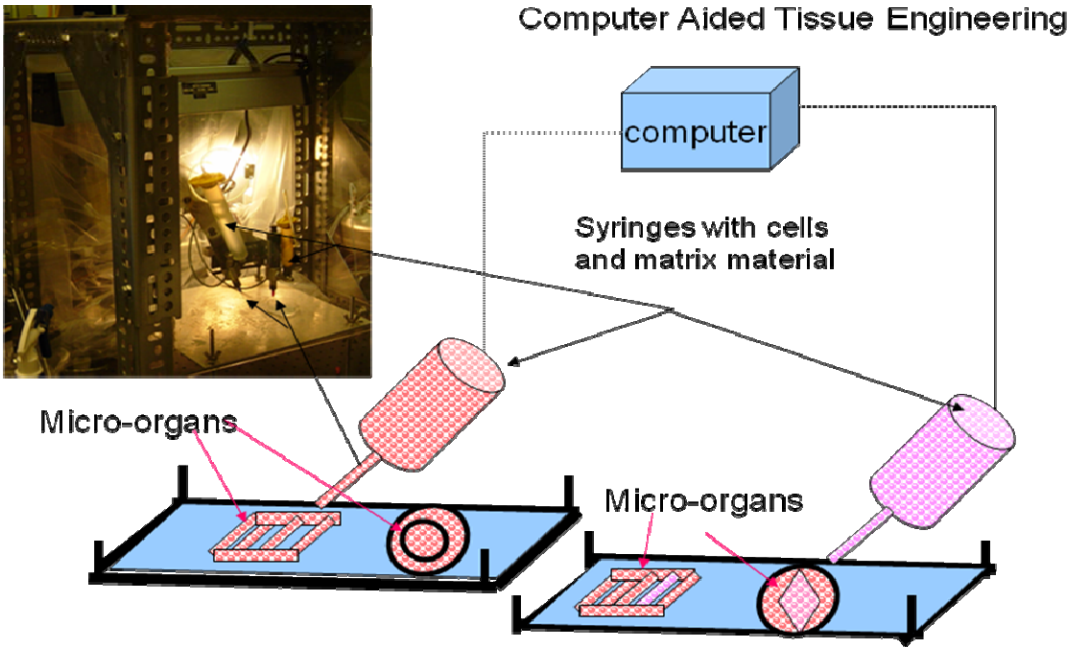

Figure 3-1: Overview of the biofabricated drug metabolism platform

3.1 Development of the Direct Cell Writing System for Freeform Fabrication of Cell-Laden Liver Tissue Constructs

In Chapter 1, the development of a proprietary multi-nozzle direct cell writing system is detailed for freeform fabricating biopolymer based three-dimensional tissue scaffolds and cell-embedded tissue constructs (Khalil et al., 2005, Khalil et al., 2007, Chang et al., 2008). However, it is the convergence of solid freeform fabrication (SFF) along with the enabling tools of microfluidics that is providing investigators with the emerging opportunity to biomanufacture and study tissues *in vitro* with heretofore unseen levels of sophistication. To give a sense of the length scales here, microfabrication techniques have traditionally been used in integrated microelectronic circuits. Now these techniques can be adopted to create microscale platforms that integrate cell, tissues, or whole animals onto a chip as shown in Figure 3-2.

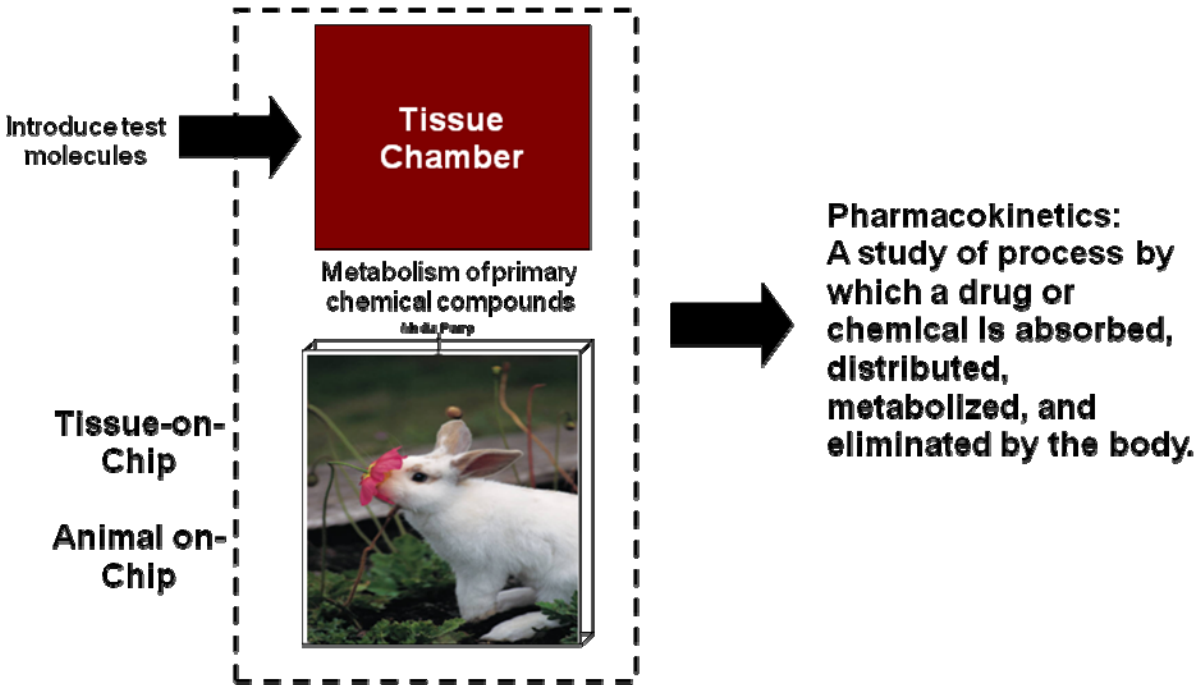

Figure 3-2: Schematic for the integration of biological tissues or whole animals onto a microfabricated device

Specifically, we are studying the liver, which is the primary organ responsible for the metabolic activities of the body. Therefore, modifications of these traditional techniques have been primed for these disciplines to work in concert for novel applications of tissue engineered liver constructs as shown in Figure 3-3.

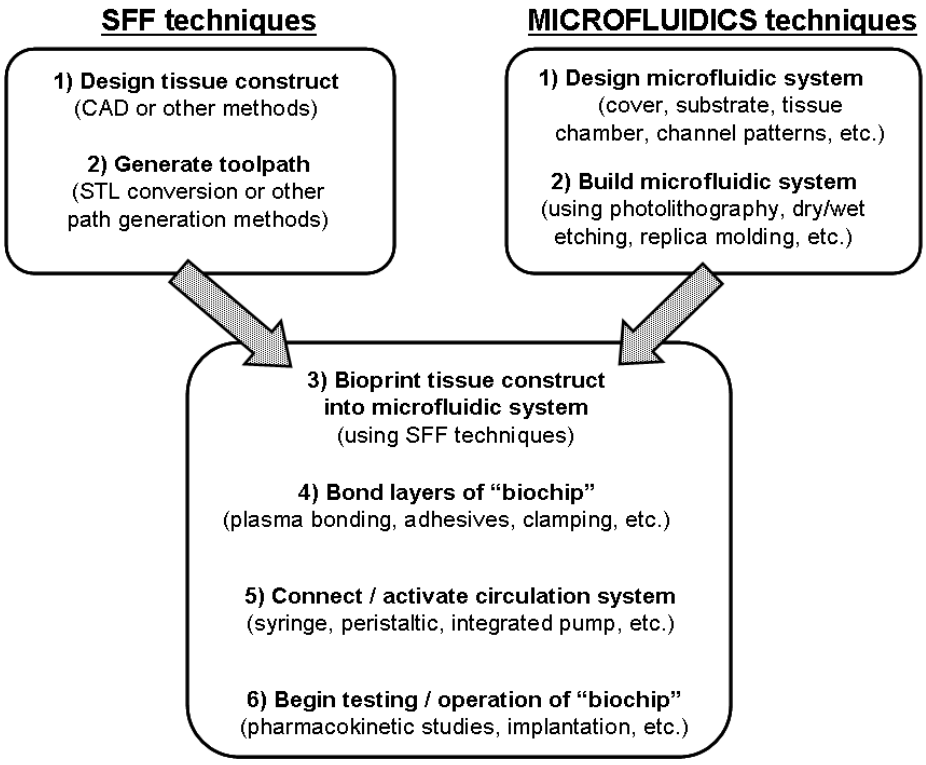

Figure 3-3: Convergence of layer-by-layer biofabrication and microfabrication techniques

The direct cell writing process is integrated with a microfluidic device to fabricate three-dimensional tissue/organ constructs/chambers in Figure 3-4, as opposed to producing two-dimensional cell monolayers.

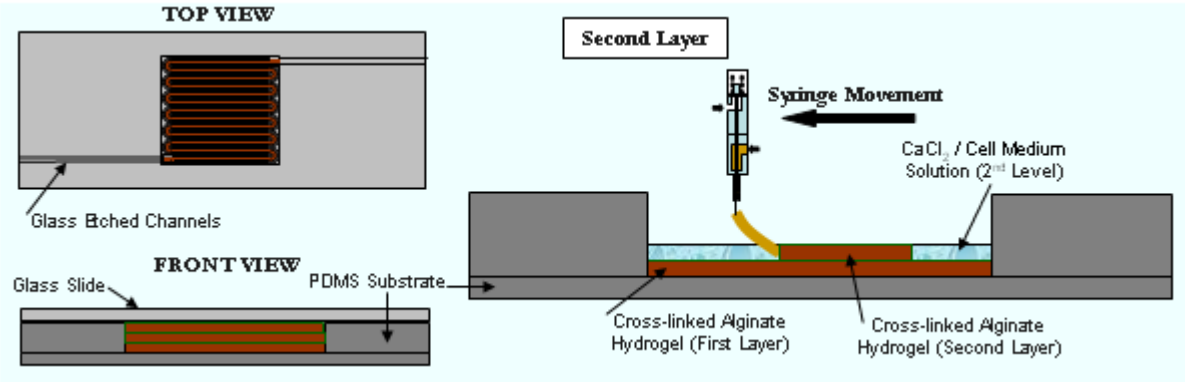

Figure 3-4: Overview of direct cell writing three-dimensional micro-organ approach

Biological studies reveal the unstable cellular phenotype and reduced tissue-specific gene expression with conventional monolayer *in vitro* culture techniques. A three-dimensional tissue model will, in contrast, foster improved retention of cell-specific function. Furthermore, direct cell deposition of encapsulated cells offers tighter control over the spatial distribution of cells, allowing one to assemble high cell density or co-culture multiple cell types within a three-dimensional construct. This can create tissue structures that more closely resemble the *in vivo* state. Cell-cell communication either from direct contact or paracrine signaling is important for proper cellular behavior, differentiation, and proliferation, along with the concomitant extracellular matrix produced by the neighboring cells. Furthermore, optimization of process parameters (e.g. nozzle pressure, motion arm velocity, nozzle tip size etc.) and material parameters (e.g. biopolymer viscosity, crosslinking agent concentrations, etc.) have been done to achieve high-fidelity three-dimensional structures and seamless integration onto a microfluidic tissue micro-organ chambers.

The first step in the biofabrication of the *in vitro* three-dimensional microfluidic microanalytical microorgan device is to establish the structural formability of liver cell-embedded tissue constructs through the direct cell writing process. A micro-scale tissue analog has been designed and fabricated for studying drug metabolism or its pharmacokinetic effects on secondary organ function via direct deposition of a three dimensional heterogeneous cell-seeded hydrogel-based matrix. First, cells were encapsulated within alginate hydrogels and bioprinted through the system into a desired pattern within the microfluidic circuits. For alginate-cell suspension, we used an air-actuated dispensing nozzle with a pre-specified internal diameter tip size. A 0.2 μm filter was attached to the compressed air cylinder. Prior to deposition, ethanol, filtered air, and deionized water were purged through the system. By integrating the bioprinting system with a CAD environment, notable feasibility and reproducibility of three-dimensional structures has been realized within micron-order dimensional specifications and hence can be used for parametric studies (Figure 3-5).

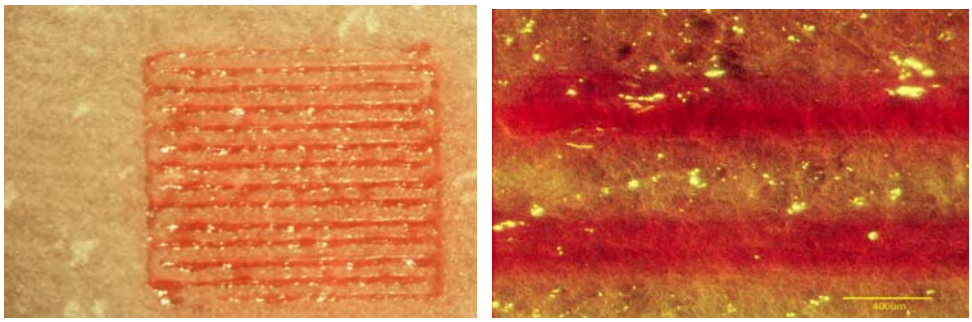

Figure 3-5: Bioprinted tissue construct structural formability

In this study, the process parameters (dispensing pressure of 2.0 psi with internal nozzle tip diameter of 200 μm) were adjusted to achieve a three-layered sinusoidal pattern with consistent strut diameters of 200 μm.

3.2 Microfabrication of the Tissue Chamber

The other major component of the three-dimensional microfluidic microanalytical micro-organ device is the micofluidic device with indented chambers that serve to house the bioprinted tissues. In order to form a closed platform for continuous drug perfusion flow studies, the micro-organ device consists of an assembly of two microfabricated components: 1) a polydimethylsiloxane (PDMS) substrate with indented chambers and 2) glass cover slide with etched microchannels that drain into and out of the tissue chamber.

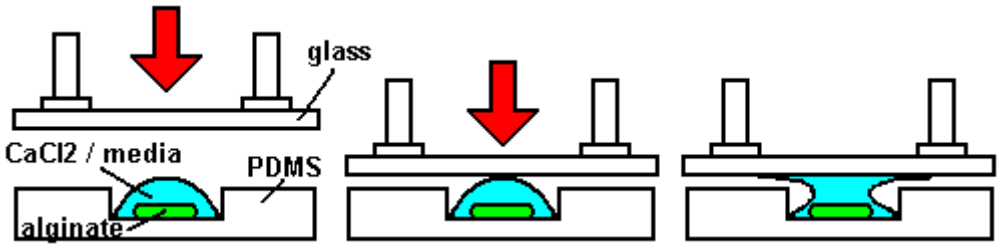

Figure 3-6: The micro-organ device represents an assembly of two microfabricated components

The preferred material for fabrication of the substrate for housing the embedded tissue is PDMS, a biocompatible silicone rubber.

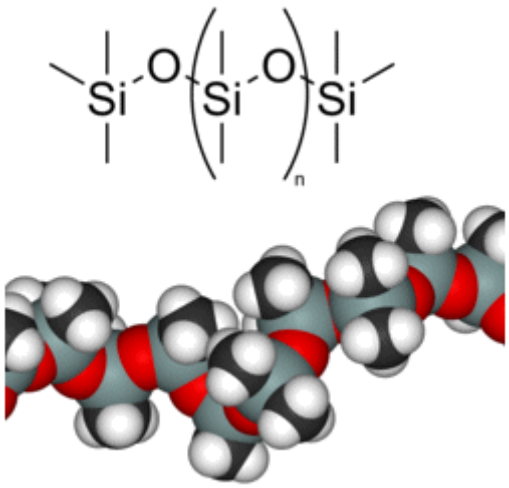

Figure 3-7: The chemical structure for polydimethylsiloxane (PDMS)

The advantages of using PDMS for these microfabricated chambers include ease of bonding, optical properties, and permeability to gases for biological applications. The process for microfabricating a PDMS substrate with a 10mm x 10mm x 750uL tissue chamber is detailed in Figure 3-8.

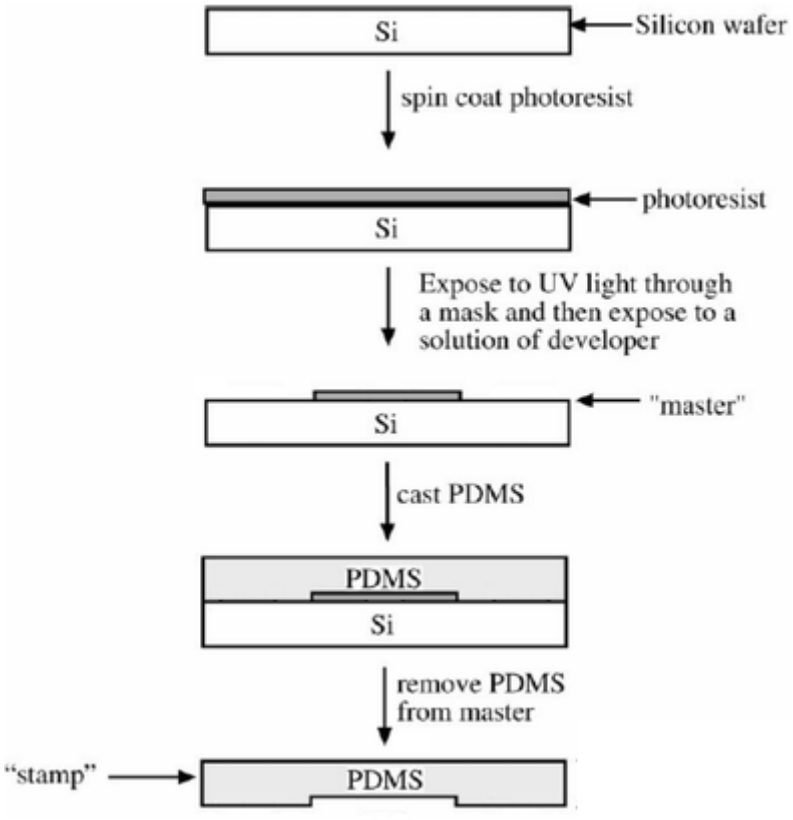

Figure 3-8: Microfabrication of a PDMS stamp

Essentially, photolithography is first applied to pattern a light-sensitive photoresist polymer (of approximate dimension 10 mm x 10 mm x 600 μm) onto a silicon wafer. Using soft lithographic techniques, PDMS is then cast onto the silicon wafer to yield a stamp (Whitesides et al., 2001). The PDMS stamp can then be used to accommodate the bioprinted micro-organ as well as a component in the microfluidic device.

The cover glass layer consists of an etched bifurcating channel pattern and inlet and outlet holes drilled into the glass shown in Figure 3-9.

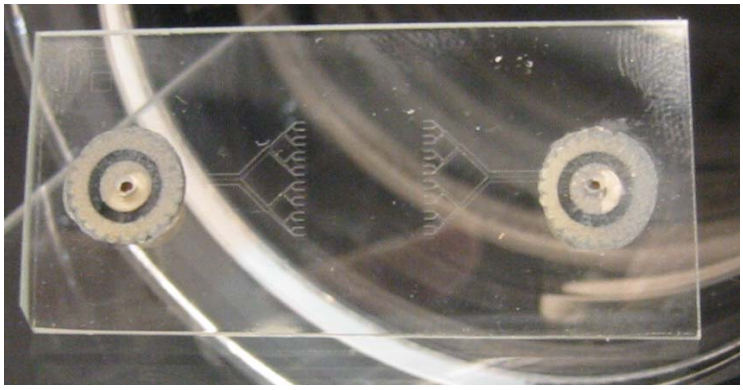

Figure 3-9: Etched microfluidic channel patterns on glass cover slide

The dimensions of the channel pattern are 20.5 μm deep, with branching channel widths ranging from 817 μm down to 88 μm. The next step is to directly write the the cell-encapsulated alginate constructs within the PDMS chamber. In order to integrate the alginate constructs onto the PDMS substrate, both the glass and PDMS layers are first cleaned with acetone and 70% ethanol and then placed into a RF plasma chamber (Harrick Plasma) to oxidize the glass and PDMS substrate surface methyl groups to form silanol groups. Therefore, a hydrophilic surface with good wettability and improved traction is attained.

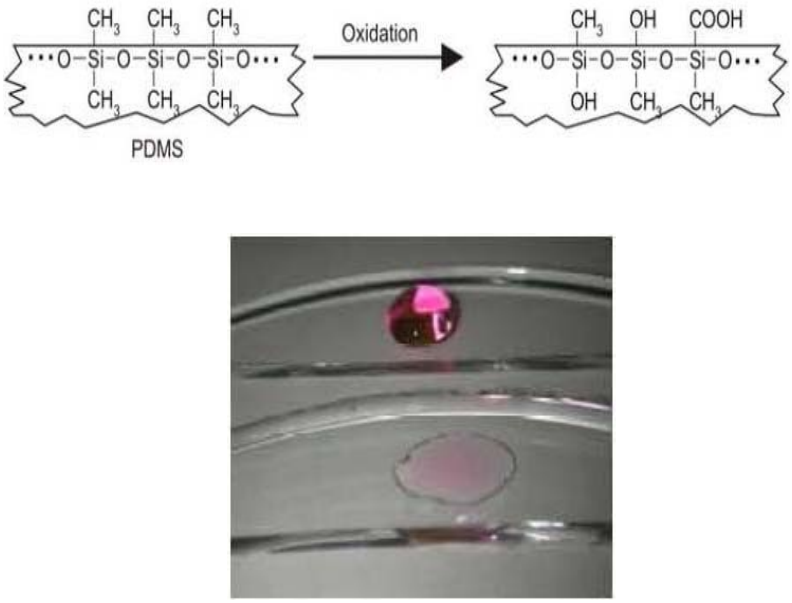

Figure 3-10: Plasma treatment of PDMS substrate results in improved wettability

Firstly, the chamber was put under vacuum for 1 min. Afterwards, the glass and PDMS surfaces were treated with air plasma for 30 sec. The PDMS layer was taken to the deposition system and the alginate-encapsulated HepG2 cell solution was deposited to create a sinusoidal flow pattern with 250 μm diameter struts (Figure 3-11) using the air-actuated EFD dispensing nozzle.

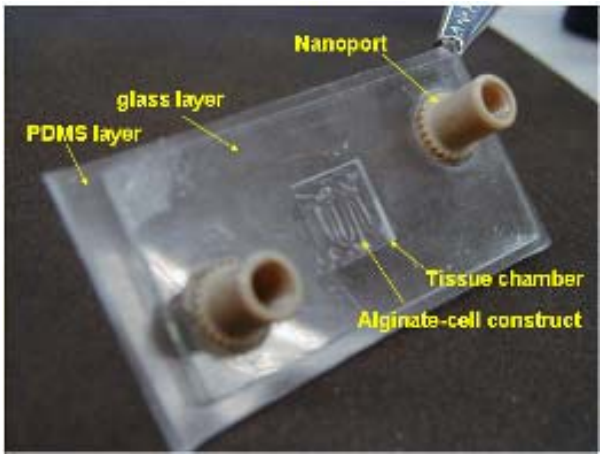

Figure 3-11: Prototype sinusoidal pattern in tissue chamber

12.5 µm of 5.0% w/v calcium chloride and media were deposited using a pipettor to crosslink the alginate and feed the cells. The PDMS was then bonded to the glass layer with the bifurcating channels aligned to the chamber. The chips were allowed to strengthen their bonding for approximately 45 min – 1 hr. Through this process, the cell-encapsulated alginate construct is directly bioprinted within the tissue chamber indentation on the PDMS microchip, thus forming an integrated three-dimensional tissue chamber unit.

3.3 Assembly of the Micro-bioreactor

The experimental apparatus setup of medium/drug flow circulation in the micro-bioreactor for parallelization of study is shown in Figure 3-12 below.

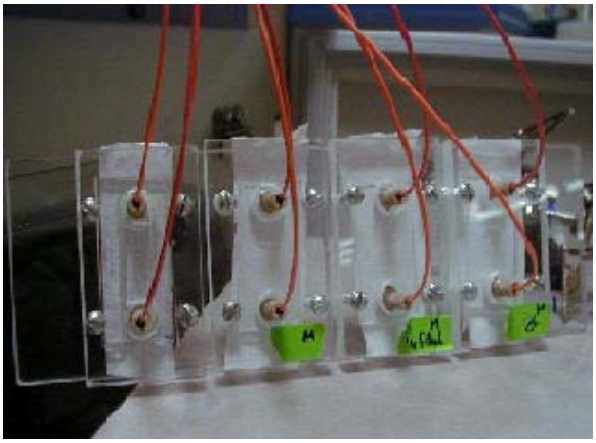

Figure 3-12: Parallelization of fully drug perfused tissue chambers

To demonstrate effective drug metabolism in the liver chamber, a non-fluorescent prodrug is fed into the system through the inlet port, metabolized by the liver chamber, and then produced an effluent fluorescent metabolite for analysis collected at the outlet port. Results of such analysis will be used in the future to understand the relative pharmacokinetic efficiency as well as relevancy of the tissue chambers design for human application. The drug flow study protocol will include 120 μL of 10 mM EFC (7-ethoxy-4-trifluoromethyl coumarin) stock solution mixed with 9.88 ml of HepG2 medium and put into a syringe to be infused by a syringe pump. The micro-organ prototype is then connected to the pump for simultaneous infusion at the inlet port and withdrawal at the outlet at a designated flow rate. The drug substrate is metabolized by the hepatocytes into the drug product or metabolite to be measured. The perfused micro-organs are subsequently incubated along with static, non-perfused controls. The effluent is collected within the withdrawal syringe and assayed with a cytofluoremeter for HFC drug metabolic conversion with a drug residence time consistent with the static controls.

3.4 Summary of Key Results and Conclusions

The feasibility of using a standard soft-lithography technique is explored to fabricate microscale *in vitro* device with microchannels and multi-chambers to house the bioprinted tissue. PDMS elastomer soft lithography is combined with micromolding techniques to fabricate three-dimensional microfluidic tissue chambers.

CHAPTER 4. MODELING FLUID DYNAMICS AND MASS TRANSFER IN THE LIVER MICRO-ORGAN

This chapter examines the modeling of fluid dynamics and mass transfer effects of a continuously perfusing drug/media flow through a channel pattern defined by a bioprinted three-dimensional liver micro-organ that biomimicks the *in vivo* liver sinusoidal capillary architecture. In macroscale bioreactors, fluid flow and mixing are expected to affect tissue formation and function in at least two ways: by enhancing mass transfer (e.g., of gases, nutrients, and drugs) and by direct physical stimulation of the cells (e.g., by hydrodynamic forces). In this thesis, a microscale fluidic device is modeled wherein the micron-sized channel features enable relatively large hydrodynamic shear forces on the liver tissue constructs while preserving predictable laminar flow regimes. In order to comprehensively evaluate the impact of fluid flow on cell-specific function, in particular liver-specific drug metabolic function, an accurate determination of the fluid flow parameters (e.g. shear stress and mass transfer) experienced by the bioprinted liver tissue is important in determining several design parameters such flow rate and microchannel dimensions to ensure that the liver cells encapsulated in the bioprinted tissue construct are subjected to the same type of fluidic microenvironment as they would inside the liver sinusoid capillaries. Below is a schematic of the configuration for the micro-organ being modeled in Figure 4-1.

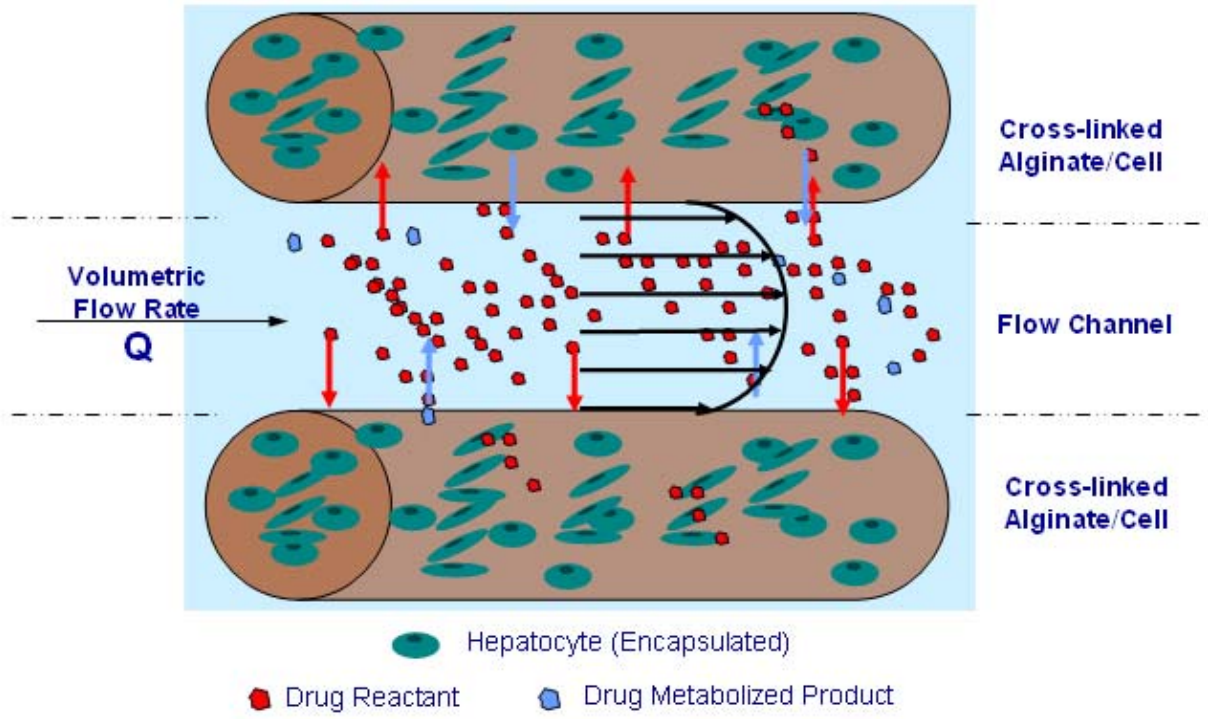

Figure 4-1: Modeling configuration for liver micro-organ

In this thesis, COMSOL Multiphysics software is implement to model fluid dynamical properties and mass transport phenomena for microfluidic flow through the liver micro-organ. COMSOL Multiphysics is a finite element analysis and solver software package for various physics and engineering applications, especially coupled phenomena, or multiphysics. The overall modeling strategy is shown in Figure 4-2.

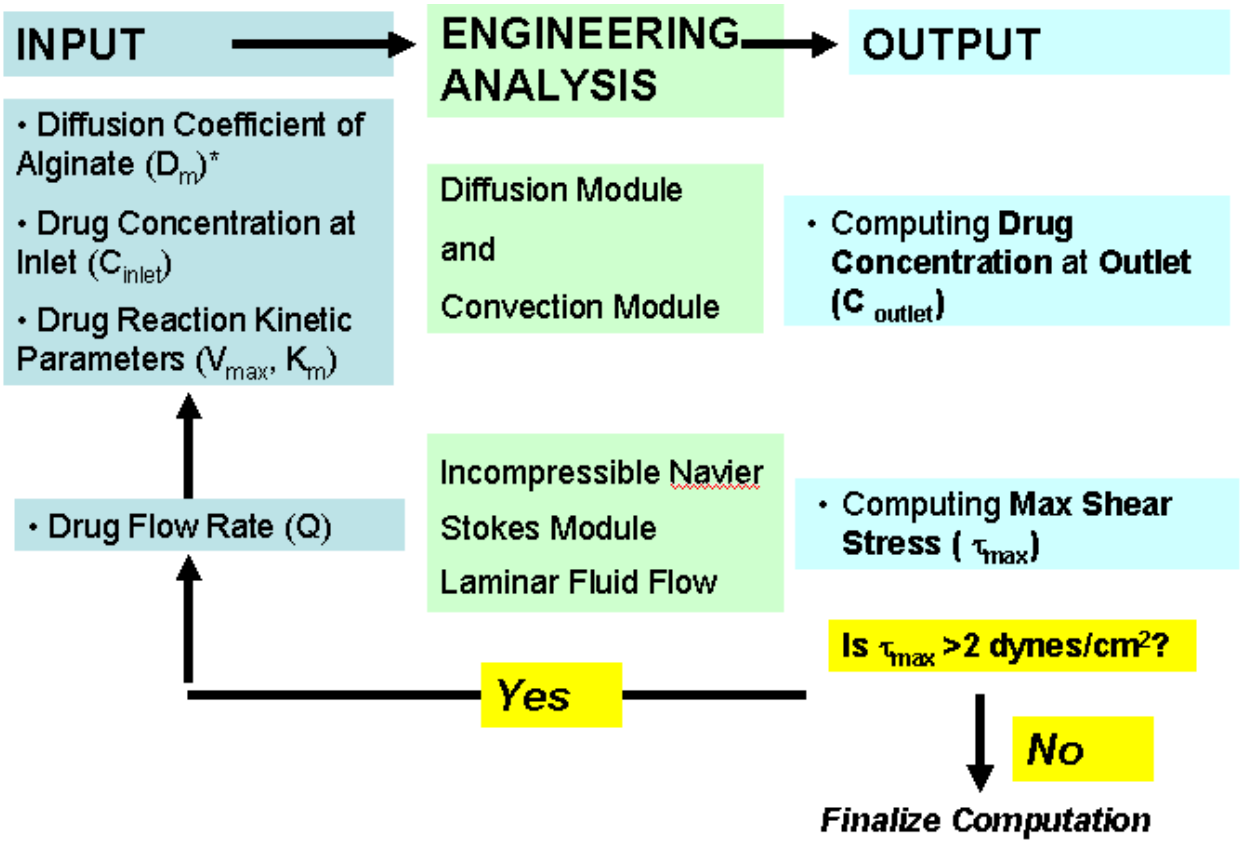

Figure 4-2: Overall modeling strategy of fluid dynamics and mass transfer in COMSOL

4.1 Computational Fluid Dynamic Model for Shear Stress Distributions

Shear stress is an inherent part of microfluidic perfusion culture systems and is often perceived as a limiting factor in microfluidic perfusion culture due to its deleterious effect on cells at high levels. However, it is possible to design and operate microfluidic perfusion culture systems such that applied shear stresses are orders of magnitude below those at which adverse effects are observed. Methods for mitigating shear stress include lower fluid velocities, designing high aspect ratio cell culture chambers, and including micropillars or microwells to shield cell cultures. On the other hand, some microfluidic

perfusion systems use high levels of shear stress to investigate biological phenomena, such as endothelial cell function or cell adhesion. In addition, acceptable levels of shear stress can vary widely depending on cell type.

Physiological values of shear stress on endothelium lining of vessels *in vivo* are in the range of 1-15+ dyne/cm^2 (Davies, 1995, Malek et al., 1999). The shear stresses on cells at the chamber/tissue inferface are well below this range, whereas the shear stresses at the fluid/tissue interface for perfusion flow in the channels approach the lower limit. Physiological values of fluid shear stress on tissue cells other than endothelium are infrequently reported or cited in the current literature. However, analysis of interstitial flow through the internal elastic lamina of blood vessels suggests that smooth muscle cells bordering the subendothelial intima experience wall shear stresses on the order of 1 dyne/cm^2 (Tada et al., 2000), a value that affects smooth muscle cell biology *in vitro* (Papadaki et al., 1998). Furthermore, as detailed in Chapter 2, the endothelial cells lining the liver perfusing capillary vasculature closely approximate the drug metabolizing hepatocytes. Therefore, one may deduce from the anatomy of the microvasculature that the highly fenestrated or porous liver endothelium depicted in Figure 4-3 results in notable transmission of fluid shear stresses to hepatocytes with significant biological consequences that may modulate drug metabolism activity.

Figure 4-3: The highly fenestrated sinusoidal liver microcirculation may lead to high fluid shear stress transmission to liver cells

In the development of a physiologically relevant microenvironment for hepatocyes in the liver, it is essential to adequately recapitulate the perfusion of the hepatocellular parenchyma by the sinusoidal capillary network. Although the effects of fluid shear stress on hepatocytes have been less well-documented than effects on blood vessel-lining endothelial cells, shear stress has been reported to induce P4501A1 activity in hepatoma cells in microcarrier culture (Mufti and Bleckwinn, 1995, Mufti and Shuler, 1995) and to simulate metabolic function and morphogenesis in two dimensional co-culture of primary rate hepatocytes with nonparenchymal cells when shear stress levels were maintained at 4.7 dyne/cm^2 compared to no shear (Kan et al., 1998). The albumin production activity of liver tissue can also be enhanced by loading an adequate shear stress (Ijima et al., 2008); thus, the mild shear stress conditions in our system are likely to be good for the expression of liver-specific functions. Furthermore, it is expected that improvements in the mass transfer around the cells will greatly improve the clearance of drugs with an

extremely high extraction ratio, such as lidocaine. For these reasons, the expression of the liver-specific functions of hepatocytes would be expected to be higher in a circulation culture than in a stationary culture.

The optimal flow conditions of a microbioreactor should not be determined through a trial-and-error approach, but rather should be supported by precise simulation methods. Computational fluid dynamic (CFD) software packages (e.g. COMSOL) have been increasingly developed during the past decade and are a powerful tool to calculate flow fields, shear stresses and mass transport within and around three-dimensional constructs. Fluid flow inside the microbioreactor may be analyzed using a computational fluid dynamic (CFD) model to estimate the velocity profiles, pressures, and fluid shear stresses present within the system. The microbioreactor flow pattern geometry, when sufficiently complicated as in the case of a liver sinusoidal capillary, requires a full computational model to supplement simple analytical calculations. Computational fluid dynamic models have been used to calculate the momentum and oxygen transport within a concentric cylinder bioreactor for cartilage tissue engineering and to design and characterize a scaled-up version. A CFD model of direct perfusion through a three-dimensional mesh demonstrated that the random fiber architecture of the scaffold would yield highly variable shear stresses; a scaffold with a homogeneous distribution of pores would therefore enable more precise control over the shear stresses. In this regard, it is becoming increasingly clear that design requirements for scaffolds used in tissue engineering should not be limited to considerations on biocompatibility and mechanical properties, but should also include a critical evaluation of pore structure and

interconnectivity, which must be tuned to the specific flow conditions used. Based on the range of flow rates seen in *in vivo* hepatic sinusoids (Davies et al., 1993, Davies, 1997, Kan et al., 1998), Powers et al sets the perfusion crossflow rate for a microfabricated perfusion bioreactor between 40 μl/min and 600 μl/min in order to mimic shear rates seen in the *in vivo* microenvironment (Powers et al., 2008). Levesque et al. uses a parallel-plate flow chamber in to study the response of bovine endothelial cells in response to fluid shear stress (Leveque et al., 1985). These results showed that endothelial cells orient with the flow direction and become more elongated when exposed to higher shear stress. Effects of microchannel sizes on this angular orientation of the endothelial cells was demonstrated by Bonnie et al. who uses microchannels with channel width decreasing from 225 μm to 25 μm (Bonnie et al., 2002). This demonstrated how endothelial cells cultured in narrower microchannels are oriented primarily along the channel lengths, while cells grown in wider channels progressively lost this preferred orientation and ultimately randomly oriented within the largest microchannels. This result was an example of how geometric control of cell shape and orientation can be accomplished by culturing cells in microchannels of different widths. Another example of dimensional considerations for microchannel flows was considered by Ledezma et al. in which the dimensional ranges were investigated for a constant perfusion rate, the chamber height strongly affected the mechanical shear stress on the cells in that significantly reduced chamber heights resulted in physiologically unrealistic shear stress values (Ledezma et al., 1999).

In this thesis, the fluid dynamics within the three-dimensional microfluidic microanalytical micro-organ can be modeled using the complete form of the Navier-Stokes equations in three dimensions, without any initial relaxations or approximations. The basic governing equations for viscous incompressible fluid flow are:

Continuity: $$v_{i,i} = 0 \tag{1}$$

Momentum: $$\rho\left[\frac{\partial v_i}{\partial t} + v_j v_{i,j}\right] = \tau_{ij,j} \tag{2}$$

$$\tau_{ij,j} = -p\delta_{ij} + 2\mu e_{ij} \tag{3}$$

where ρ is the mass density of the fluid, v_i is a component of the fluid velocity and τ_{ij} is the ij^{th} component of the stress tensor and where

$$e_{ij} = \frac{v_{i,j} + v_{j,i}}{2} \tag{4}$$

p is the fluid pressure and μ is the coefficient of viscosity.

Therefore, the primary outputs from the computational fluid dynamical analysis are the fluid velocity profile and the wall shear stress. For microfluidic perfusion culture simplified as a two dimensional Poiseuille flow system, the resulting parabolic flow profile yields a simple estimate of shear stress at the wall:

$$\tau = \frac{6\mu Q}{h^2 w} \qquad \text{where } \mu = \text{viscosity } [\frac{\text{kg}}{\text{m}\cdot\text{s}}], \tag{5}$$

$$Q = \text{flow rate } [\frac{\text{m}^3}{\text{s}}],$$

$$h = \text{channel height [m], and}$$

w = channel width [m].

In COMSOL, this wall shear stress is modeled using Navier-Stokes equation for incompressible fluid in the laminar flow regime. Based on the tissue chamber dimension of 10 mm x 10 mm x 600 μm, and a minimum 4 hr drug/media incubation period required for appreciable drug conversion in static cultures of bioprinted tissue constructs, the volumetric flow rate is set as 0.015 ml/hr for the drug flow perfusion studies. For all simulations performed in COMSOL, tetrahedral elements were used to set the mesh distribution in the geometry shown in Figure 4-4.

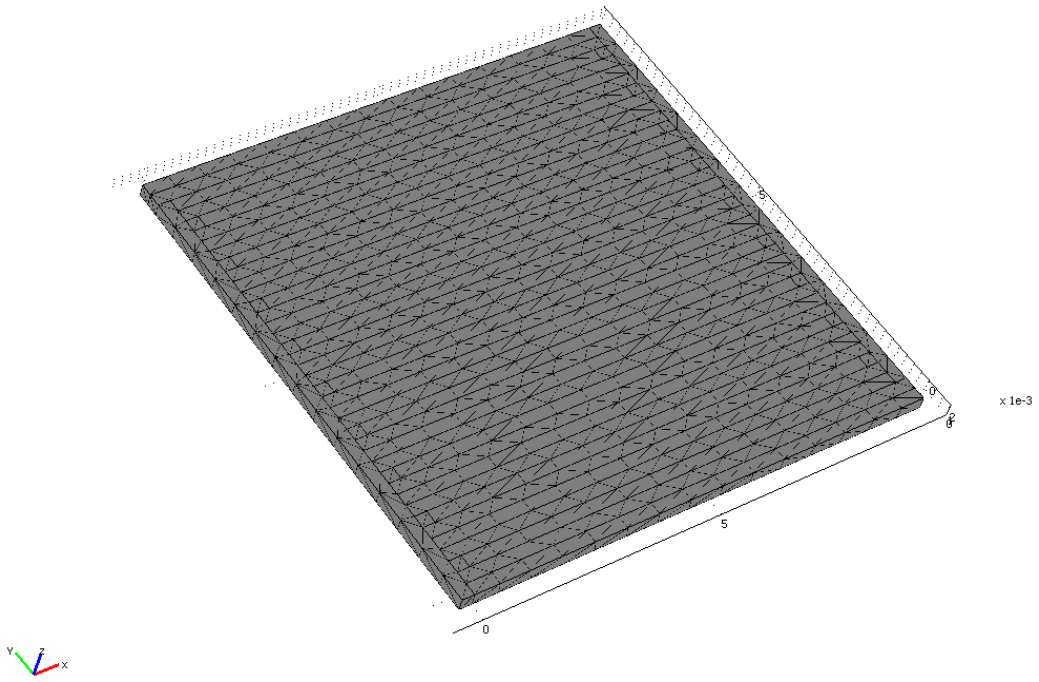

Figure 4-4: Tetrahedral mesh element distribution in COMSOL

The conditions for this simulation include an inlet volumetric flow rate of 1.5 x 10^{-2} ml/hr, 3.0% w/v bioprinted alginate concentration, 1 x 10^{6} total HepG2 liver cells

encapsulated. Different channel widths of 150 μm, 250 μm, and 400 μm are simulated to predict effect of varying channel dimensions on drug wall shear stress in Figure 4-5.

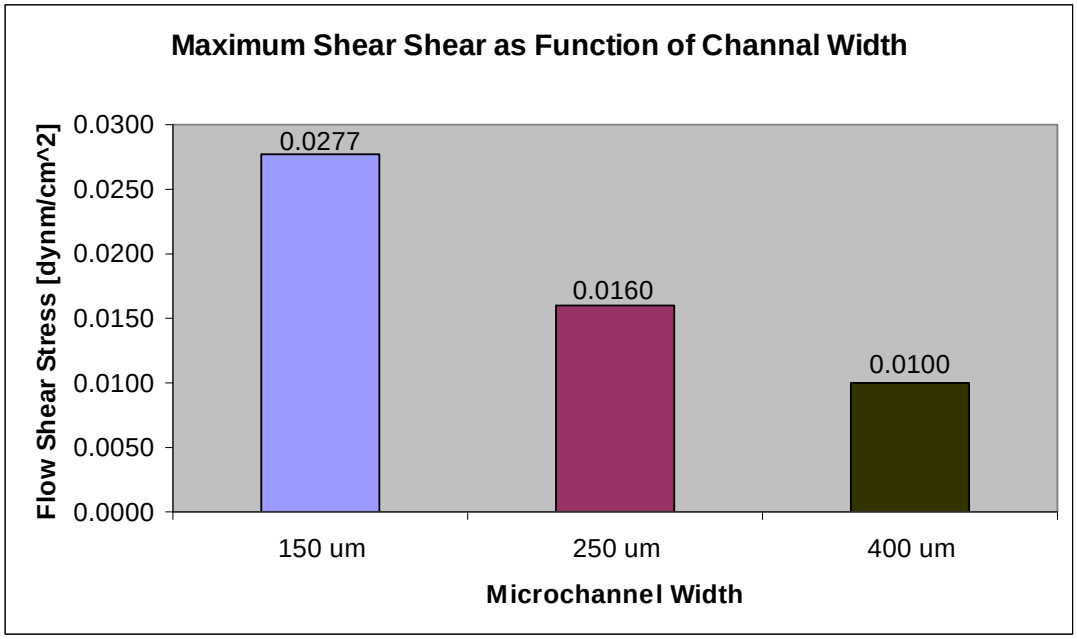

Figure 4-5: Effect of varying channel width dimension on wall shear stress

These results show that decreasing the channel width results in an elevated maximum wall shear stress. A simulation on varying velocities for a given channel width gave expected results with proportionately higher wall shear stresses for higher initial volumetric flow rates.

4.2 Mass Transfer Model in COMSOL

The microbioreactor offers the benefit of improved mass transfer that is provided by perfusion, stirring, or rotation. The physical system that is being modeled in COMSOL is that of a hollow fiber through which drug reactant solute in nutrient media

flows with a fully developed laminar parabolic velocity profile. The wall of the tube constitutes a membrane phase made up of cells encapsulated in alginate. Media and drug transport in the hollow fibers occurs through a non-trivial interaction of convection and diffusion, modulated by a number of factors. The drug reactant is transported by convection and diffusion in the liquid media phase, whereas diffusion is the only transport mechanism in the membrane phase. To describe the system, the following mass transport equations can be formulated:

$$\nabla \cdot (-D\nabla c_1 + c_1\mathbf{u}) = 0 \qquad \text{in liquid phase} \qquad (6)$$

$$\nabla \cdot (-D_m \nabla c_2) = 0 \qquad \text{in membrane phase} \qquad (7)$$

where c_i denotes the concentration of the drug reactant (mol/m^3) in the respective phases, D denotes the diffusion coefficient (m^2/s) in the liquid phase and D_m is the diffusion coefficient in the membrane, while u denotes the velocity (m/s) in the liquid phase.

The convection-diffusion equation is applied to both domains and coupled to the fluid velocities of the momentum transport equations. An idealized tissue-channel geometry containing cylindrical conduits for convective flow forms the basis for the numerical analysis with a mass transfer model. Species diffusion and enzymatic reaction are assumed as the only contributing factors to mass conservation within the tissue. The basis species conservation equations can be used to solve for the coupled tissue-conduit species concentration profile. These equations in their most generalized form are (assuming constant density and diffusivity):

$$\frac{DC_i}{Dt} = D_i \nabla^2 C_i + R_{vi} \tag{8}$$

where

$$\frac{D}{Dt} = \frac{\partial}{\partial t} + v_r \frac{\partial}{\partial r} + \frac{v_\theta}{r} \frac{\partial}{\partial \theta} + v_z \frac{\partial}{\partial z} \tag{9}$$

and D_i is the diffusivity of the i^{th} species, C_i is the concentration of the i^{th} species in the tissue, R_{vi} is the cellular uptake or release rate of the i^{th} species, and r, θ, and z represent the cylindrical coordinates used to describe the system. Since the tissue can be assumed solid and non-porous, the species conservation equation at steady state applicable to the tissue reduces to:

$$D_i \nabla^2 C_{i,tissue} + R_{vi} = 0 \tag{10}$$

where $C_{i,tissue}$ represents the i^{th} metabolite concentration in the tissue.

The cell uptake or release rate of the drug metabolite is assumed to follow Michaelis-Menten kinetics:

$$R_{vi} = \frac{V_{\max} C}{C + K_m} \tag{11}$$

where V_{max} and K_m are the appropriate Michaelis-Menten parameters respresenting the maximal enzyme activity and the substrate concentration at which the activity is half the maximal, respectively.

The appropriate boundary conditions needed to solve for the concentration profile in the tissue include the insulation boundary condition at the walls of the chip, flux-continuity at the tissue-fluid interface, and appropriate concentrations at the top and bottom plane surfaces of the tissue construct.

$$-D\nabla C_{i,tissue}\Big|_{wall} = 0 \tag{12}$$

The species conservation equation in the channel with the Poiseuille flow approximation (which follows from the fluid dynamic modeling described in the previous section) reduces at steady state to:

$$-v_z \frac{\partial C_{i,fluid}}{\partial z} = D\nabla^2 C_{i,fluid} \tag{13}$$

The appropriate boundary conditions needed to simulate the metabolite distribution in the channel include the continuity of fluxes at the fluid-tissue interface and a valid inlet concentration of the substrate C_o.

$$-D\nabla C_{i,tissue}\Big|_{tissue-fluid} = -D\nabla C_{i,fluid}\Big|_{fluid-tissue} \tag{14}$$

Prior to modeling mass transfer in COMSOL, the constants V_{max} and K_m first need to be determined through experimentation. Assuming Michaelis-Menten kinetics, it is important to determine the maximum rate of an enzyme mediated reaction through a series of experiments carried out with varying substrate concentration ([*S*]) and the initial rate of product formation is measured. Initial here is taken to mean that the reaction rate is measured after a relatively short time period, during which complex builds up but the

substrate concentration remains approximately constant and the quasi-steady-state assumption will hold. For Michaelis-Menten kinetics, the enzymatic reaction is assumed to be irreversible, and the product does not bind to the enzyme:

$$E + S \underset{k_{-1}}{\overset{k_1}{\rightleftarrows}} ES \xrightarrow{k_2} E + P \tag{15}$$

The first key assumption in this derivation is the quasi-steady state assumption (or pseudo-steady-state hypothesis), namely that the concentration of the substrate-bound enzyme ([*ES*]) changes much more slowly than those of the product ([*P*]) and substrate ([*S*]). The second key assumption is that the total enzyme concentration does not change over time, thus we can write the total concentration of enzyme as the sum of the free enzyme in solution and that which is bound to the substrate.

Using the drug substrate EFC (7-ethoxy-4-trifluoromethylcoumarin) for our model, varying substrate concentrations are reacted with bioprinted hepatocyte-encapsulated samples of a given cell density in static culture (see Chapter 6). The specific enzyme being probed for this kinetic reaction is 7-Ethoxycoumarin O-deethylase selected for in the cytochrome P450 CYP2B6. A saturation curve for an enzyme showing the relation between the concentration of substrate and rate allows for the determination of K_m and V_{max}. In literature, reported values for CYP2B6 catalyzed EFC O-deethylation as the test reaction include an EFC Km value of 4.0 μM (1.6–6.4 μM, 95% confidence interval) and a V_{max} value of 2.4 nmol/(min x nmol CYP) (1.8–3.0 nmol/(min x nmol CYP)) (Korhonen et al., 2007). Another set of kinetic characteristics have been tabulated

using the EFC fluorescent probe assays in intact CYP2B6-expressing cells and found K_m and V_{max} values of 4.2±2.8 μM and 35.1±4.9 pmol/min·mg, respectively. (Donato et al., 2004). In this thesis, K_m and V_{max} are determined by evaluating the rate of EFC metabolism in cultured cells over a substrate concentration range of 0.3 to 100 μM. From this analysis, the K_m and V_{max} values for a bioprinted HepG2 encapsulated tissue constructs of initial cell number of 1 x 10^6 cells are 3.8 μM and 0.3 nmol/s·cell, respectively. Based on size of EFC (MW=258.2 g/mol), the diffusion coefficient D_m and partition coefficient for EFC through 3.0% w/v alginate concentration are set at 5.0 x 10^{-5} cm^2/s and 0.98, respectively, as interpolated for literature values.

In order to establish a predictive model of drug metabolism in bioprinted liver tissue constructs, the flow rate must be sufficiently high enough to recapitulate nutrient/waste exchange as in the in vivo vasculature, but at the same time provide sufficient drug/media residence time in the perfused tissue chamber to ensure a measurable drug metabolic response. Based on the tissue chamber dimension of 10 mm x 10 mm x 600 μm, and a minimum 4-hr drug/media incubation period required for appreciable drug conversion in static cultures of bioprinted tissue constructs, the volumetric flow rate is set as 0.015 ml/hr for the drug flow perfusion studies.

The effluent concentration of drug metabolite (i.e. HFC) can be predicted by simulating the sinusoidal drug flow pattern in COMSOL's convection-diffusion module. The conditions for this simulation include an inlet volumetric flow rate of 1.5 x 10^{-2} ml/hr, 3.0% w/v bioprinted alginate concentration, 10^6 total HepG2 liver cells

encapsulated. Different channel widths of 150 μm, 250 μm, and 400 μm are simulated to predict effect of varying channel dimensions on drug conversion in Figure 4-6.

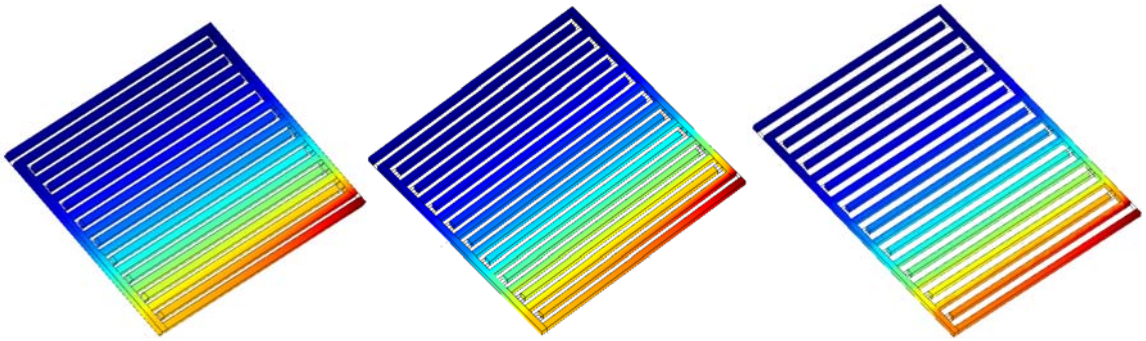

$[HFC]_{max} = 0.769\ \mu M$	$[HFC]_{max} = 0.770\ \mu M$	$[HFC]_{max} = 0.770\ \mu M$
$[HFC]_{min} = 0.705\ \mu M$	$[HFC]_{min} = 0.755\ \mu M$	$[HFC]_{min} = 0.765\ \mu M$
(a) 150 um channel width	(b) 250 um channel width	(c) 400 um channel width

Figure 4-6: Effect of varying channel width dimension on drug metabolite concentration

Tissue construct strut widths of 250 μm and overall construct volume is maintained as a constant for all samples to maintain cell numbers across all dimensional variations. While the differences in drug metabolic conversion are small for the different channel widths, the minimum HFC concentration at steady-state is observed to increase as the channel width increases since the linear transit time of the drug increases for larger channel widths, thereby exposing the substrate EFC to enzymatic conversion by the cells for a longer duration.

For a channel width of 250 μm, initial volumetric flow rates of 1.5 x 10^{-4} ml/hr, 1.5 x 10^{-2} ml/hr, and 1.5 ml/hr are simulated to predict effect of varying initial volumetric flow rates on drug conversion in Figure 4-7.

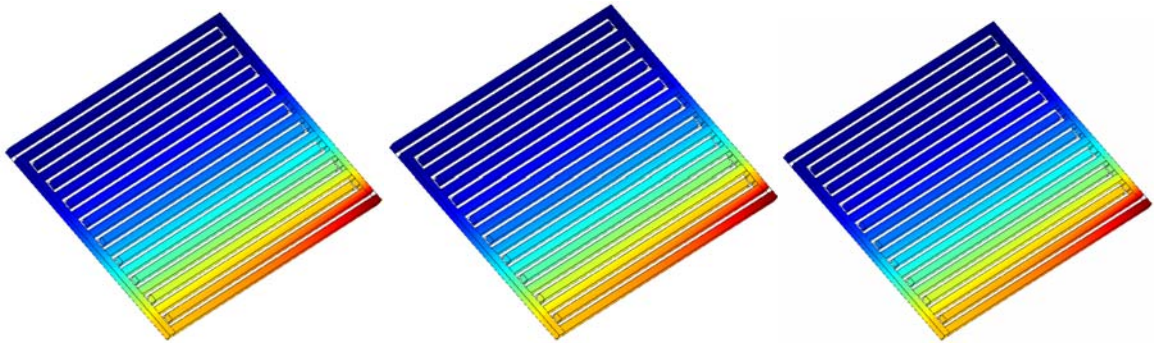

$[HFC]_{max}$ = 0.770 μM	$[HFC]_{max}$ = 0.770 μM	$[HFC]_{max}$ = 0.769 μM
$[HFC]_{min}$ = 0.770 μM	$[HFC]_{min}$ = 0.755 μM	$[HFC]_{min}$ = 0.206 μM
(b) Q = 1.5 x 10^{-4} ml/hr	(b) Q = 1.5 x 10^{-2} ml/hr	(c) Q = 1.5 ml/hr

Figure 4-7: Effect of varying volumetric inlet flow rate on drug metabolite concentration

For a given channel width, the HFC concentration at steady-state is observed to decrease as the initial volumetric flow rate increases since the overall transit time of the drug decreases at higher volumetric flow rates, thereby exposing the substrate EFC to enzymatic conversion by the cells for a shorter duration.

4.3 Summary of Key Results and Conclusions

Fluid shear has been shown to activate cell signaling pathways and influence differentiated function of both hepatocytes and endothelial cells. An accurate determination of the shear stress experienced by the biomanufactured tissue is therefore

important in determining several design parameters such as flow rate and geometry to ensure that the cells in the bioreactor are subjected to the same kind of environment as they would inside the liver capillaries. The shear stresses at the fluid/tissue interface for perfusion flow in the channels approach the lower limit of physiological values for shear stress on endothelium lining of vessels *in vivo*. The microbioreactor flow pattern geometry, when sufficiently complicated as in the case of a liver sinusoidal capillary, requires a full computational model to supplement simple analytical calculations. This section reviews in detail approaches to the fluid dynamical and transport modeling of flow in microscale bioreactors in which biological tissue is maintained in channels by continuous perfusion of culture medium. In addition, to better understand the tissue disposition of a candidate drug, a comprehensive mass transfer model is also considered and developed. For fluid dynamical predictions, wall shear stress is calculated by solving Navier-Stokes equations for incompressive fluid flow in a laminar flow regime in COMSOL to predict the effect of microchannel dimensions and flow rate on wall shear stress. The simulations showed that for a given initial volumetric flow rate, decreasing the channel width results in an elevated maximum wall shear stress. A simulation on varying velocities for a given channel width gave expected results with proportionately higher wall shear stresses for higher initial volumetric flow rates. In the study of mass transfer effects, the effluent concentration of drug metabolite (i.e. HFC) can be predicted by simulating the sinusoidal drug flow pattern in COMSOL's convection-diffusion module. By varying the microchannel dimensions, it was observed from the simulation that the minimum HFC concentration at steady-state is observed to increase as the

channel width increases since the linear transit time of the drug increases for larger channel widths, thereby exposing the substrate EFC to enzymatic conversion by the cells for a longer duration. Finally, for a given channel width, the HFC concentration at steady-state is observed to decrease as the initial volumetric flow rate increases since the overall transit time of the drug decreases at higher volumetric flow rates, thereby exposing the substrate EFC to enzymatic conversion by the cells for a shorter duration.

CHAPTER 5. CELL VIABILITY CHARACTERIZATION ON EFFECT OF KEY BIOFABRICATION PROCESS PARAMETERS

Novel technologies such as the direct cell writing process are emerging that incorporate cells as part of the building blocks for various layered biomanufacturing processes for the freeform fabrication of tissue constructs in tissue regeneration, 3D pharmacokinetic models, cell-based MEMS, sensors, and microfluidic devices. Now, we are attempting to use cells as building blocks to manufacture biological structures. However, the effects of these biomanufacturing processes on cells have not been fully studied.

Cells, bioactive substances, and scaffold materials are the three major elements of tissue engineering. It is often overlooked that cells may not remain viable and/or of the desired phenotype after undergoing the mechanical forces used to process bioactive substances and scaffolding materials during the biofabrication. Furthermore, mechanical models of cell manipulation are often based on assumptions of a standard viscous or viscoelastic continuum or an elastic nucleus within a viscous cytoplasm (Evans et al., 1989, Schmid-Schoenbein et al., 1995, Dong et al., 1991). Biological studies show that living cells are dynamic structures that change their growth, locomotion, and differentiation under external mechanical influences (Wang et al., 2001). Alteration in mechanical signals caused by changes of cell geometry may result in chemical signals that modulate downstream cellular development (Clark et al., 1995, Plopper et al., 1995). During the biofabrication process, cells are invariably subjected to mechanical forces.

These process-induced mechanical forces may affect the intracellular structures of the cell (Ingber, 1993, Ingber, 1997). For many biological applications, it is important to know whether cells remain viable and/or the desired phenotype after undergoing the mechanical forces applied during the process. Taking a syringe-based cell dispensing as an example, different process parameters will produce different effects on cells: decreasing in the dispensing nozzle size will increase the dispensing shear forces experienced by cells inside the nozzle; varying the nozzle head movement speed could also induce additional compressive or tensile forces on the deposited strands with respect to the substrate, for example, at a high speed, the deposited strand may be "stretched" and cause an additional tensile force to the embedded cells, while at a low speed, the forces may be lower, or even compressive in nature. Therefore, it is important that any process-induced effects on cells during the biofabrication are better understood.

This chapter specifically examines the effect of the solid freeform fabrication based direct cell writing process, focusing on dispensing pressure and nozzle size, on the viability of liver cells within alginate. Cell viability assays are conducted to evaluate the effect of varying cell/material dispensing process parameters on cell survival. Sodium alginate is chosen as the biopolymer material to be utilized during the testing of the cell dispensing process.

5.1 Effect of Dispensing Pressure and Nozzle Size on Cell Viability

In this set of studies, hepatocytes are bioprinted and encapsulated within a three-dimensional alginate tissue construct. To prepare the polymer solution, medium viscosity

sodium alginate powder (Sigma, St. Louis, MO) is dissolved in deionized water as a 3.0% (w/v) solution. The ionic crosslinking solution is prepared by dissolving 5.0% (w/v) calcium chloride (Sigma, St. Louis, MO) in deionized water. The cells selected are HepG2 liver cells (ATCC, MA) which are cultured and maintained in Dulbecco's Modified Eagle's Medium (DMEM, ATCC), supplemented with 10% (w/v) fetal bovine serum and maintained in the incubator at 5% CO_2 and 37°C. The cells were gently mixed in viscous sodium alginate solution with Pasteur pipet to ensure a uniform cell distribution. Hemocytometer readings measured the cell concentration at $1x10^6$ cells/mL of alginate biopolymer solution. HepG2 cells are chosen because of its usefulness in pharmacokinetic studies and potential for *in vitro* tissue-on-chip applications.

For the cell viability study, each bioprinted sample are submitted to the Live/Dead Assay (Molecular Probes, Inc). The samples are viewed in a Leica fluorescence microscope under 40X magnification. In order to quantify the cell viability and assign a cell viability percentage throughout the time course study, each bulk sample is visualized and a live-dead cell count is performed at five different locations. The 5 different locations for the bulk sample are chosen using a protocol whereby the locations were 3 peripherally and 2 centrally. All 5 sample locations for the bulk samples are observed to reside on the surface due to focal constraints.

Two studies are performed, one short-term and another at longer time points. The aim of the short-term study is to evaluate the cell viability ratios at three incremental time points: 0 hr, 12 hr, 24 hr. The aim of the longer time point study is to evaluate the cell

viability ratios at three incremental time points: 0 day, 3 day and 7 day. The experimental setup for each parametric study involves twelve experimental groups and one control group. Two basic cell dispensing process parameters are studied: the nozzle tip internal diameters at 150 um, 250 um, 400um and the dispensing pressures at 5 psi, 10 psi, 20 psi, and 40 psi. Each experimental group comprises a sample size of four (i.e. n = 4). The control group consists of collecting alginate-cell solution directly from the reservoir under the passive effect of gravity. All experimental samples are dispensed as bulk material and weighed with a mass balance to a previously determined uniform mass. Upon completion of deposition, each sample is immediately submerged into a 5.0% (w/v) $CaCl_2$ crosslinking solution for a five-minute duration before perfusion with media and incubation. All samples in the long-term study are cross-linked daily to maintain both cell immobilization and structural integrity.

A first set of parametric experimental studies are conducted to assess the effect of the dispensing pressure and the nozzle size on the viability of cells. Each data point is an average of five representative Live/Dead images for each sample. Analysis is first performed by segregating the samples into three experimental groups according to different nozzle diameters of 150 μm, 250 μm, and 400 μm. Results of the parameter study are presented in Figure 5-1a for cell viability as function of dispensing pressure and Figure 5-1b as a function of nozzle diameter, respectively.

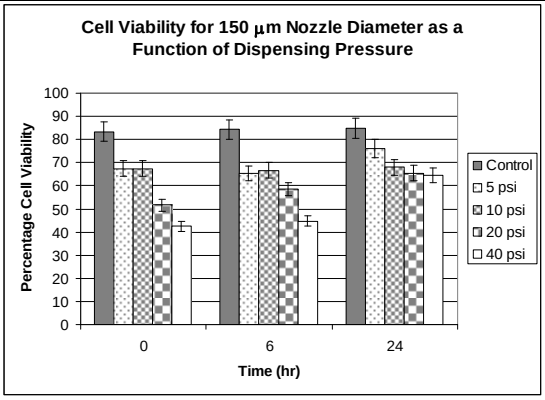

(a) cell viability as function of dispensing pressure

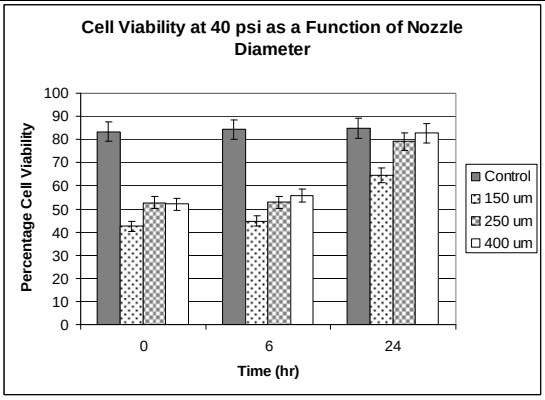

(b) cell viability as function of nozzle diameter

Figure 5-1: Effect of process parameter on cell viability for 24-hr study

It can be observed from the figures that cell viability varies with dispensing pressure and nozzle diameter. Cell viability increases as dispensing pressure decreases and/or nozzle diameter increases.

The first general observation from the cell proliferation assay is that the control group demonstrated no change in cell proliferation during the 24-hr period as well as the 7-day period due to the cell-immobilizing alginate gel matrix which is daily replenished with crosslinking ions. The consequence is that no cell proliferation occurs throughout the studied periods and any increase in cell viability in the experimental groups may be attributed to cell recovery from mechanical cell damage. For the experimental group varying nozzle diameters, there is a statistical drop in cell viability between the control group and the bioprinted cell encapsulated tissue constructs immediately after dispensing (0 hr) and at the 6 hr time point. Cell viabilities of the experimental samples at the 0 hr

time point for the nozzle diameters studied (150, 250, and 400 μm) are 68.60%, 76.15%, and 76.41% respectively of the control values.

For the experimental group varying dispensing pressures, there also exists a significant difference in cell viability over the time course, especially at the initial time point. Observed is a statistically significant drop in cell viability between the control group and the bioprinted cell encapsulated tissue constructs immediately after dispensing (0 hr) and at the 6 hr time point. The cell viabilities of the experimental samples at time 0 hr for the dispensing pressures studied (i.e., 5, 10, 20, and 40 psi) are 84.30%, 82.71%, 68.99%, and 58.89% respectively of the control values.

5.2 Effect of Dispensing Pressure and Nozzle Size on Cell Recovery

Cell recovery is also observed as a function of the process parameters and quantitative date is calculated for the percentage of cell recovery at the different culture times. Figure 5-2 shows a trend of cell recovery as a function of dispensing pressure (Figure 5-2a) and nozzle tip diameter (Figure 5-2b) referenced to the control group sample measured at 0 and 24 hr culture time points. The results of cell recovery data is presented in the following way: to study the cell recovery as a function of dispensing pressure as shown in Figure 5-2a, for a given pressure, the cell recovery experimental data is first measured for every nozzle diameter, and then averaged together and plotted in the figure; to study the cell recovery as a function of nozzle diameter as shown in Figure 5-2b, for a given nozzle diameter, the cell recovery experimental data is first

measured for every dispensing pressure, then averaged over all the data together and plotted in the figure.

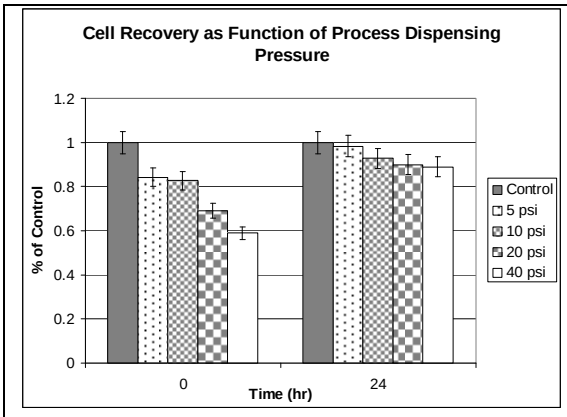

(a)

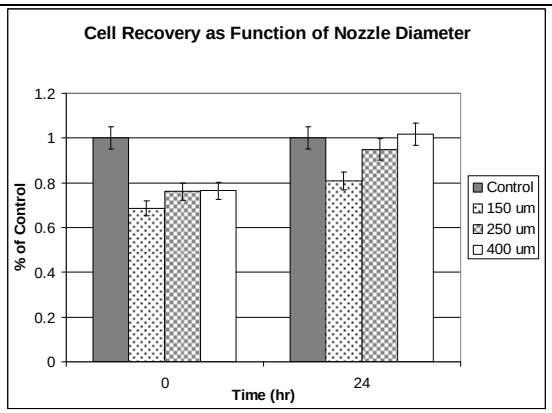

(b)

Figure 5-2: Cell recovery as referenced to control group for 24-hr study. (a) cell recovery as function of dispensing pressure; (b) cell recovery as function of nozzle diameter

All experimental groups for dispensing pressure (i.e., 5, 10, 20, and 40 psi) show significant cell recovery at the 24 hr time endpoint with cell viabilities at 98.34%, 92.69%, 89.98%, and 88.94% respectively of the control values. The smallest nozzle diameter group (i.e., 150 μm) demonstrates significantly diminished cell recovery with percentage cell viability of the control at 24 hr of 80.82%. The larger nozzle tip diameter experimental groups (250 and 400 μm) show comparatively higher cell recovery at the study's endpoint with cell viability at 94.91% and 100% respectively of the control values. The results of cell recovery at a longer time point are shown in Figure 5-3 as a function of the dispensing pressure (Figure 5-3a) and as a function of nozzle tip diameter

(Figure 5-3b), referenced to the control group sample measured at 0 and 7day culture time points.

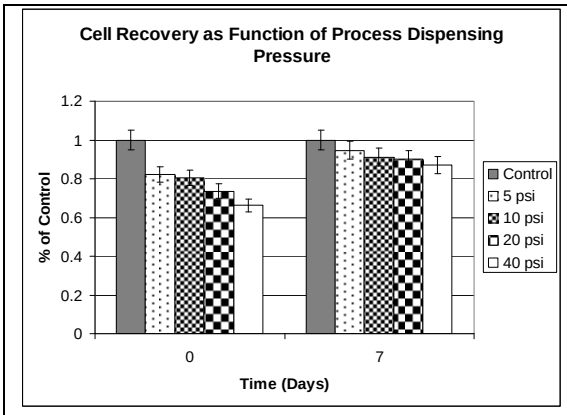

(a)

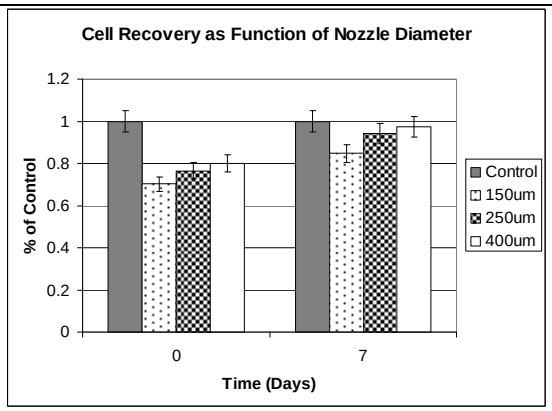

(b)

Figure 5-3: Cell recovery as referenced to control group for 7-day study. (a) cell recovery as function of dispensing pressure; (b) cell recovery as function of nozzle diameter

All experimental groups for dispensing pressure (i.e., 5, 10, 20, and 40 psi) show significant cell recovery at the 7-day study endpoint with cell viability at 94.67, 91.07%, 90.02%, and 87.06% of control values. The smallest nozzle diameter group (i.e., 150 μm) shows significantly diminished cell recovery with percentage cell viability of the control at 7 days of 84.70%. The larger nozzle diameter experimental groups (250 and 400 μm) again shows comparatively higher cell recovery at the study's endpoint with cell viability at 94.13% and 97.33% of the control values.

Figure 5-4 shows the percentage of cell recovery by comparison of the cell viabilities at two culture time windows: 0 hr to 6 hr and 0 hr to 24 hr as a function of pressure (Figure 5-4a) and nozzle tip diameter (Figure 5-4b).

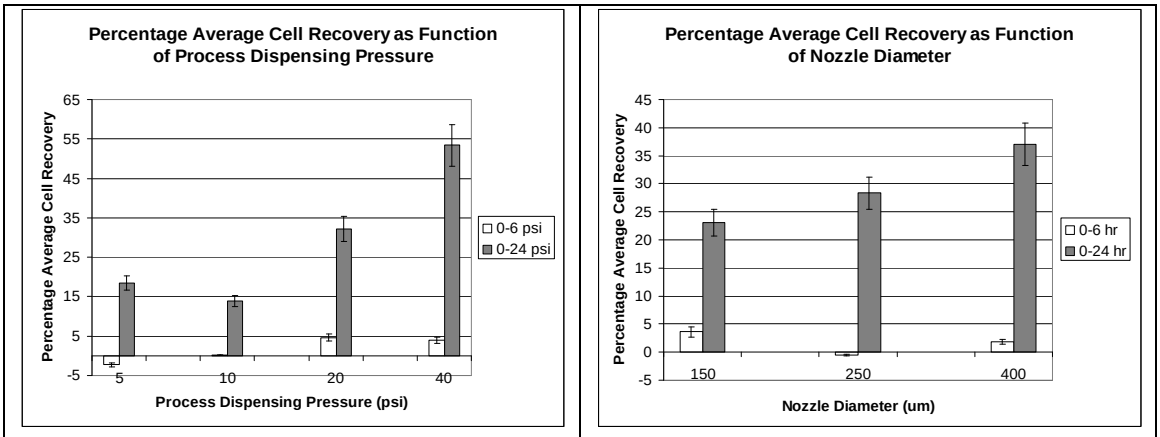

(a) (b)

Figure 5-4: Percentage of cell recovery for 24-hr study. (a) percentage of cell recovery function of dispensing pressure; (b) percentage of cell recovery as function of nozzle diameter

From the cell recovery data presented in Figure 5-4, different cell recovery sensitivities are observed for the process parameters: cell recovery is higher for high pressure (i.e., percentage recovery: 53.39% at 40 psi averaged over all nozzle tip diameters), see Figure 5-4a, and cell recovery is less for small nozzle tip diameter (i.e, percentage recovery: 23.07% at 150 um average over all pressures), see Figure 5-4b. The observed values for percentage recovery over the first 6 hours of study for the three nozzle tips (i.e., 150, 250, 400 μm) are 3.64%, -0.54%, and 1.81% respectively. The percentage recovery over the 24-hr period for the three nozzle diameters (i.e., 150, 250, and 400 μm) is 23.07%,

28.31%, and 37.04% respectively. The percentage recovery over the first 6 hours of study for the dispensing pressures (i.e., 5, 10, 20, and 40 psi) is -2.23%, 0.20%, 4.59%, and 4.03% respectively. The percentage recovery over the 24-hr period for the dispensing pressure (i.e., 5, 10, 20, and 40 psi) is 18.44%, 13.84%, 32.23%, and 53.39% respectively.

Figure 5-5 shows the percentage of cell recovery by comparison of the cell viabilities at two culture time windows corresponding to the longer study period: 0 day to 3 day and 0 day to 7 day as a function of pressure (Figure 5-5a) and nozzle tip diameter (Figure 5-5b).

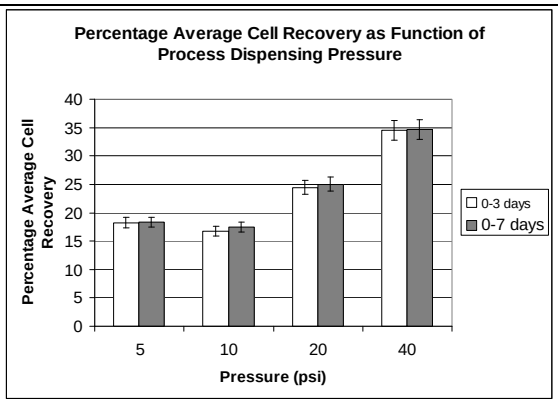

(a)

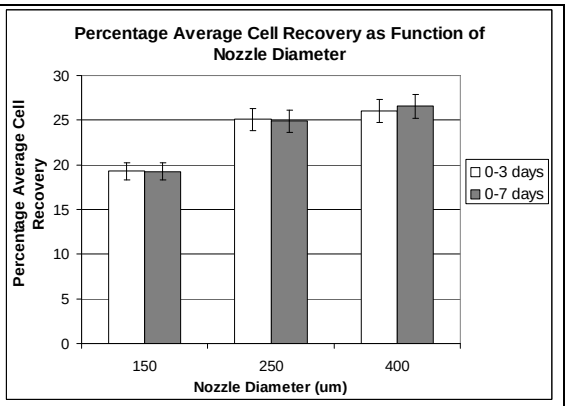

(b)

Figure 5-5: Percentage of cell recovery for 7-day study. (a) percentage of cell recovery function of dispensing pressure; (b) percentage of cell recovery as function of nozzle diameter

Comparing the cell recovery data from these two culture windows presented in Figure 5-5, no new significant cell recovery occurs after a certain time point for both process

parameters studied. The observed values for percentage recovery over the first 3 days of study for the three nozzle tips (i.e., 150, 250, 400 μm) are 19.29%, 25.09%, and 26.07% respectively. The percentage recovery over the entire 7-day period for the three nozzle parameters (i.e., 150, 250, 400 μm) is 19.26%, 24.90%, and 26.56%, respectively. The percentage recovery over the first 3 days of study for the dispensing pressures (i.e., 5, 10, 20, 40 psi) is 18.25%, 16.74%, 24.47%, and 34.45% respectively. The percentage recovery over the 7-day period for the dispensing pressures (i.e., 5, 10, 20, 40 psi) is 18.35%, 17.46%, 25.04%, and 36.64% respectively.

5.3 Summary of Key Results and Conclusions

In the solid freeform fabrication based direct cell writing process, the application of external loads to cells is likely to occur at different spatial, temporal, and material levels during dispensing. Taking the reported cell dispensing system as an example, the mechanical disturbance may be contributed by the dispensing pressure, deposition speed, the dispensing nozzle size and length, and the hydrogel rheological properties. The preliminary cell viability and recovery data suggest that during and after dispensing, cells may have three distinct responses: (1) survival with desired phenotype (i.e., capable of proliferation), (2) survival but quiescent, or (3) necrosis. As time passes, cells in a quiescent state may also demonstrate three further behaviors: (1) sustain mechanical stress but able to recover original capabilities, (2) phenotypic change and/or de-differentiation, or (3) have undergone damage leading to apoptosis.

During the 24-hr study, increases in quantitative cell viability (cell recovery) over time may have been attributed to initial process-induced mechanical cellular attrition, which is reversible with time for quiescent cells. This is a safe assumption as the control group demonstrates no change in cell viability during 24-hr period due to a cell-immobilizing alginate gel matrix. Therefore, no cell proliferation is observed throughout the study period and we considered that the increases in cell viability after time may be attributed to cell recovery from the mechanical pertubation. Comparing the two dispensing parameters studied (i.e., dispensing pressure and nozzle diameter) during the 24-hr cell viability study, the average cell viability and/or cell recovery appears more likely to increase due to reduced dispensing pressure than increased nozzle diameter. Furthermore, different cell recovery results at the extreme conditions are observed (i.e. 53.39% at 40 psi versus 23.07% at 150 um). Differences in the initial viability and eventual recovery may indicate differences in the severity and type of mechanical on the dispensed cells. Furthermore, the cell recovery for the longer time point 7-day study shows no significant cell recovery between the initial culture window to the study endpoint, which indicates that the majority of cell recovery occurred over the first 24 hours.

When a functioning live cell is impinged upon by the dispensing process, the array of mechanical forces sustained by the cell may result in a number of distinctive outcomes. Specifically, mechanically-induced damage to cell viability, as shown during short-term studies (i.e., 24 hr), appears likely to affect construct viability more than all other scaffold rendering parameters. The results of this study suggest that the effect of

dispensing parameters on cell viability initially may be reversible with time, and the severity of the effects of the two parameters studied here, cell dispensing pressure and nozzle diameter, on cell viability and/or eventual recovery response was not equally contributory. Also, taking both the 24-hr and 7-day cell recovery studies herein into account, a significant cell recovery from mechanical process-induced damage appears to take place over the first 24 hours with no significant cell recovery thereafter. This may provides a necessary temporal benchmark for functional study and perfusion flow studies of dispensed hepatocytes through the direct cell writing process.

CHAPTER 6. BIOLOGICAL CHARACTERIZATION OF BIOPRINTED THREE-DIMENSIONAL MICRO-ORGAN

6.1 The Rational for Bioprinting Three-dimensional Tissue Constructs

6.1.1 Three-dimensional Scaffolds for Enhanced Osteoblastic Function

Although microfluidics has naturally catalyzed the development of miniaturized two-dimensional culture for *in vitro* use, development of three-dimensional microscale bioreactors is a relatively novel approach in tissue engineering (Khetani et al., 2006, Eschbach et al., 2005, Kane et al., 2006). The ability to bioprint three-dimensional structures into a microfluidic system is extremely important because of studies indicating that three-dimensional culture can produce significant differences in cell functional behavior (Abbot 2003, Weaver et al., 1997, Wolf et al., 2003, Sahai et al., 2003).

A comparison study of biological cell proliferation and function of osteoblasts cultured using two types of 3D Insert™ versus two-dimensional conventional monolayer is conducted. The 3D Insert™ are polymeric three-dimensional porous constructs designed for use with multi-well polystyrene tissue culture plates. They are fabricated by 3D Biotek, LLC through a precision extrusion deposition (PED) type freeform fabrication process, with a layer pattern of a 0°/90° orientation and defined, controlled three-dimensional porous structures of variable pore sizes ranging from 300 μm to 500 μm. The 3D InsertTM materials include both a biodegradable polymer: polycaprolactone (PCL), and a non-biodegradable polymer: polystyrene (PS), respectively. PCL has been extensively studied as a biodegradable scaffold material for bone tissue engineering

applications and PS is a transparent, non-cytotoxic material conventionally used in various two-dimensional cell culture vessels. A 14-day study using a rat osteoblast cell line was conducted comparing 3D Insert™ of PCL and PS with two-dimensional monolayer culturing, as well as the effect of varying pore size and relative enhancement over a two-dimensional monolayer control group. A fluorometric indicator of cell metabolic activity was performed to determine cell proliferative capacity along with ALP activity, a measure of osteoblast cell function. The ability to fabricate porous PCL and PS 3D Insert™ using freeform fabrication system was demonstrated with accuracy and process repeatability for defined, controlled microstructures and physiologically relevant pore sizes. Biological characterization data of osteoblastic cell function are shown in Figure 6-1.

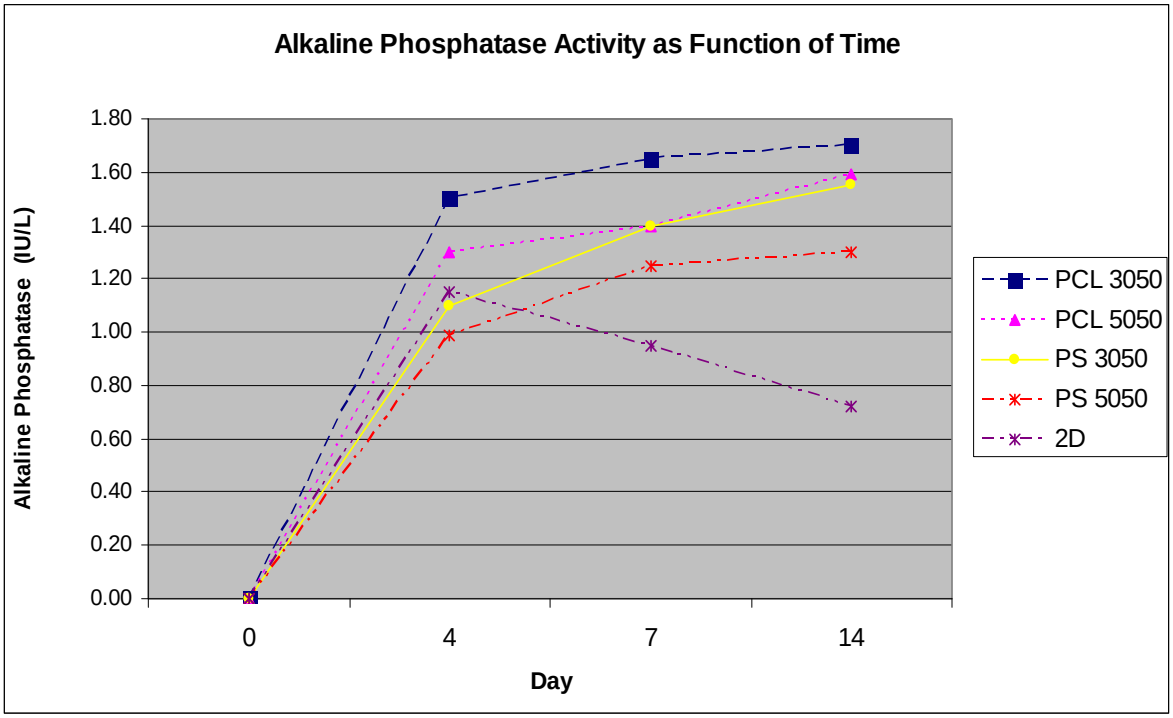

Figure 6-1: Comparison of alkaline phosphatase activity for PCL and PS 3D InsertTM with two-dimensional conventional monolayer culture

For the same number of cells, the experimental data suggests that at certain time points, the precipitous decrease in fluorescent intensity in the case of two-dimensional monolayer culture is due to the over-confluence of cells on the two-dimensional surface in which case cells can no longer spread, undergo contact inhibition, and leads to gradual loss of viability. Cell functions in the 3D Inserts™, for both the PS and PCL samples are improved from two-dimensional monolayer culture. From proliferation studies, PS is observed to exhibit a steeper proliferation curve compared to PCL. For both 3D Inserts™, the smaller pore size of 300 um (samples 3050 in Figure 6-1) had a steeper proliferation curve compared to that of with the larger pore size of 500 um (samples 5050 in Figure 6-

1). This may be attributed to larger pore sizes leading to lower seeding efficiency initially (as cells may fall through larger pores). The general trend of the graph of alkaline phosphatase activity (Figure 6-1) shows that the cell function is higher in the three-dimensional case early on. This advantage conferred to the three-dimensional culture systems becomes even more significant at days 7 and 14 as cells grow on the three-dimensional structure and the two-dimensional counterpart reaches overconfluence.

6.1.2 Three-dimensional Tissue Constructs for Enhanced Hepatocyte Function

Three-dimensional cell growth does not merely resemble the geometry of *in vivo* tissue, but is a basic requirement for the cells to retain their differentiated phenotype through cell-to-cell interactions as three-dimensional cellular aggregates. The aim of this 3-day functional study is to evaluate the implications of a bioprinted three-dimensional structure on a measure of hepatocyte-specific function, namely urea synthesis. The experimental setup for this study involved one experimental test sample and one control. The experimental test sample was the bioprinting of a three-dimensional hepatocyte/alginate tissue construct. The control group selected is a two-dimensional hepatocellular monolayer with equivalent cell number as the test sample. In Figure 6-2, urea synthesis is quantitatively detected with a cell-based colorimetric assay, allowing comparison of time-dependent phenotype for bioprinted cell-encapsulated hepatocytes with controls cultured as a hepatocellular monolayer.

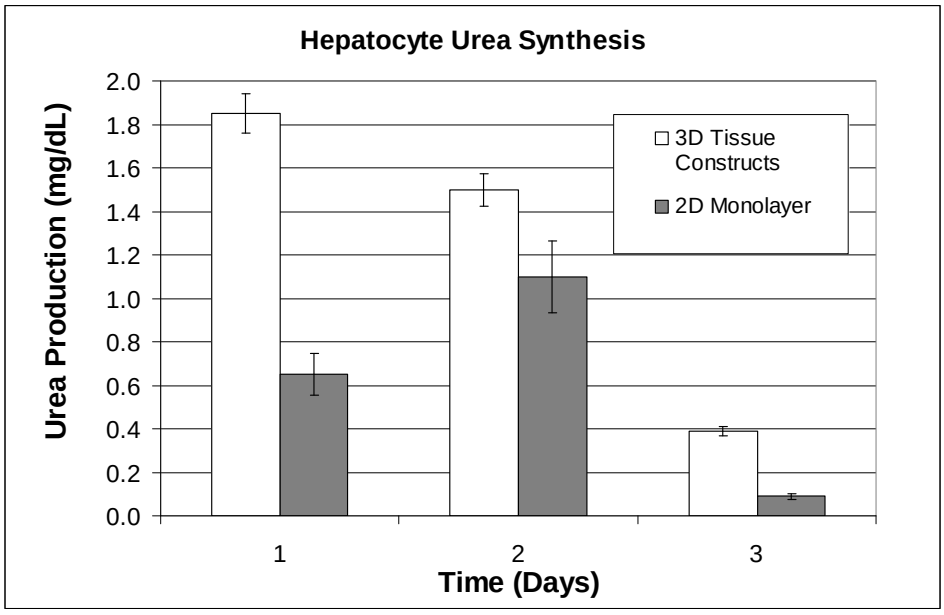

Figure 6-2: Results of 3-day urea synthesis study of bioprinted hepatocyte embedded alginate tissue constructs

Cell medium is replenished for both the test sample and control once per day. Each data point constitutes an average of 5 samples taken at Days 1, 2, and 3 after bioprinting. This data suggests that a hepatocytes encapsulated in a three-dimensional alginate/hepatocyte tissue construct synthesizes a higher amount of urea than the same number of hepatocytes cultured as a two-dimensional hepatocyte cell monolayer. This difference is most striking on Day 1, where the three-dimensional tissue construct shows a marked urea concentration of 1.90 mg/mL compared to a two-dimensional hepatocyte cell monolayer urea concentration of 0.65 mg/mL. While the marked dropoff in urea synthesis at Day 3 is typical of *in vitro* culture, the three-dimensional microenvironmental structure confers an ability for increased urea production relative to the two-dimensional monolayer case.

Therefore, this demonstrated that the bioprinting process for microencapsulation of hepatocytes in three-dimensional alginate tissue constructs is compatible with enhancement of hepatotocellular specific function compared to its two-dimensional counterpart.

5.2 Effect of Material Properties on Liver Cell Metabolic Function

Prior to drug perfusion flow cultures, experiments are conducted to first establish optimal experimental conditions for the drug metabolic response of hepatocytes encapsulated in a three-dimensional bulk alginate tissue constructs under bioprinted conditions and subsequent static culture. In the first set of experiments, the quantitative effect of alginate concentration in variable media volumes upon the drug metabolism of the HepG2 cells encapsulated in alginate bioprinted constructs is assessed. In the second set of experiments, the effect of cell type, cell confluency, cell seeding density, and media volume on drug metabolism is evaluated for HepG2 cells encapsulated in alginate bioprinted constructs.

In the liver, cytochrome P450 enzyme complexes are the major players in the oxidative metabolism of a wide range of structurally diverse xenobiotics including drugs. Several model probe substrates for specific P450 enzymes have been identified that can produce highly fluorescent metabolites in aqueous solutions. The measurement of drug metabolism in this thesis are all based on the metabolic conversion of the drug 7-Ethoxy-4-(trifluoromethyl)coumarin (EFC) to 7-Hydroxy-4-(trifluoromethyl)coumarin (HFC) by

the enzyme 7-Ethoxycoumarin O-deethylase found in several P450 enzymes as shown in the metabolic reaction in Figure 6-3.

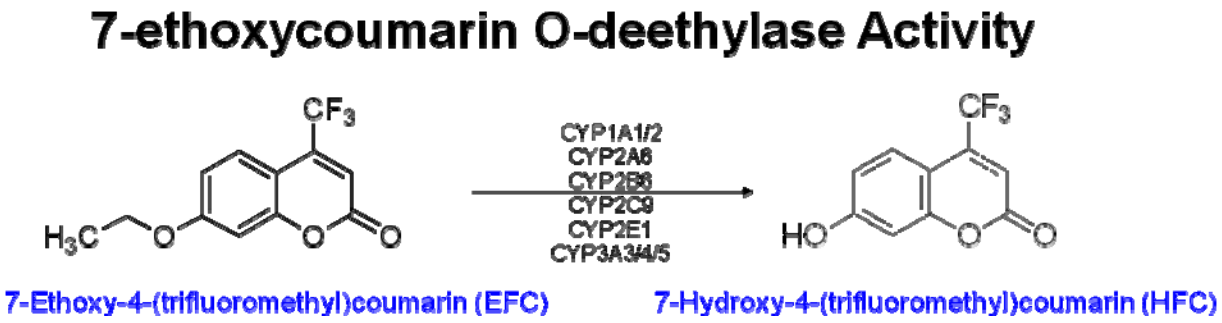

Figure 6-3: EFC as a suitable fluorogenic substrate probe

Although the P450 enzymes are heterogously expressed in the hepatocyte (e.g. O-deethylation of EFC is known to occur in several different P450 enzymes), for CYP2B6 activity, EFC has been demonstrated to have the best fluorescent probe properties with highest metabolic rates and lowest background fluorescence (Donato et al. 2004).

In all experiments, drug metabolism by measuring fluorescent readings correlating with drug metabolite HFC concentrations. The fluorescent emission and excitation behavior of both drug reactant and metabolite are assessed and shown in Figure 6-4.

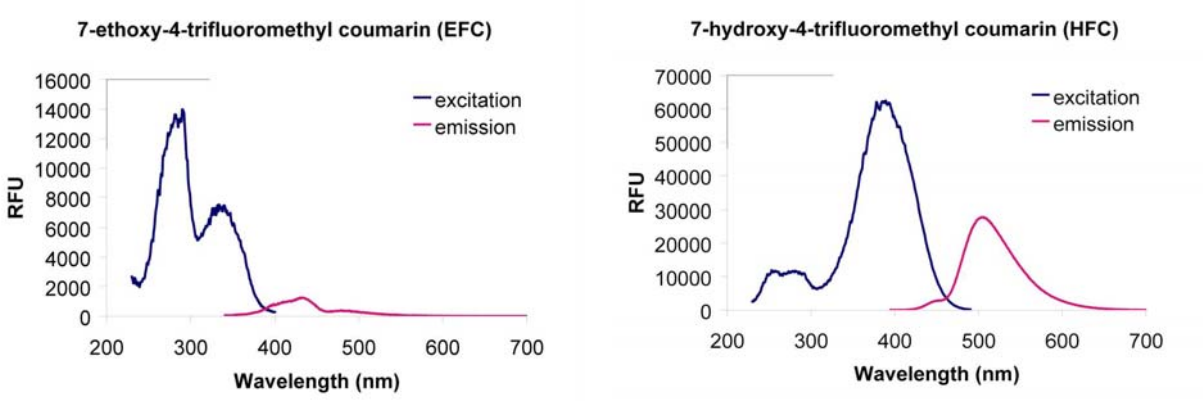

Figure 6-4: Emission and excitation wavelengths of EFC and HFC.

Based on these results, we are able to optimally measure drug excitation and emission at 360 nm and 520 nm, respectively, with the cytofluoremeter.

The quantitative effect of alginate concentration upon the drug metabolism of the HepG2 cells encapsulated in alginate bioprinted constructs is first studied. Each sample comprises of a bioprinted bulk HepG2-embedded construct. The results are tabulated below in Figure 6-5.

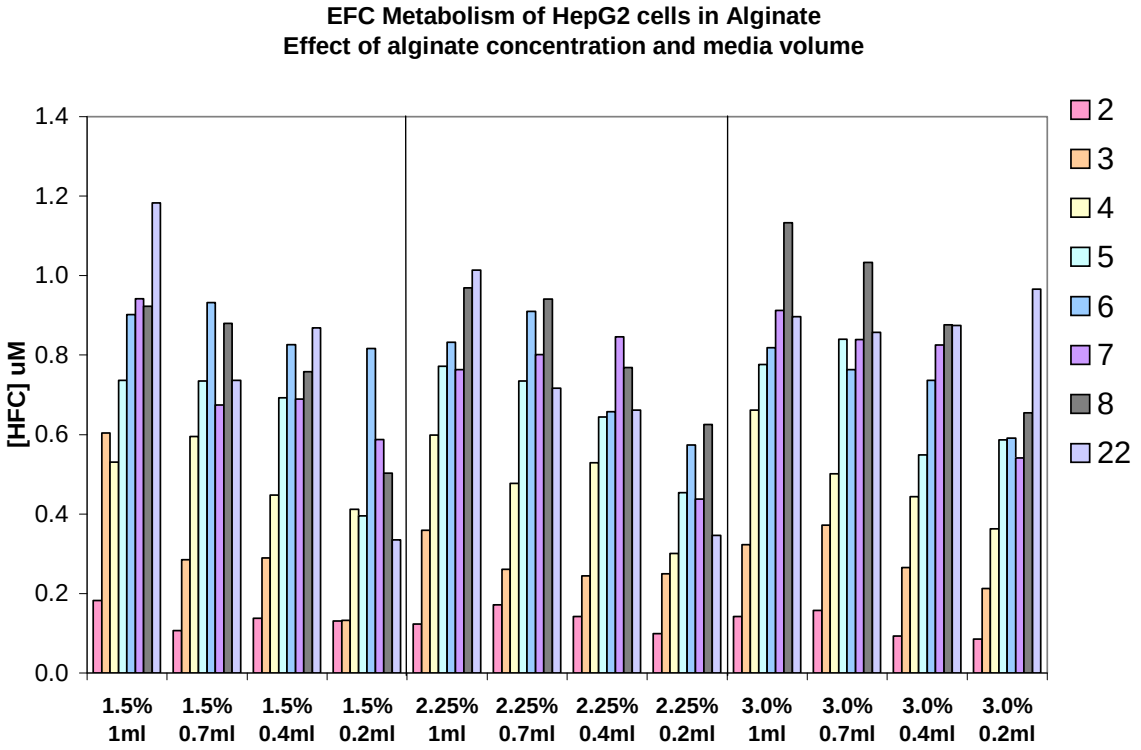

Figure 6-5: Effect of alginate concentration and media volume on bioprinted HepG2-embedded alginate constructs

Since the cell concentration of encapsulated hepatocytes can vary over a wide range, the cell concentration would be expected to have a major influence on the metabolic activity of encapsulated hepatocytes, which are affected by influences like cell-cell contact or mass transfer limitation at higher concentrations. However, the study for the variation of alginate concentration (1.5%, 2.25%, 3.0% w/v) on drug metabolism does not demonstrate any effect on percentage of drug conversion. The explanation for this may be attributable to the small solute size (i.e. drug) which, as a virtue of its small molecular weight , increasing the amount of material (and therefore decreasing the amount and size

of micro-pore spaces between alginate chains for the drug to diffuse through) is not enough to hinder diffusion of such a small solute. Therefore, from the perspective of the drug particles, navigating through the 3.0% alginate is as easily accessible to the encapsulated cells as the 1.5% alginate. While this is the window for the material parameters that we studied since literature values for alginate are typically between 1.5-3.0% as well as suitable for our biomanufacturing process, appreciable differences in drug conversion may be observed at lower or higher concentrations if such a study were conducted. The study for the variation of media volume on drug metabolism also does not show any differences on percentage of drug conversion. It should be clarified that the media volume did have an effect on the amount of drug being metabolized, however, not on the percentage of drug being metabolized. The reason is that the concentration of drug in all of the studies are kept constant. Therefore, for example, a volume of 0.2mL would have only one-fifth of the amount of drug solute in a volume of 1.0mL. Therefore, the media volume with 1.0mL will have higher HFC product because it had more EFC reactant to begin with. However, the drug conversion, i.e. the percentage of drug actually converted is the same for all media volumes studied, whether working at higher or lower media volumes.

6.3 Effect of Cell Culture Conditions on Liver Cell Metabolic Function

In this set of experiments, the effect of various cell culture conditions (i.e. cell confluency, cell type, cell seeding density) on drug metabolism is evaluated for HepG2 cells encapsulated in alginate bioprinted constructs. The nutrient media conditions are particularly essential in the culture of hepatocytes which are highly metabolic cells that

have high oxygen uptake rates compared to many other types of mammalian cells (Balis et al., 1999, Foy et al., 1994).

In conventional two-dimensional cell culture biology, confluency refers to the coverage or proliferation that the cells are allowed over or throughout the culture medium. Typically, after confluence is reached (i.e. all the available growth area is utilized and cells make close contact with one another), specific cells whose growth is sensitive to density limitations and subsequent contact inhibition will stop dividing. Therefore, maintaining a low cell density (e.g. 40-60% confluence helps to presernve the normal phenotype in cultures such as mouse fibroblasts, in which spontaneous transformants tend to overgrow at high cell densities (Todaro et al., 1963). However, a general trend observed for many cell types, e.g. hepatocytes and chondrocytes, is that cells permitted to aggregate in culture are more functional and longer survivability due to enhanced cell-cell interactions (Glicklis et al., 2000). Therefore, a prefatory study of cell confluency is conducted in which the experimental groups are categorized into 3 groups of increasing culture confluency before trypsinization and subsequent bioprinting and assay: confluence, 3-day confluence, and 5-day confluence. The results are shown in Figure 6-6 at an initial reactant concentration of 120 uM EFC and variable initial cell seeding densities.

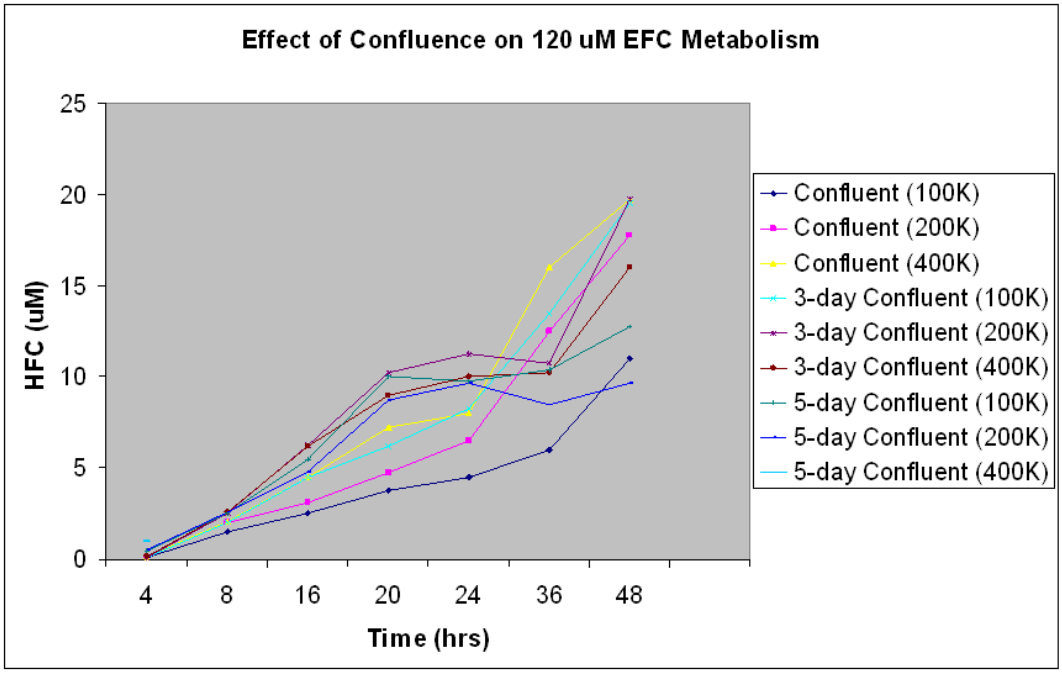

Figure 6-6: Effect of cell confluency on 120 uM EFC metabolism

This result indicates the 3-day confluent cells are most suitable for conducting short term drug metabolism studies.

In this thesis, immortalized hepatocytes are used in lieu of primary hepatocytes due to ease in handling, stable phenotype over time, and amenability to multiple generation of subcultures. Primary human hepatocytes represent the more pertinent model for short-term *in vitro* drug metabolism since they express higher levels of the P450 enzymes. However, as with other mammalian primary hepatocytes, they exhibit a limited growth activity and early phenotypic alterations. Hepatocyte cell lines, mainly originating from tumors (e.g. the hepatoblastoma HepG2), possess an indefinite capacity for proliferation (Castell et al., 2006). In the next set of studies, two human cell lines of

immortalized hepatocytes are compared for their relative drug conversion capabilities as shown in Figure 6-7.

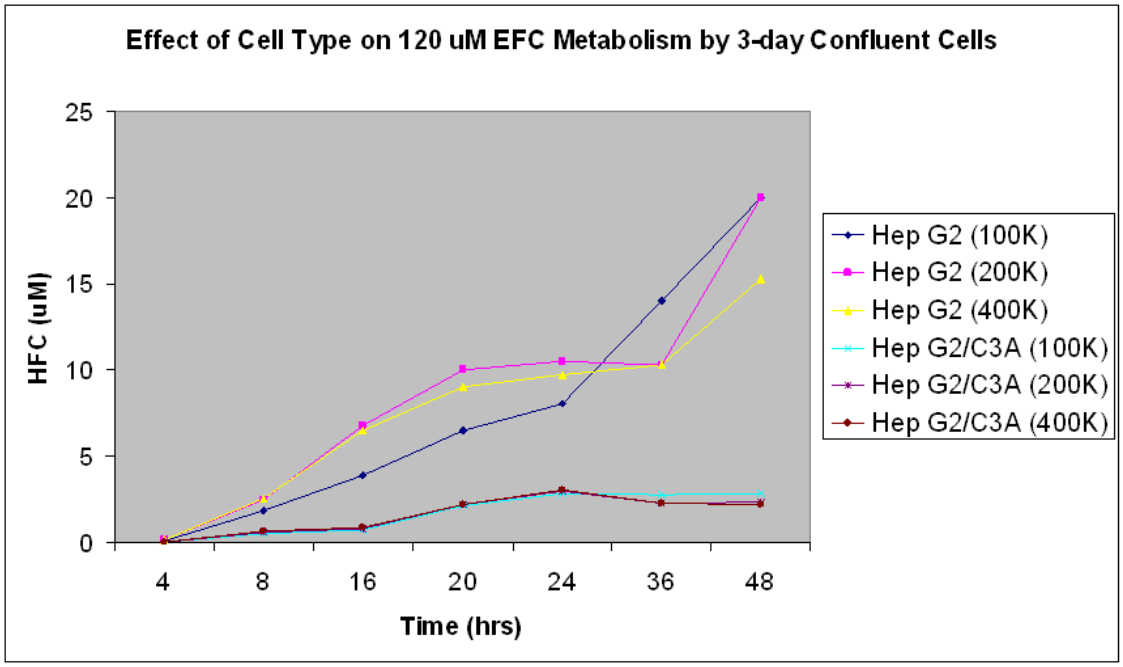

Figure 6-7: Effect of cell type on 120 uM EFC metabolism

HepG2 shows betters metabolic conversion compared to the HepG2/C3A subclone. This difference is even more pronounced for initial reactant concentrations of 30 uM EFC and 60 uM EFC, respectively, shown in Figure 6-8 and 6-9.

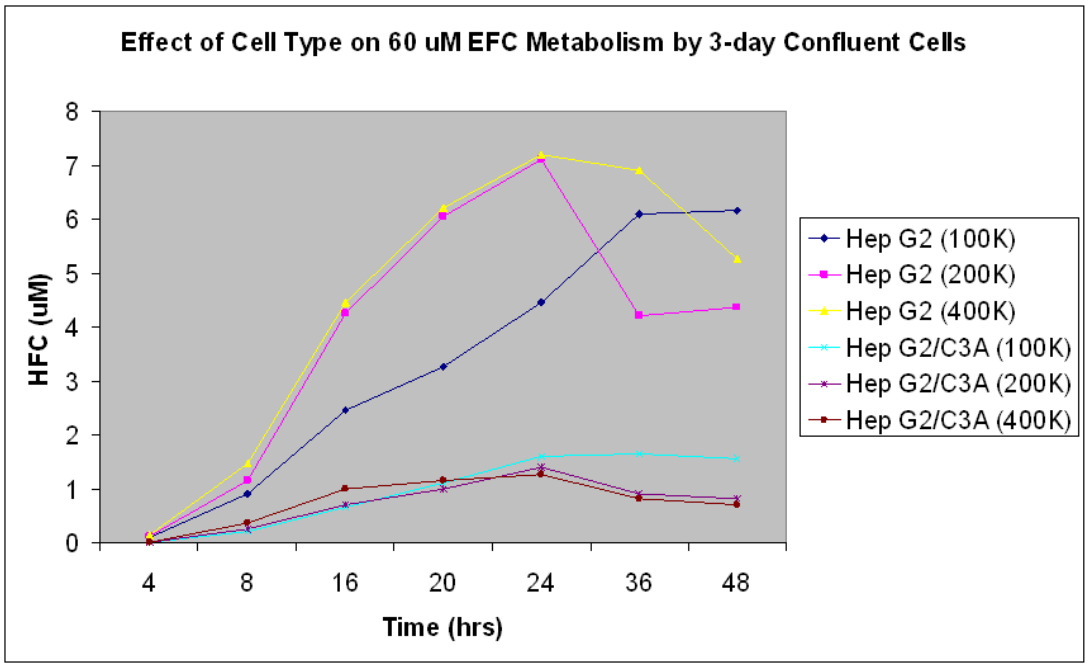

Figure 6-8: Effect of cell type on 60 uM EFC metabolism

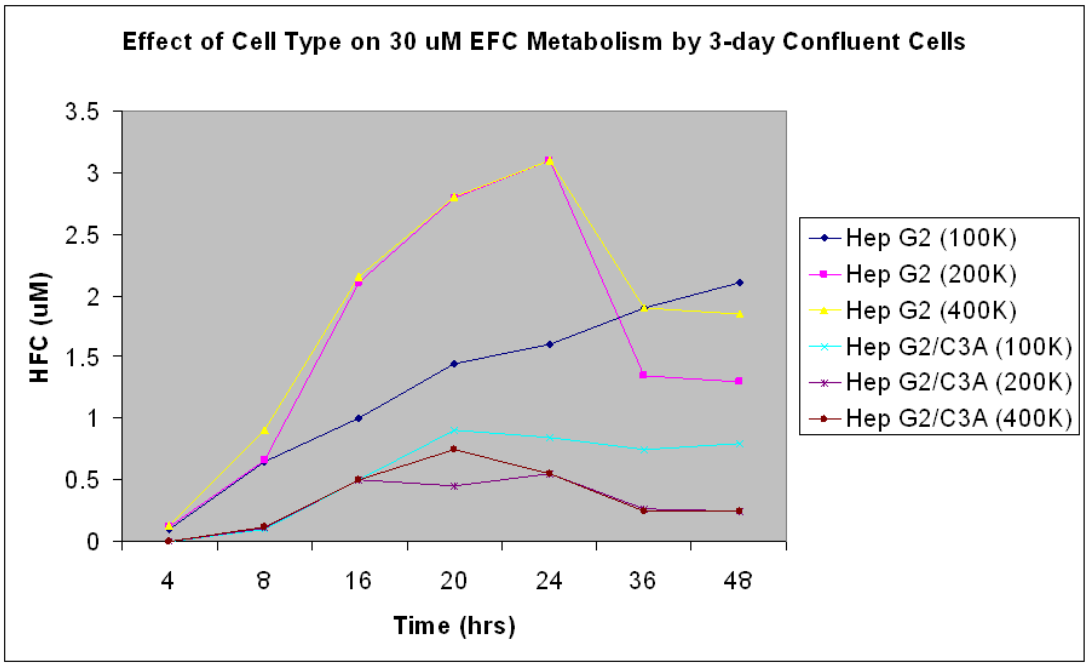

Figure 6-9: Effect of cell type on 30 uM EFC metabolism

6.4 Drug Perfusion Studies

6.4.1 Structural Formability of Bioprinted Sinusoidal Liver Micro-pattern

The ability to manufacture porous scaffold structures based on designed porosity, pore size, and pore interconnectivity in a reproducible, precise, and timely manner would be quite valuable for tissue engineering constructs. With the direct cell writing system, due to variable ambient conditions during the biopolymer deposition, there may exist slight differences between the designed construct pattern dimensions and the manufactured ones. In order to assess the reproducibility and detect variability of this biofabrication process for precise three-dimensional structural formability, a series of measurements are done on five different location of each tissue construct. A live/dead assay was performed on representative roadwidths for each strut size specification with encapsulated live cells indicated as green in Figure 6-10:

(a) 150 um road widths

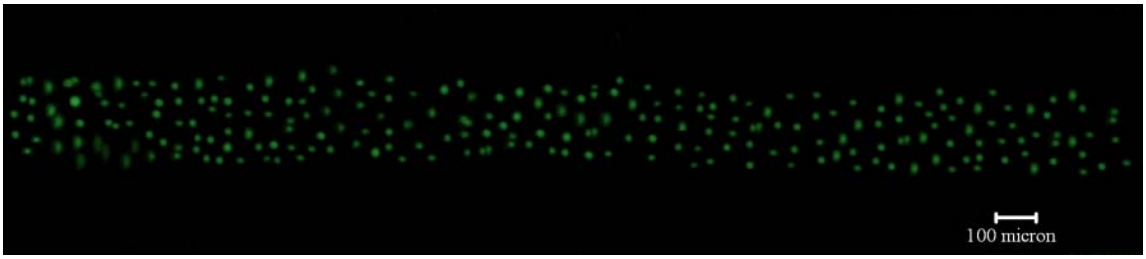

(b) 250 um road widths

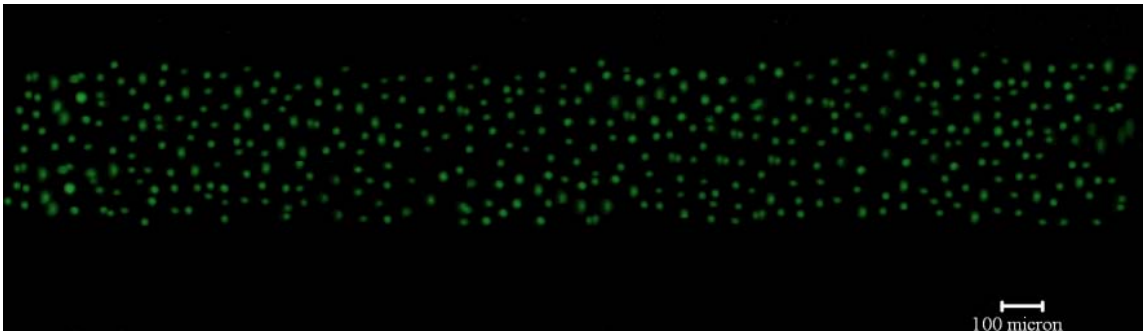

(c) 400 um road widths

Figure 6-10: Structural formability for design specifications

The measurement data for 15 scaffolds (n=5 for each strut width design specification) and the solid model of the designed tissue construct are summarized in Table 6-1

Strut Width Design Specification	Strut Width	Pore size (μm)
1A (250 um)	235±8	240±7
2A (250 um)	240±4	241±5
3A (250 um)	239±6	239±7
4A (250 um)	242±5	252±3
5A (250 um)	239±9	251±6
1B (150 um)	158±5	251±6
2B (150 um)	155±10	246±9
3B (150 um)	149±6	248±11
4B (150 um)	147±3	240±6
5B (150 um)	157±7	248±11
1C (400 um)	420±7	251±7
2C (400 um)	417±7	253±9
3C (400 um)	415±7	258±6
4C (400 um)	409±7	252±8
5C (400 um)	410±7	256±7

Table 6-1. The strut width and pore size measurements of fifteen tissue constructs manufactured by direct cell writing

Based on the measurements data given in Table 6-1, the average strut width for the 250 um, 150 um, and 400 um strut width design specifications are 239 μm, 152 μm, and 411 μm. The ± represents standard deviation of five different measurements of the constructs. This corresponds to an accuracy of 90% based for the designed strut widths. This data demonstrates a highly precise and reproducible biofabrication process typical of layered biomanufacturing techniques.

6.4.2 Drug Metabolic Function of Liver Micro-organ Under Continuous Perfusion Flow

A study is conducted to see the effect of dynamic drug perfusion flow through an *in vitro* three-dimensional Microfluidic Microanalytical Micro-organ Device (3MD) on the metabolic drug conversion in bioprinted alginate-encapsulated HepG2 liver cells. The tissue constructs (n=8) are first bioprinted into specified sinusoidal geometry directly into the PDMS tissue chamber.

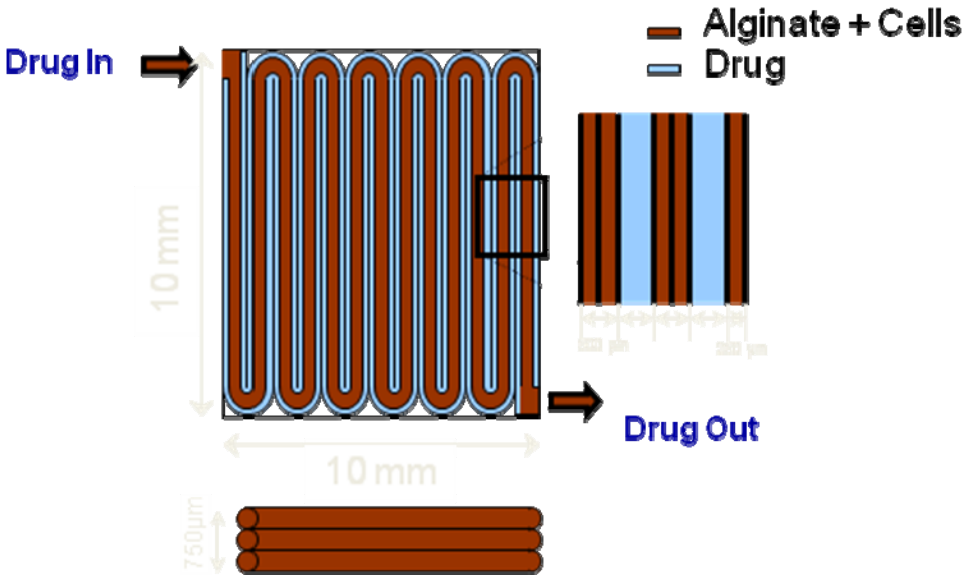

Figure 6-11: Specified three-dimensional sinusoidal design pattern for bioprinted liver construct

The controls (n=8) selected for the flow experiments are 1.) bioprinted three-dimensional static culture and 2.) two-dimensional monolayer in 24-well plate. In the control groups, both cell viability via live/dead stain and drug metabolic conversion are assessed at approximately 4 hrs and 24 hrs after bioprinting. For the experimental flow group, the

bioprinted cells are permitted to “recover” from the bioprinting process for 24 hrs. This recovery phase maintains the tissue chamber under media flow for adequate nutrient delivery. After 24 hours of media infusion, media/drug is infused at a rapid enough rate to fully purge system of the original media volume as shown in Figure 6-12.

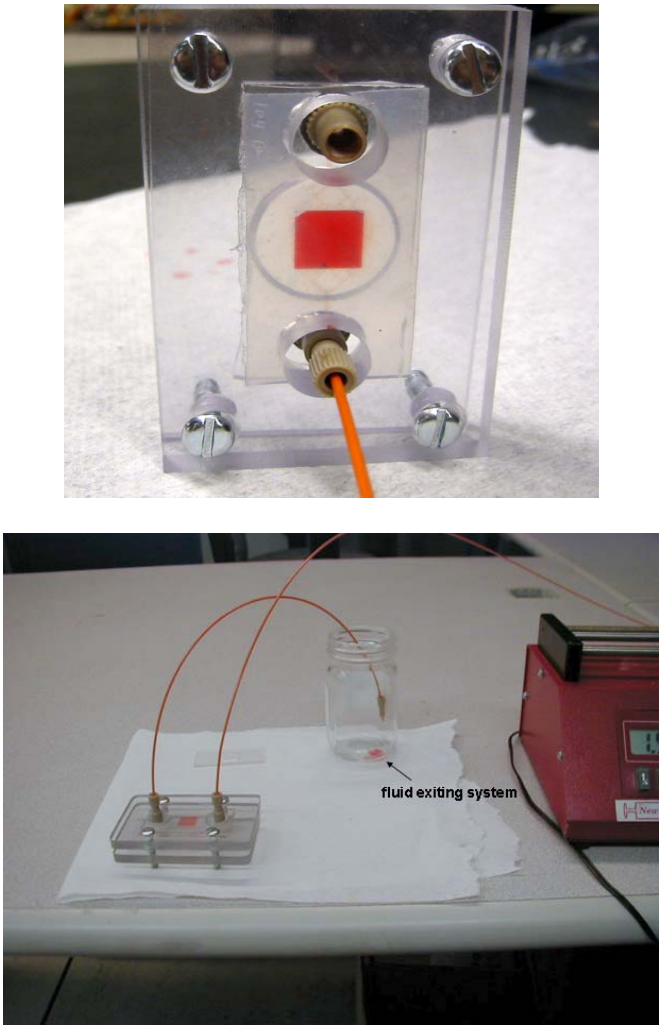

Figure 6-12: A fully perfused tissue chamber with drug and nutrient media and clamping device to maintain leakage-free flow

The flow perfusion setup or micro-bioreactor with simultaneous pumping and withdrawal of drug/media is incubated under physiological conditions and shown in Figure 6-13 below.

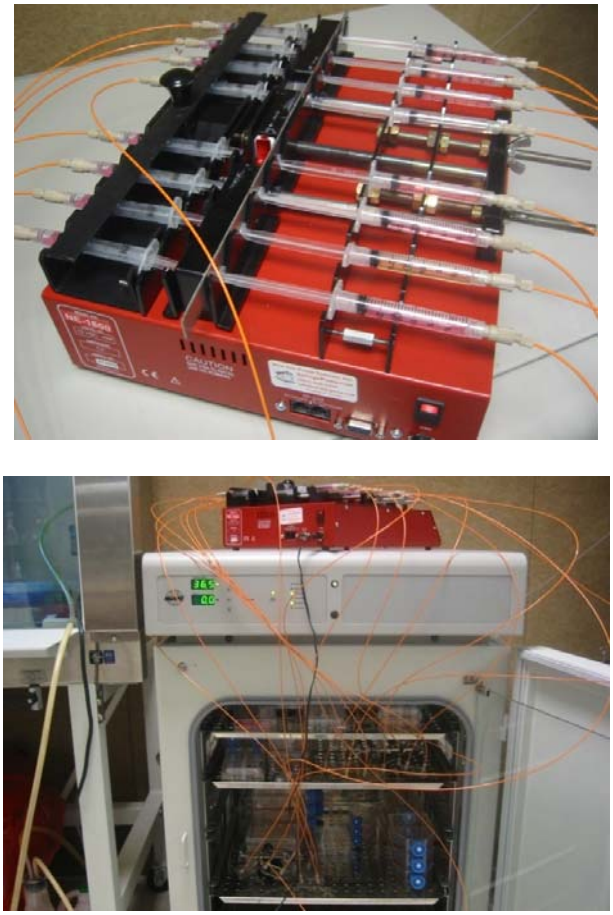

Figure 6-13: Drug flow perfusion setup for parallelization study

In order to ensure 4-hour residence time in the tissue chamber, the infusion flow rate is calculated and adjusted to 0.015 mL/hr. This flow rate is maintained for another 48 hours to purge tubing and collect adequate drug effluent volume in the withdrawal tube for cytofluoremeter sampling.

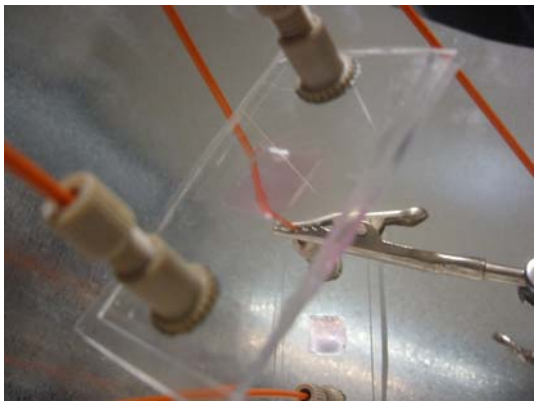

Figure 6-14: A fully perfused tissue chamber with drug/media

Therefore, the fully perfused tissue chamber is a single micro-organ that is assayed for HFC drug metabolic conversion in Figure 6-14 with a drug residence time of 4 hours. The bioprinted three-dimensional static (n=4) is cultured in the incubator for an equivalent 4 hours. The bioprinted three-dimensional flow conditions confers an approximately 26% increase in HFC drug metabolic conversion as compared to the bioprinted three-dimensional static conditions in Figure 6-15.

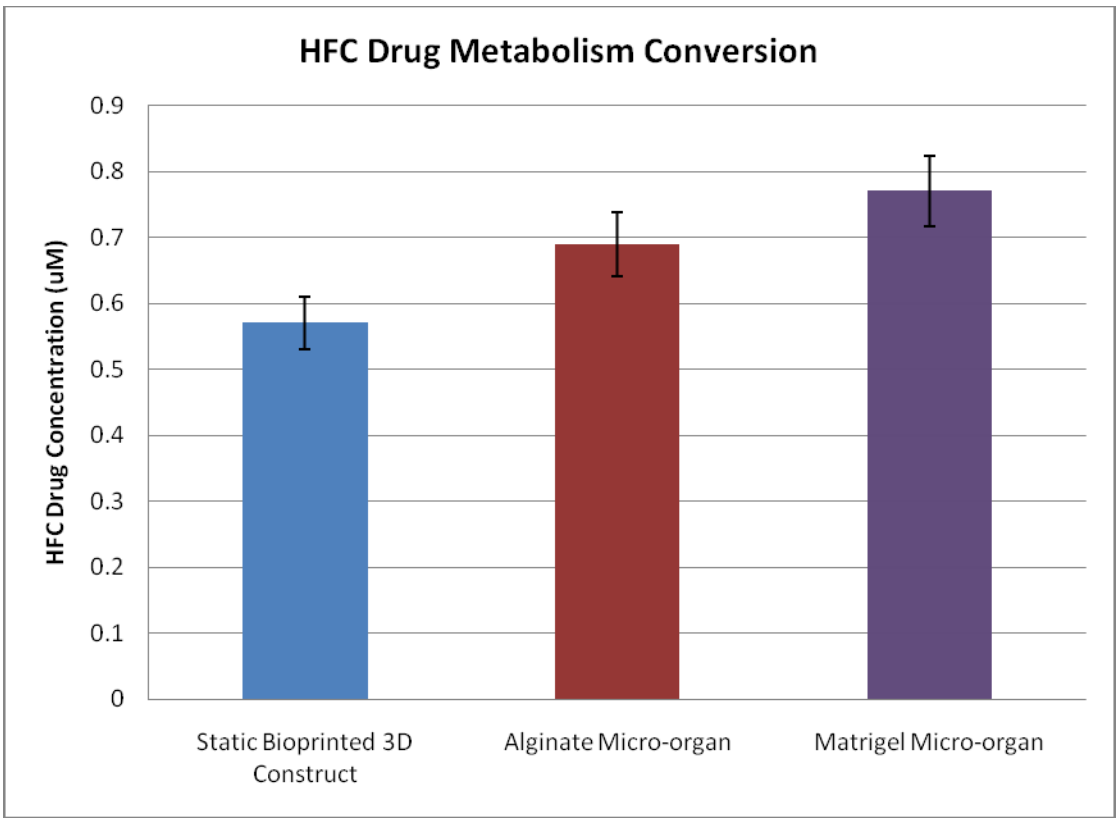

Figure 6-15: Metabolic drug conversion of bioprinted three-dimensional tissue constructs under static versus dynamic flow conditions with 4 hr residence time in tissue chamber

6.4 Summary of Key Results and Conclusions

In this chapter, the liver micro-organ is characterized biologically for its suitability as an *in vitro* drug metabolism platform under continuous perfusion flow. Preliminary to conducting the drug perfusion flow studies, static culture experiments are carried out to 1) validate the need for a three-dimensional microenvironment and 2) elicit the material parameters and nutrient media requirements favorable for optimal drug conversion. The rationale for a three-dimensional microenvironment is first tested, with enhanced

osteoblastic function exhibited on polystyrene scaffolds and liver-specific urea synthetic function exhibited in bioprinted tissue constructs. For drug metabolic function, the cell encapsulant material parameters varying alginate concentrations (1.5%, 2.25%, 3.0% w/v) on drug metabolism does not demonstrate any effect on the percentage of drug conversion. In a study of the extent of cell confluence on drug metabolism 3-day confluent cells are found to be most suitable for conducting short term drug metabolism studies. In a study of nutrient media requirements for bioprinted liver cell-embedded constructs, media volume did have an effect on the amount of drug being metabolized, however, not on the percentage of drug being metabolized. Finally, structural formability of sinusoidal patterned tissue constructs with the direct cell writing system was also assessed, demonstrating a highly precise and reproducible biofabrication process typical of layered biomanufacturing techniques. In the drug perfusion study, dynamic flow conditions for the bioprinted three-dimensional micro-organ device conferred an approximately 26% increase in HFC drug metabolic conversion as compared to the bioprinted three-dimensional static conditions, consistent with the that predicted from numerical methods and fundamental understanding of the liver microenvironment.

CHAPTER 7. SUMMARY, CONCLUSION, AND RECOMMENDATIONS

7.1 Summary of Research

A specific targeted novel application of biomanufacturing approaches includes the development of an *in vitro* drug metabolism model. Such an *in vitro* drug metabolism model can be realistically and reliably implemented to predict human response to various drug administration and toxic chemical exposure for NASA's interest of a flight-suitable drug metabolism platform in microgravity and planetary environments. A high-fidelity *in vitro* drug metabolism model is also important for the biopharmaceutical industry's interest in drug and toxicology screening prior to the pursuance of clinical drug trials. This research details the fabrication process development and adaptation of microfluidic devices for the creation of a pharmacokinetic model involving the combinatorial setup of an automated syringe-based, layered direct cell writing (DCW) bioprinting process with soft lithographic micro-patterning techniques to fabricate a microscale *in vitro* device housing a chamber of bioprinted three-dimensional micro-organ that biomimics the cell's natural microenvironment for enhanced performance and functionality. By designing and biofabricating various microscale three-dimensional physiological tissue engineered constructs within tissue chambers on a microfluidic chip, one can selectively model an interconnected network of differentiated mammalian tissues for a number of applications, among them pharmaceutical screening for drug efficacy and toxicity along with apprehension of the disposition and metabolic profile of a candidate drug. This thesis addresses issues related to the development and implementation of a unique bioprinting

process for freeform biofabrication of three-dimensional cell-encapsulated hydrogel-based tissue constructs with defined patterns, the direct integration onto a microfluidic device for drug metabolism study, and the underlying engineering science behind the flow pattern design and hydrodynamic conditions (e.g. wall shear stress) for perfusion of the three-dimensional microscale tissue chamber for drug metabolism study. To this end, a prototype three-dimensional microfluidic tissue chamber embedded with cells encapsulated within a hydrogel matrix construct is bioprinted as a physiological *in vitro* model for drug metabolic investigation.

7.2 Conclusion and Remarks

For millions of years, cells have been thought of as nature's building blocks that assemble to make us what we are. Broadly speaking, biomanufacturing uses cells and other bioactive factors as nature's basic building blocks from which biological models, systems, devices, and products are assembled. Biomanufacturing techniques encompass a broad range of physical, chemical, biological, and/or engineering processes, with various applications in tissue science and engineering, disease pathogeneses and drug pharmacokinetic studies, biochips and biosensors, cell printing, patterning, and assembly, and emerging organ printing. Many different cell manipulation techniques have been explored, such as syringe-based cell deposition for tissue constructs; bioassembly tools; rapid prototyping of hydrogel structures; inkjet-based cell printing; laser direct writing of mammalian cells and bacteria; microcontact printing; cell manipulation by mechanical, optical, electrical, magnetic, ultrasound, and ionic methods for microfluidics; and cell

patterning by photo- or electroetching, and soft lithography. As an interdisciplinary research area, tissue science and engineering will increasingly rely on biomanufacturing technologies to help establish a new knowledge base in applications including, as presented in this thesis, *in vitro* drug metabolism models.

7.3 Research Contributions

My research science and engineering contributions are as follows:

1) Developed the direct cell writing system to biofabricate three-dimensional patterned tissue constructs for direct integration on a microfluidic substrate to enable novel creation of a micro-organ device for *in vitro* drug metabolism study.

2) Studied bioprinting process parameters to optimize cell viability in drug perfusion studies.

3) Studied material/culture conditions to optimize drug metabolic function in drug perfusion studies.

4) Developed a framework of an engineering analysis model to predict effect of liver flow pattern design/conditions on drug metabolism.

7.4 Future Work and Recommendations

7.4.1 Novel Temperature-Controlled Printing System for the Solid Freeform Fabrication of Cell-Laden Matrigel Constructs

Matrigel is a promising natural biomaterial that is currently being studied as a basis for pharmacokinetic models. Matrigel's composition of natural biopolymers mimics *in vivo*

microenvironments, facilitating better cell viability, differentiation, and function in a cell-embedded tissue construct. However, Matrigel's use in solid freeform fabrication techniques, the sequential delivery of cell-seeded biomaterials to specified points in space, has been limited by its unique thermo-physical properties as it is a fluid that liquifies below 4^{o}C and constitutes a cross-linked gel at physiological temperature of 37^{o}C. Current biofabrication systems such as the direct cell writing system cannot be trivially adapted to bioprint Matrigel, as the material occludes the bioprinting apparatus, which operates at room temperature. To overcome these current obstacles in the biofabrication of Matrigel constructs, the development of a miniaturized temperature-controlled printing system has been proposed with the ability to maintain a suitable temperature at or below 4^{o}C and create cell-laden patterned Matrigel constructs. During an early research and development phase, temperature-controlled enclosure has already been produced along with a Matrigel delivery system, and an integrated and automated motion system. Currently, the prototype is being tested by printing rat tail tendon collagen type I as a Matrigel model material, as the high cost of Matrigel limits its availability for testing. Successful patterned constructs have been created, with significant increase in printing ability in the sample maintained at approximately 4^{o}C as compared to the room temperature control.

7.4.2 Direct Cell Writing Into Multichambers for In Vitro Radiation Model

An ongoing extension of the collaboration with NASA is the creation of a multichamber, multicellular *in vitro* model for studying drug radioprotection. Firstly, the direct cell writing system is implemented to bioprint patterned three-dimensional constructs of

viable epithelial cells. The two distinct cell types, hepatocytes (HepG2) and melanoma cells (M10) will be encapsulated in Matrigel and printed via a temperature/motion controlled direct cell writing system. Next, the dual micro-organ is assembled and sealed to complete the microfluidic circuit. The serially connected M10 and HepG2 tissue chambers are perfused with media (for nutrients) and anti-radiation pro-drug Amiphostine (for select samples) over the bioprinted constructs. To assess the protective efficacy of anti-radiation drug on irradiated cells, the tissue constructs will be exposed to a low dose of Gamma Radiation after pro-drug treatment. Drug effectiveness can be analyzed via DNA damage quantified by micronuclei staining. The hypothesis is that in comparing the extent of pro-drug to active drug conversion, HepG2 cells express a much lower capacity than M10 to convert the pro-drug Amiphostaine to its active form. In the dual micro-organ, drug perfuses the M10 construct, is converted to active form, and then fed downstream to exert an effect on the HepG2 target construct.

7.4.3 Tissue Integrated Microbioreactor-on-a-Chip to Enable In Vitro Nanotoxicity Evaluation

A proposed future plan is to develop an optical measurement technique to directly identify and evaluate novel nanoprobes designed to target cells of an *in vitro* tissue-engineered model. *In vitro* cell model systems are versatile instruments with great potential to advance both toxicological and tissue engineering research by simulating signaling and mechanistic phenomena under physiological conditions. Such models are particularly attractive as tremendous positive impacts of nanotechnology in medicine become ubiquitous, and limited data on the potential risks of nano-sized particles to

human health and the environment emerge. Currently, however, robust quantification, evaluation, prediction, and verification of the biological fate, distribution, and risks of nanoparticles *in vivo* are lacking. In the proposed work, a 3D tissue-based model subject to physiological perfusion flow will enable broad application as an *in vitro* testbed for nanoparticle toxicity evaluation on tissues under *in vivo*–like conditions. Specifically, the convergence of several key enabling technologies in the fields of solid freeform fabrication (SFF) and microfabrication will feasibly lead to a complex and physiologically pertinent 3D tissue integrated microbioreactor-on-a-chip model amenable to long-term nanotoxicological study. To illustrate this model's applicability in nanotoxicology, dynamical optical imaging techniques will be applied to a fabricated microbioreactor-on-a-chip tissue testbed using novel quantum dot multimodal imaging probes called upconverting nanoparticles (UCNPs).

LIST OF REFERENCES

[1] Abbot, A. 2003. Biology's new dimension. Nature 424: 870-872.

[2] Abilez, O., Benharash, P., Mehrotra, M., Miyamoto, E., Gale, A., Picquet, J., Xu, C., and Zarins, C. 2006. A novel culture system shows that stem cells can be grown in 3D and under physiologic pulsatile conditions for tissue engineering of vascular grafts. J Surg Res 132(2): 170-178.

[3] Abu-Absi, S.F., Friend, J.R., Hansen, L.K., and Hu, W.S. 2002. Structural polarity and functional bile caniliculi in rat hepatocyte spheroids. Exp Cell Res 274(1): 56-67.

[4] Babensee, J.E., De Boni, U., and Sefton, M.V. 1992. Morphological assessment of hepatoma cells (HepG2) microencapsulated in a HEMA-MMA copolymer with and without Matrigel. J Biomed Mater Res 26(11): 1401-1418.

[5] Bader, A., Zech, K., Crome, O., Christians, U., Ringe, B., Pichlmayr, R., and Sewing, K.F. 1994. Use of organotypical cultures of primary hepatocytes to analyse drug biotransformation in man and animals. Xenobiotica 24(7): 623-633.

[6] Baker, T.K., Carfagna, M.A., Gao, H., Dow, E.R., Li, Q., Searfoss, G.H., and Ryan, T.P. 2001. Temporal gene expression analysis of monolayer cultured rat hepatocytes. Chem Res Toxicol 14(9): 1218-1231.

[7] Balis, U.J., Behnia, K., Bhatia, S.N., Sullivan, S.J., Yarmush, M.L., and Toner, M. 1999. Oxygen consumption characteristics of porcine hepatocytes. Metab Eng 1: 49-62.

[8] Baudoin, R., Corlu, A., Griscom, L., Legallais, C., and Leclerc, E. 2007. Trends in the development of microfluidic cell biochips for in vitro hepatotoxicity. Toxicol In Vitro 21(4): 535-544.

[9] Ben-Ze'ev, A., Robinson, G.S., Bucher, N.L., and Farmer, S.R. 1988. Cell-cell and cell-matrix interactions differentially regulate the expression of hepatic and cytoskeletal genes in primary cultures of rat hepatocytes. Proc Natl Acad Sci USA 85(7): 2161-2165.

[10] Bhatia, SN, Yarmush, ML, and Toner, M. 1997. Controlling cell interactions by micropatterning in co-cultures: hepatocytes and 3T3 fibroblasts. J Biomed Mater Res 34(2): 189-199.

[11] Bian, W., and Bursac, N. 2009. Engineered skeletal muscle tissue networks with controllable architecture. Biomaterials 30(7): 1401-1412.

[12] Boland, T., Tao, X., Damon, B. J., Manley, B., Kesari, P., Jalota, S., and Bhaduri, S. 2007. Drop-on-demand printing of cells and materials for designer tissue constructs. Mater Sci Eng C 27(3): 372–376.

[13] Boland, T., Xu, T., Damon, B., and Cui, X. 2006. Application of Inkjet Printing to Tissue Engineering. Biotechnology J 1(1): 910–917.

[14] Bonnie, L.G., Deborah, K.L., Scott, D.C., Rosemary, L.S., and Abdul, I.B. 2002. Microchannel platform for the study of endothelial cell shape and function. Biomed Microdevices 4(1): 9-16.

[15] Borenstein, J.T., Weinberg, E.J., Orrick, B.K., Sundback, C., Kaazempur-Mofrad, M.R., and Vacanti, J.P. 2007. Microfabrication of three-dimensional engineered scaffolds. Tissue Eng 13(8): 1837-1844.

[16] Brandon, E.F., Raap, C.D., Meijerman, I., Beijnen, J.H., and Schellens, J.H. 2003. An update on in vitro test methods in human hepatic drug biotransformation research: pros and cons. Toxicol Appl Pharmacol 189(3): 233-246.

[17] Bratten, C.D.T., Cobbold, P.H., and Cooper, J.M. 1998. Single-cell measurements of purine release using a micromachined electroanalytical sensor. Anal Chem 70: 1164-1170.

[18] Brouwer, K.L. and Thurman R.G. 1996. Isolated perfused liver. Pharm Biotechnol 8: 161-192.

[19] Castell, J.V., Jover, R., Martinez-Jimenez, C.P., and Gomez-Lechon, M.J., 2006. Hepatocyte cell lines: their use, scope and limitations in drugmetabolism studies. Expert Opin Drug Metab Toxicol 2(2): 183–212.

[20] Catania, J.M., Pershing A.M., and Gandolfi, A.J. 2007. Precision-cut tissue chips as an in vitro toxicology system. Toxicol In Vitro 21(5): 956-961.

[21] Chang, R., Nam, J. and Sun, W. 2008a. Effects of dispensing pressure and nozzle diameter on cell survival from solid freeform fabrication-based direct cell writing. Tissue Eng 14(1): 41-48.

[22] Chang, R., Nam, J. and Sun, W. 2008b. Direct cell writing of 3D micro-organ for in vitro pharmacokinetic model. Tissue Eng C 14(2): 157-166.

[23] Chen, A.A., Tsang, V.L., Albrecht, D.R., and Bhatia, S.N. 2006. 3-D Fabrication Technology for Tissue Engineering In: Springer US, BioMEMS and Biomedical Nanotechnology: 23-28.

[24] Chen, C.S., Mrksich, M., Huang, S., Whitesides, G.M., and Ingber, D.E. 1997. Geometric control of cell life and death. Science 276: 1425-1428.

[25] Chen, H.L., Wu, H.L., Fon, C.C., Chen, P.J., Lai, M.Y., and Chen, D.S. 1998. Long-term culture of hepatocytes from human adults. J Biomed Sci 5(6): 435-440.

[26] Chen, P., Xu, B., Tokranova, N., Feng, X., Castracane, J., Gillis, K.D. 2003. Amperometric detection of quantal catecholamine secretion from individual cells on micromachined silicon chips. Anal Chem 75: 518-524.

[27] Clark, E.A. and Brugge, J.S. 1995. Integrins and signal transduction pathways: the road taken. Science 268: 233-239.

[28] Cortesini, R. 2005. Stem cells, tissue engineering and organogenesis in transplantation. Transpl Immunol 15: 81-89.

[29] Cross, D.M. and Bayliss, M.K. 2000. A commentary on the use of hepatocytes in drug metabolism studies during drug discovery and development. Drug Metab Rev 32(2): 219-240.

[30] Davies, P.F. and Tripathi, S.C. 1993. Mechanical stress mechanisms and the cell: an endothelial paradigm. Circ Res 72(2): 239-245.

[31] Davies, P.F. 1995. Flow-mediated endothelial mechanotransduction. Physiol Rev 75: 519-560.

[32] Davies, P.F. 1997. Overview: temporal and spatial relationships in shear stress-mediated endothelial signaling. J Vasc Res 34(3): 208-211.

[33] Davila, J.C., Rodriguez, R.J., Melchert, R.B., Acosta, D. 1998. Predictive value of in vitro model system in toxicology. Annu Rev Pharmacol Toxicol 39: 63-96.

[34] De Bartolo, L. and Bader, A. 2001. Review of a flat membrane bioreactor as a bioartificial liver. Ann Transplant 6(3): 40-46.

[35] DiMasi, J.A., Hansen, R.W., and Grabowski, H.G. 2003. The price of innovation: new estimates of drug development costs. J Health Econ 22: 151–185.

[36] DiMasi, J.A. and Grabowski, H.G. 2007. The cost of biopharmaceutical R&D: is biotech different? Managerial and Decision Economics 28(4): 469–479.

[37] Donato, M.T., Gómez-Lechón, M.J., and Castell, J.V. 1990. Drug metabolizing enzymes in rat hepatocytes co-cultured with cell lines. In Vitro Cell Dev Biol 26(11): 1057-1062.

[38] Donato, M.T., Jiménez, N., Castell, J.V., and Gómez-Lechón, M.J. 2004. Fluorescence-based assays for screening nine cytochrome P450 (P450) activities in intact cells expressing individual human P450 enzymes. Drug Metab Dispos 32(7): 699-706.

[39] Dong, C., Skalak, R., and Sung, K.L. 1991. Cytoplasmic rheology of passive neutrophils. Biorheology 28: 557-567.

[40] Drury, J.L. and Mooney, D.J. 2003. Hydrogels for tissue engineering: scaffold design variables and applications. Biomaterials 24: 4337-4351.

[41] Dunn, J.C., Yarmush, M.L., Koebe, H.G., and Tompkins, R.G. 1989. Hepatocyte function and extracellular matrix geometry: long-term culture in a sandwich configuration. FASEB J 3(2): 174-177.

[42] Evans, E. and Yeung, A. 1989. Apparent viscosity and cortical tension of blood granulocytes determined by micropipet aspiration. Biophys J 56: 151-160.

[43] Foy, B.D., Rotem, A., Toner, M., Tompkins, R.G., and Yarmush, M.L. 1994. A device to measure the oxygen-uptake rate of attached cells—importance in bioartificial organ design. Cell Transplant 3: 515-527.

[44] Gebhardt, R., Wegner, H., Alber, J. 1996. Perifusion of co-cultured hepatocytes: optimization of studies on drug metabolism and cytotoxicity in vitro. Cell Biol Toxicol 12(2): 57-68.

[45] Ghanem, A. and Shuler, M.L. 2000. Combining cell culture analogue reactor designs and PBPK models to probe mechanisms of naphthalene toxicity. Biotechnol Prog 16: 334-345.

[46] Glicklis, R., Shapiro, L., Agbaria, R., Merchuk, J.C., and Cohen, S. 2000. Hepatocyte behavior within three-dimensional porous alginate scaffolds. Biotechnol Bioeng 67(3):344-53.

[47] Griffith, L.G. and Naughton, G. 2002. Tissue engineering--current challenges and expanding opportunities. Science 295:1009-1014.

[48] Guguen-Guillouzo, C., Clément, B., Baffet, G., Beaumont, C., Morel-Chany, E., Glaise, D., and Guillouzo, A. 1983. Maintenance and reversibility of active albumin secretion by adult rat hepatocytes co-cultured with another liver epithelial cell type. Exp Cell Res 143(1): 47-54.

[49] Holmes, T.C., de Lacalle, S., Su, X., Liu, G., Rich, A., and Zhang, S. 2000. Extensive neurite outgrowth and active synapse formation on self-assembling peptide scaffolds. Proc Nat Acad Sci USA 97: 6728-6733.

[50] Ijima, H. and Kakeya, Y. 2008. Monolayer culture of primary rat hepatocytes on an Arg-Gly-Asp (RGD)-immobilized polystyrene dish express liver-specific functions of albumin production and p-acetamidophenol metabolism the same as for spheroid culture. Bioch Eng J 40(2): 387-391.

[51] Ingber, D.E. 1993. Cellular tensegrity: defining new rules of biological design that govern the cytoskeleton. J Cell Sci 104: 613-627.

[52] Ingber, D.E. 1997. Tensegrity: the architectural basis of cellular mechanotransduction. Annu Rev Physiol 59: 575-599.

[53] Jukes, J.M., Moroni, L., Van Blitterswijk, C.A., and Boer, J.D. 2008. Critical steps toward a tissue-engineered cartilage implant using embryonic stem cells. Tissue Eng A 14: 135-147.

[54] Kan, P., Miyoshi, H, Yanagi, K., and Ohshima, N. 1998. Effects of shear stress on metabolic function of the co-culture system of hepatocyte/nonparenchymal cells for a bioartificial liver. ASAIO J 44(5): M441-M444.

[55] Kaplowitz, N. 2005. Idiosyncratic drug hepatotoxicity. Nat Rev Drug Discov 4: 489–499.

[56] Khalil S, Nam J, and Sun W. 2005. Multi-nozzle deposition for construction of 3D biopolymer tissue scaffolds. Rapid Prototyping J 11(1): 9-17.

[57] Khalil, S. and Sun, W. 2007. Biopolymer deposition for freeform fabrication of hydrogel tissue constructs. Mater Sci Eng C 27: 469-478.

[58] Khetani, S., Szulgit, G., Del Rio, J., Barlow, C., and Bhatia, S.N. 2004. Exploring mechanisms of stromal-epithelial cell interactions using gene expression profiling. Hepatology 40(3): 545-554.

[59] Khetani, S.R. and Bhatia, S.N. 2006. Engineering tissues for in vitro applications. Curr Opin Biotechnol 17(5): 524-531.

[60] Kjavin, I.J., and Madison, R.D. 1991. Peripheral nerve regeneration within tubular prostheses: effects of laminin and collagen matrices on cellular ingrowth. Cells Mat 1: 17.

[61] Koide, N., Sakaguchi, K., Koide, Y., Asano, K., Kawaguchi, M., Matsushima, H., Takenami, T., Shinji, T., Mori, M., and Tsuji, T. 1990. Formation of multicellular spheroids composed of adult rat hepatocytes in dishes with positively charged surfaces and under other nonadherent environments. Exp Cell Res 186(2): 227-235.

[62] Kono, Y., Yang, S., and Roberts, E.A. 1997. Extended primary culture of human hepatocytes in a collagen gel sandwich system. In Vitro Cell Dev Biop Anim 33: 467-472.

[63] Korhonen, L.E., Turpeinen, M., Rahnasto1, M., Wittekindt, C., Poso, A., Pelkonen, O., Raunio, H., and Juvonen, R.O. 2007. New potent and selective

cytochrome P450 2B6 (CYP2B6) inhibitors based on three-dimensional quantitative structure-activity relationship (3D-QSAR) analysis. British J of Pharm 150: 932–942.

[64] Kreeger, P.K., Woodruff, T.K., and Shea, L.D. 2003. Murine granulosa cell morphology and function are regulated by a synthetic Arg-Gly-Asp matrix. Molecular and Cellular Endocrinology 205: 1-10.

[65] Landers, R., Hubner, U., Schmelzeisen, R., and Mulhaupt, R. 2002. Rapid prototyping of scaffolds derived from thermoreversible hydrogels and tailored for applications in tissue engineering. Biomaterials 23: 4437–4447.

[66] Langer, R. and Vacanti, J.P. 1993. Tissue engineering. Science 260(5110): 920-926.

[67] LeCluyse, E.L., Bullock, P.L., and Parkinson, A. 1996. Strategies for the restoration and maintenance of normal hepatic structure and function in long term cultures of rat hepatocytes. Adv Drug Delivery Rev 22:133-186.

[68] LeCluyse, E.L. 2001. Human hepatocyte culture systems for the in vitro evaluation of cytochrome P450 expression and regulation. Eur J Pharm Sci 13(4): 343-368.

[69] LeCluyse, E.L., Alexander, E., Hamilton, G.A., Viollon-Abadie, C., Coon D.J., Jolley, S., and Richert, L. 2005. Isolation and culture of primary human hepatocytes. Methods Mol Biol 290: 207-229.

[70] Ledezma, G.A., Folch, A., Bhatia, S.N., Balis, U., Yarmush, M.L., and Toner, M. 1999. Numerical model of fluid flow and oxygen transport in a radial-flow microchannel containing hepatocytes. ASME J Biomech Eng 121: 58-64.

[71] Lee, J.K., Leslie, E.M., Zamek-Gliszcazynski, M.J., and Brouwer, K.L. 2008. Modulation of trabectedin hepatobiliary disposition by multidrug reistance-associated proteins may prevent hepatotoxicity. Toxicol Appl Pharmacol 228(1): 17-23.

[72] Leinfelder, U., Brunnenmeier, F., Cramer, H., Schiller, J., Arnold, K., Vasquez, J.A., and Zimmermann, U. 2003. A highly sensitive cell assay for validation of purification regimes of alginates," Biomaterials 24: 4161-4172.

[73] Leong KF, Cheah CM, and Chua CK. 2003. Solid freeform fabrication of three-dimensional scaffolds for engineering replacement tissues and organs. Biomaterials 24(13):2363–2678.

[74] Lerche-Langrand, C. and Toutain, H.J. 2000. Precision-cut liver slices: characteristics and use for in vitro pharco-toxicology. Toxicology 153: 221-253.

[75] Levesque, M.J. and Nerem, R.M.. 1985. The elongation and orientation of cultured endothelial cells in response to shear stress. ASME J Biomech Eng 107:341-347.

[76] Li, G.N., and Hoffman-Kim, D. 2008. Tissue-engineered platforms of axon guidance. Tissue Eng B 14: 33.

[77] Lu, S.H., Wang, H.B., Liu, H., Wang, H.P., Lin, Q.X., Li, D.X., Song, Y.X., Duan, C.M., Feng, L.X., and Wang, C.Y. 2008. Reconstruction of engineered uterine tissues (EUTs) containing smooth muscle layer in collagen/matrigel scaffold in vitro. Tissue Eng A 15: 1.

[78] Lutolf, M.P. and Hubbell, J.A. 2005. Synthetic biomaterials as instructive extracellular microenvironments for morphogenesis in tissue engineering. Nature Biotechnology 23(1): 47-55.

[79] Madison, R. 1985. Increased rate of peripheral nerve regeneration using bioresorbable nerve guides and a laminin-containing gel. Exp Neuro 88: 767.

[80] Malek, A.M., Alper, S.L., and Izumo, S. 1999. Hemodynamic shear stress and its role in atherosclerosis. J Am Med Assoc. 282: 2035-2042.

[81] McBeath, R., Pirone, D.M., Nelson, C.M., Bhadriraju, K., and Chen, C.S. 2004. Cell shape, cytoskeletal tension, and RhoA regulate stem cell lineage commitment. Dev Cell 6: 483-495.

[82] Meyvantsson, I. and Beebe, D.J. 2008. Cell culture models in microfluidic systems. Ann Rev Anal Chem 1: 423-449.

[83] Mironov, V., Markwald, R. R., and Forgacs, G. 2003. Organ printing: self-assembling cell aggregates as bioink. Sci and Med 9(2): 69-71.

[84] Mitaka, T. 1998. The current status of primary hepatocyte culture. Int J Exp Pathol 79(6): 393-409.

[85] Modrinos, M.J., Koutzaki, S., Jiwanmall, E., Li, M., Dechadarevian, J., Lelkes, P.I., and Finck, C.M. 2006. Engineering three-dimensional pulmonary tissue constructs. Tissue Eng 12: 717.

[86] Mufti, NA, Bleckwenn, NA, Babish, JG, Shuler, ML. 1995a. Possible involvement of the Ah receptor in the induction of cytochrome P-4501A1 under conditions of hydrodynamic shear in microcarrier-attached hepatoma cell lines. Biochem Biophy J Res Comm 208: 144-152.

[87] Mufti, N.A, Shuler, M.L. 1995b. Induction of cytochrome P450Ia1 activity in response to sublethal stresses in microcarrier-attached hepatocytes. Biotechnol Prog. 11: 659-663.

[88] Norman, J.J., Collins, J.M., Sharma, S., Russell, B., and Desai, T.A. 2008. Microstructures in 3D biological gels affect cell proliferation. Tissue Eng A 14: 379.

[89] Nussler, A.K., Wang, A., Neuhaus, P., Fischer, J., Yuan, J., Liu, L., Zeilinger K., Gerlach, J., Arnold, P., and Albrecht, W. 2001. The suitability of hepatocyte culture models to study various aspects of drug metabolism. Altex 18: 91-101.

[90] Papadaki, M., Tilton, R.G., Eskin, S.G., and McIntire, L.V. 1998. Nitric oxide production by cultured human aortic smooth muscle cells: stimulation by fluid flow. Am J Physiol. 278:H616-J626.

[91] Peshwa, M.V., Wu, F.J., Sharp, H.L., Cerra, F.B., and Hu, W.S. 1996. Mechanistics of formation and ultrastructural evaluation of hepatocyte spheroids. In Vitro Cell Dev Biol Anim 32(4): 197-203.

[92] Plopper, G.E., McNamee, H.P., Dike, L.E., Bojanowski, K., and Ingber, D.E. 1995. Convergence of integrin and growth factor receptor signaling pathways within the focal adhesion complex. Mol Biol Cell 6: 1349-1365.

[93] Polykandriotis, E., Arkudas, A., Horch, R.E., and Kneser, U. 2008. To Matrigel or not to Matrigel. Am J Pathol 172: 1441.

[94] Porter, N.L., Pilliar, R.M., and Grynpas, M.D. 2001. Fabrication of porous calcium polyphosphate implants by solid freeform fabrication: A study of processing and in vitro degradation characteristics. J Biomed Mater Res 56: 504–515.

[95] Powers, M.J., Domansky, K., Kaazempur-Mofrad, M.R., Kalezi, A., Capitano, A., Upadhyaya, A., Kurzawski, P., Wack, K.E., Stolz, D.B., Kamm, R., and Griffith, L.G. 2002a. A microfabricated array bioreactor for perfused 3D liver culture. Biotechnol Bioeng 78(3): 257-269.

[96] Powers, M.J., Janigian, D.M., Wack, K.E., Baker, C.S., Stolz, D.B., and Griffith, L.G. 2002b. Functional behavior of primary rat liver cells in a three-dimensional perfused microarray bioreactor. Tissue Eng 8: 499-513.

[97] Pritchard, J.F., Jurima-Romet, M., Reimer, M.L., Mortimer, E., Rolfe, B., and Cayen, M.N. 2003. Making better drugs: Decision gates in non-clinical drug development. Nat Rev Drug Discov 2: 542–553.

[98] Ringeisen, B. R., Othon, C. M., Barron, J. A., Young, D., and Spargo, B. J. 2006. Jet-based methods to print living cells. Biotechnology J 1(9): 930–948.

[99] Sahai E. and Marshall C.J. 2003. Differing Modes of Tumour Cell Invasion Have Distinct Requirements for Rho/ROCK Signaling and Extracellular Proteolysis. Nature Cell Biology. 5(8): 711-719.

[100] Schmid-Schoenbein, G.W., Kosawada, T., Skalak, T., Chien, S. 1995. Membrane model of endothelial cells and leukocytes: A proposal for the origin of a cortical stress. ASME J Biom Eng 117:171.

[101] Semino, C.E., Merok, J.R., Crane, G.G., Panagiotakos, G., and Zhang, S. 2003. Functional differentiation of hepatocytelike spheroid structures from putative liver progenitor cells in three-dimensional peptide scaffolds. Differentiation 71:262.

[102] Schuetz, E.G., Li, D., Omiecinski, C.J., Muller-Eberhard, U., Kleinman, H.K., Elswick, B., and Guzelian, P.S. 1988. Regulation of gene expression in adult rat hepatocytes cultured on a basement membrane matrix. J Cell Physiol 134(3): 309-323.

[103] Shoichet, M.S., Li, R.H., White, M.L. and Winn, S.R. 1996. Stability of hydrogels used in cell encapsulation: an in vitro comparison of alginate and agarose. Biotechnol Bioeng 50: 374-381.

[104] Shor, L., Guceri, S., Wen, X., Gandhi, M., and Sun, W. 2008. Fabrication of three-dimensional polycaprolactone/hydroxyapatite tissue scaffolds and osteoblast-scaffold interactions in vitro. Biomaterials 28(35): 5291-5297.

[105] Shuler, M.L., Ghanem, A., Quick, D., Wong, M.C., and Miller, P. 1996. A self-regulating cell culture analog device to mimic animal and human toxicological responses. Biotechnol Bioeng 52: 45-60.

[106] Sivaraman, A., Leach, J.K., Townsend, S., Iida, T., Hogan, B.J., Stolz, D.B., Fry, R., Samson, L.D., Tannenbaum, S.R., and Griffith, L.G. 2005. A microscale in vitro physiological model of the liver: predictive screens for drug metabolism and enzyme induction. Curr Drug Met 6: 569-591.

[107] Sun, W., Yan, Y., Lin, F., and Spector, M. 2006. Biomanufacturing: a US-China National Science Foundation-sponsored workshop. Tissue Eng 12(5): 1169-1181.

[108] Surapaneni, S., Pryor, T., Klein, M.D., and Matthew, H.W. 1997. Rapid hepatocyte spheroid formation: optimization and long-term function in perfused microcapsules. ASAIO J 43(5): M848-M853.

[109] Tada, S. and Tarbell, J.M. 2000. Interstitial flow through the internal elastic lamina affects shear stress on arterial smooth muscle cells. Am J Physiol Heart Circ Physiol. 278: H1589-H1597.

[110] Tan, K.H., Chua, C.K., Leong, K.F., Cheah, C.M., Cheang, P., Abu Bakar, M.S., and Cha, S.W. 2003. Scaffold development using selective laser sintering of polyetheretherketone–hydroxyapatite biocomposite blends. Biomaterials 24: 3115–3123.

[111] Thomas, C.H., Collier, J.H., Sfeir, C.S., and Healy, K.E. 2002. Engineering gene expression and protein synthesis by modulation of nuclear shape. Proc Natl Acad Sci USA 99: 1972-1977.

[112] Todaro, G.J. and Green, H. 1963. Quantitative studies of the grough of mouse embryo cells in culture and their development into established lines. J Cell Biol 17: 299-313.

[113] Tsang, L.T. and Bhatia, S.N. 2004. Three-dimensional tissue fabrication. Adv Drug Delivery Rev 56: 1635-1647.

[114] Venkatesh, S. and Lipper, R.A. 2000. Role of the development scientist in compound lead selection and optimization. J Pharm Sci 89(2):145-154.

[115] Viravaidya, K., Sin, A., and Shuler, M.L. 2004. Development of a microscale cell culture analog to probe naphthalene toxicity. Biotechnol Prog 20: 316.

[116] Vozzi, G., Flaim, C., Ahluwalia, A., and Bhatia, S. 2003 Fabrication of PLGA scaffolds using soft lithography and microsyringe deposition. Biomaterials 24: 2533–2540.

[117] Wang, N., Naruse, K., Stamenovic, D., Fredberg, J., Mijailovich, S., and Tolit-Norrelykke, I. 2001. Mechanical behavior in living cells consistent with the tensegrity model. Proc. Natl. Acad. Sci. U.S.A. 98(14): 7765-7770.

[118] Wang, L., Shelton, R.M., Cooper, P.R., Lawson, M., Triffitt, J.T., and Barralet, J.E. 2003. Evaluation of sodium alginate for bone marrow cell tissue engineering. Biomaterials 24: 3475-3481.

[119] Weaver, V.M., Petersen, O.W., Wang, F., Larabell, C.A., Briand, P., Damsky, C., and Bissell, M.J. 1997. Reversion of the malignant phenotype of human breast cells in three-dimensional culture and in vivo by integrin blocking antibodies. J Cell Biology 137(1): 231-245.

[120] Whitesides, G.M., Ostuni, E., Takayama, S., Jiang, X., and Ingber, D.E. 2001. Soft lithography in biology and biochemistry. Annu Rev Biomed Eng 3: 335-373.

[121] Williams, D. and Sebastine, I. 2005. Tissue engineering and regenerative medicine: manufacturing challenges. IEE Proc. Nanobiotechnol 152: 207–210.

[122] Wolf K., Mazo I., Leung H., Engelke K., von Andrian U.H., and Deryugina E.I. 2003. Compensation Mechanism in Tumor Cell Migration: Mesenchymal-amoeboid transition after blocking of pericellular proteolysis. J Cell Biology 160(2): 267-277.

[123] Wong, A.P., Perez-Castillejos, R., Love, J.C., and Whitesides, G.M. 2008. Partitioning microfluidic channels with hydrogel to construct tunable 3-D cellular microenvironments. Biomaterials 29: 1853.

[124] Wu, F.J., Friend, J.R., Remmel, R.P., Cerra, F.B., and Hu, W.S. 2000. Enhanced cytochrome P450 IA1 activity of assembled rat hepatocyte spheroids. Cell Transplant 8: 233-246.

[125] Yang, S., Leong, K.F., Du, Z., and Chua, C.K. 2002. The design of scaffolds for use in tissue engineering: Part II. Rapid prototyping techniques. Tissue Eng 8: 1–11.

[126] Yu, L.J., Matias, J., Scudiero, D.A., Hite, K.M., Monks, A. Sausville, E.A., Waxman, D.J. 2001. P450 enzyme expression patterns in the NCI human tumor cell line panel. Drug Metabol Dispos 29(3): 304-312.

[127] Zein, I., Hutmacher, D., Tan, K.C., and Teoh, SH. 2002. Fused deposition modeling of novel scaffold architectures for tissue engineering applications. Biomaterials 23: 1169–1185.

APPENDICES

The direct cell writing protocol presented below is established for a reliable, high-throughput drug screening model.

A. Cell-alginate biopolymer solution preparation:

1. To prepare the pre-polymer solution, dissolve medium viscosity sodium alginate powder in DI water as a 3.0% (w/v) solution.
2. Mix with magnetic stir bar overnight.
3. Sterilize sodium alginate solution by serial filtration using 0.85 μm, 0.45 μm, and 0.20 μm syringe filters.
4. To prepare the ionic cross-linking solution, dissolve calcium chloride in DI water as a 5.0% (w/v) solution.
5. Prepare HepG2 liver cells by culturing and maintaining in Dulbecco's Modified Eagle's Medium (DMEM), supplemented with 10% (w/v) fetal bovine serum, and maintained in the incubator at 5% CO2 and 37°C.
6. Centrifuge prepared HepG2 cell suspension (e.g. 8,000 × *g* for 5 min).
7. Resuspend the cells in sodium alginate pre-polymer solution with gentle pipetting.

B. Preparation of microfluidic components for bioprinting:

1. Wash glass cover slide successively x 3 with acetone, ethanol, and DI water.
2. Leave recently baked PDMS substrate as is (i.e. without washing).

C. Plasma treatment of microfluidic components for bioprinting:

1. Use tweezers to gently place clean glass cover slide and PDMS substrate onto quartz plate inside plasma chamber.
2. Turn on vacuum of plasma chamber for 1 minute.
3. Expose glass cover slide and PDMS substrate to RF plasma for 30 seconds.

D. Direct cell writing into tissue chamber of microfluidic device:

1) Take plasma-treated PDMS layer to the printing system.
2) Align tissue chamber and height.
3) Print cell/alginate suspension into the tissue chamber using defined toolpath.
4) Specify and adjust the printing process parameters according the design specifications.
5) $CaCl_2$ crosslinking agent dispensed at regular intervals using second pneumatic nozzle.
6) Affix glass layer to the PDMS layer to seal the system.
7) Place chips in sterile container / seal container.

E. Adaptation of microprinted tissue construct for pharmacokinetic study:

1) Take sealed container to hood and place into chip holder/clamps.
2) Attach to syringe pump using tubing and Nanoports.
3) Place inside incubator.

F. Assessment of cell viability for three-dimensional cell-alginate constructs:

1) Add 1mL of Live/Dead assay to each sample.

2) Incubate for 45 minutes.

3) View under a Leica fluorescence microscope at 40X magnification

4) In order to quantify the cell viability and assign a cell viability percentage throughout the time course study, each sample is visualized and a live-dead cell count performed at five different locations (three peripheral, two central) for the bulk sample.

G. Cell counting in three-dimensional cell-alginate constructs using microplate reader:

1) Use hemocytometer to obtain the number of cells/ml in cell solution.

2) Cell solutions are made at different concentrations ranging from 250,000 cells/ml to 2,000,000 cells/ml at 250,000 cells/ml intervals.

3) X volume of Alamar Blue is added to Y volume of each cell solution concentration in step (2) to give a total volume Z.

4) Each Z volume of different cell concentration/Alamar Blue solution is placed into 6 wells in a 6x8 well plate.

5) The well plate is placed in the cytofluorimeter and a reading is given out for each well plate. Measure concentration of reduced Alamar Blue solution using a

microplate reader with an excitation filter wavelength of 535 nm and an emission filter wavelength of 595 nm.

6) A curve is obtained presenting the number of cells versus the microplate reading.

7) Scaffold is immersed in a known cell solution volume for 1 hour in incubator.

8) Scaffold is removed from cell solution and kept in a new culture dish.

9) Alamar Blue (fluorescence dye) is added at volume A (depending on scaffold size) to the cells seeded scaffold in the new culture dish and kept in the incubator for 3 hours. This step allows the cells in the printed construct to metabolize the Alamar Blue.

10) The Alamar Blue solution is removed from the scaffold and the W volume is divided into 6 wells in a 6x8 well plate. Each well contains Z ml of the Almar Blue solution.

11) Fresh medium is added to the scaffold and is replaced back in the incubator

12) The well plate is placed in the microplate reader and a reading is given out for each well plate.

13) The data from step (6) is used to obtain the number of cells in step (12). Step (8) to (13) could be repeated over a number of days to obtain the proliferation of cells in the scaffold over a couple of days.

H. Assessment of liver cell-specific urea synthesis function:

1) 1 mL of QuantiChrome Urea Assay (BioAssay Systems, Hayward, CA) solution, a fluorometric indicator of liver cell urea synthetic activity, is added to each printed sample.
2) Replenish media with assay daily.
3) Measure concentration of urea using a microplate reader with an absorbance filter wavelength of 520 nm.

I. Drug Metabolism Protocol for Liver Cells:

1) Drug substrate EFC = 7-ethoxy-4-trifluoromethyl coumarin 25 mg of drug comes in a glass amber vial and should be reconstituted in 9.68ml of DMSO to create a 10mM stock solution of EFC.

2) Drug product HFC (for standard curve) = 7-hydroxy-4-trifluoromethyl coumarin 100 mg of drug comes in a glass amber vial and is reconstituted in 43.5 ml of DMSO to create a 10 mM stock solution of HFC.

3) Carry out formation of EFC and HFC stock solutions in the laminar flow hood using good sterile technique and sterile DMSO. Store stock solutions dessicated in the refrigerator.

4) Once the drug and standard stock solutions have been made, they can be diluted to the desired working concentration in cell culture media just prior to an

experiment. 120 μM EFC has been found to work quite well for drug metabolism studies in the HepG2 cells.

5) To create 10 ml of a 120 μM EFC test solution:

   Dilute 120 μL of the 10 mM EFC stock solution into 9.88 ml of HepG2 medium and mix well.

6) To create 5 ml of HFC standard solutions ranging from 0.1 – 64 μM:

   Dilute 64 μL of the 10 mM HFC stock solution into 9.936 mL of HepG2 medium containing 120 μM EFC.

7) Serially dilute the 64 μM standard to achieve the desired standards. For example, add 5 ml of 64 μM HFC solution to 5 ml of 120 μM EFC test solution and mix well. This will be 32 μM HFC standard. Then add 5 ml of the 3 μM HFC standard to 5 ml of 120 μM EFC test solution etc. until 0.125 μM HFC standard is reached. Use the 120 μM EFC test solution as the "zero" HFC standard.

8) To start a metabolism experiment:

   Remove medium covering test cells. Replace with desired amount of 120 μM EFC test solution.

8) Measure concentration of urea using a microplate reader with an excitation filter wavelength of 360 nm and an emission filter wavelength of 520 nm.

VITA

EDUCATION:

B.S., Department of Chemical Engineering (2000), University of Pennsylvania

Ph.D., Department of Mechanical Engineering (2009), Drexel University

SELECTED PUBLICATIONS:

1. **Chang R**., Nam J., and Sun W. "Direct Cell Writing of 3D Micro-organ for In Vitro Pharmacokinetic Model," Tissue Engineering Part C, 14(2), 157-169, 2008.
2. **Chang R.,** Nam J., and Sun W. "Computer-Aided Design, Modeling, and Freeform Fabrication of Micro-organ Flow Patterns for Pharmacokinetic Study," CAD Applications, Vol. 5, p. 21-29, 2008.
3. **Chang R**., Nam J., and Sun W. "Effects of Dispensing Pressure and Nozzle Diameter on Cell Survival from Solid Freeform Fabrication-based Direct Cell Writing," Tissue Engineering, 14(1): 41-48, 2008.
4. **Chang R**., Emami K., Jeevarajan A., Wu H., and Sun W. "Direct Cell Writing of 3D Micro-organ for Drug Metabolism Studies," Biofabrication, in preparation.
5. Shor L., Guceri S., **Chang R.**, Sun W., Gordon J., Kang Q., Hartstock L., and An Y. "Precision Extruding Deposition (PED) Fabrication of Poly-e-Caprolactone (PCL) Scaffolds for Bone Tissue Engineering," Biofabrication, in press.

AWARDS:

Drexel Best Dissertation Award (2009)

BP Young Scientists and Students Award (2008)

Lawrence Baida Business Student Business Plan Winner (2008)

NASA Technology Transfer Award (2008)

Koerner Family Fellowship (2007)

TERMIS Student Travel Award, NIH (2008)

Drexel Student Outreach Award (2008)

TERMIS Student Travel Award, NIH (2007)

GAANN Fellowship, Drexel University (2006)